The Institute of Paper Chemistry

Appleton, Wisconsin

Doctor's Dissertation

Effects of Physical Structure on the Alkaline Degradation of Hydrocellulose

Victor M. Gentile

June, 1986

EFFECTS OF PHYSICAL STRUCTURE ON THE ALKALINE DEGRADATION OF HYDROCELLULOSE

A thesis submitted by

Victor M. Gentile

B.S. 1977, St. Joseph's College

M.S. 1980, Lawrence University

in partial fulfillment of the requirements
of The Institute of Paper Chemistry
for the degree of Doctor of Philosophy
from Lawrence University
Appleton, Wisconsin

June, 1986

TABLE OF CONTENTS

SUMMARY

The alkaline degradation of cellulose involves random cleavage of the glycosidic linkages and stepwise elimination of monomer units from the reducing end (peeling). Random chain cleavage only occurs at significant rates in native cellulose (i.e., wood and cotton fibers) at relatively high temperatures (>150°C). In contrast, the peeling reaction occurs rapidly even at much lower temperatures (<100°C) and is manifested in losses in cellulose yield. Cellulose molecules are stabilized toward peeling by a competing reaction which converts the reducing end group to an alkali-stable carboxylic acid end group (chemical stopping). In addition, physical stopping of the peeling reaction reportedly occurs when a molecule is peeled back to a crystalline region in the cellulose structure, causing the reducing end group to become inaccessible to the alkaline medium.

In the present study, the concept of physical stopping and the effects of cellulose physical structure on the alkaline reaction rates were assessed by studying alkaline degradations of a fibrous cotton hydrocellulose (predominantly cellulose I) and an amorphous hydrocellulose (noncrystalline). Differences in reactivities of the two substrates could therefore be attributed to the substantial differences in physical structures. The reactions were conducted in oxygen-free 1.0M sodium hydroxide at 60 and 80°C. The degradative and stabilizing reactions were characterized by monitoring yield loss and end group composition. In addition, changes in the hydrocellulose physical structures were evaluated using hydroxyl accessibility measurements, x-ray diffraction, and Raman and solid-state ^{13}C-NMR spectroscopy.

The fibrous hydrocellulose exhibited no significant change in physical structure during degradation. In contrast, the amorphous hydrocellulose

underwent partial recrystallization (cellulose II) and preferential loss of amorphous material due to peeling.

During the early reaction periods, peeling and chemical stopping occurred more rapidly in the amorphous regions of the amorphous hydrocellulose than in the disordered regions of the fibrous hydrocellulose. In addition, random chain cleavage only occurred in the amorphous regions of the amorphous hydrocellulose. These results are indicative that the reducing end groups and glycosidic linkages in the disordered regions of the fibrous substrate were less reactive than those in amorphous regions of the amorphous substrate. Therefore, it is postulated that the disordered regions of the fibrous hydrocellulose consisted of slightly distorted cellulose I crystalline domains and crystallite surfaces rather than amorphous regions. Preferential removal of material from such regions by peeling would not be expected to cause a significant increase in the crystalline fraction, because the molecules would exhibit some level of cellulose I character.

The peeling reaction was drastically inhibited by the cellulose I domains of the fibrous hydrocellulose and by the cellulose II domains that formed in the amorphous hydrocellulose. This is apparently due to the crystalline domains essentially blocking the peeling reaction from progressing along the cellulose molecule, despite the fact that its reducing end group is accessible to the alkaline medium. In contrast, chemical stopping was significantly more inhibited by cellulose I than by cellulose II. This effect is attributed to both the degree of structural order and the conformational environment of an accessible reducing end group dictating its reactivity toward chemical stopping. In addition, the rate of chemical stopping increased relative to the rate of

peeling for both substrates with increasing temperature, consistent with chemical stopping having a higher activation energy than peeling.

Physical stopping of peeling was more rapid and extensive in reactions of the fibrous hydrocellulose due to the larger number of molecules extending into crystalline domains compared to the amorphous hydrocellulose. Consequently, the dominant stabilization mechanism for the fibrous hydrocellulose was physical stopping, while chemical stopping dominated in the reactions of the amorphous hydrocellulose. The occurrence of physical stopping in both substrates demonstrates that cellulose I and cellulose II crystallites provide sites at which the reducing end group can be inaccessible to the alkaline medium. In addition, the cessation of physical stopping in the later periods of the 80°C reactions indicates that a maximum number of potential physical stopping sites is present in a particular cellulose substrate. As would be expected, this number was greater for the fibrous hydrocellulose.

INTRODUCTION

PERSPECTIVE

Over the past fifty years, the sulfate or kraft process has become the dominant method for pulping wood.[1] Its popularity is attributable to its relative insensitivity to wood species and the resultant pulp strength properties.[1-3] Ideally, the primary objective in chemical pulping of wood is to isolate cellulosic fibers with desirable properties in the highest possible yield. Unfortunately, the alkaline kraft and soda processes are not selective delignification processes, and the loss of wood polysaccharides can equal the lignin removed,[4] resulting in low fiber yields.

During the last several decades, a great deal of research has been focused on elucidating the alkaline reaction mechanisms of wood polysaccharides, particularly cellulose, the major wood component.[4-16] Alkali-soluble compounds have frequently been employed in mechanistic studies,[5,12-16] since cellulose and its degradation products are not easily characterized. However, most reactions of cellulose are dictated to some extent by the physical structure.[5,17-18] More specifically, the tendency of cellulose molecules to form highly-ordered structures places accessibility and mobility limitations on the molecules, thereby modifying their response to the reaction medium. Although a few studies of alkaline degradation of cellulose have indicated that cellulose structure is important in controlling its degradation,[7,11,19] the manner in which physical structure affects the reactions has not been thoroughly examined. This investigation was directed at clarifying the role of cellulose physical structure in its alkaline reactions.

CELLULOSE STRUCTURE

The cellulose molecule is a linear polymer composed of anhydro-D-glucopyranose monomer units which are connected by β-glucosidic bonds between the anomeric carbon (C-1) of one monomer unit and C-4 of the adjacent monomer unit (Fig. 1). The cellulose molecule has nonequivalent end units referred to as the reducing and nonreducing ends. Thus, the main functional groups responsible for cellulose reactivity are the hydroxyl groups at C-2, C-3, and C-6 of each anhydroglucose unit, the glycosidic linkages, and the hemiacetal at C-1 of the reducing end.[2]

The chemistry of cellulose as it relates to alkaline pulping is discussed in a later section.

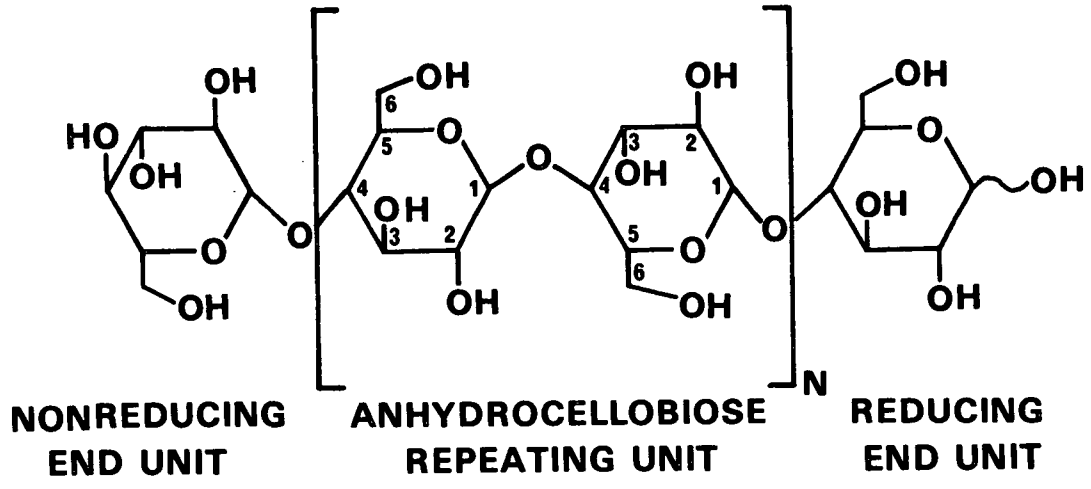

Figure 1. Cellulose molecule.

With its hydroxyl groups, glycosidic oxygen atoms, and ring oxygen atoms, the linear cellulose molecule has the capability of forming numerous hydrogen bonds along the entire length of the polymer chain. These bonds bind together parallel segments of adjacent cellulose molecules, thereby forming the basic structural elements of native cellulose fibers.[17]

The disposition of the molecules within the basic structural elements has been a topic of debate for more than a century.[20,21] With the development of modern analytical tools many of the earlier postulates were either discarded or reformulated. However, it is generally agreed that cellulose molecules form highly-ordered (crystalline) aggregates. Cellulose reactivity is therefore dependent on functional group accessibility, which is dictated by the location of the molecular chain within the basic structural element.[17,22] Thus, the following discussion deals mainly with the current concepts of cellulose structure at this organizational level.

The fringed-micelle theory was the first widely accepted concept for the aggregation of cellulose molecules.[21] Frey-Wyssling[23] and Hermans[24] have reviewed the development of this theory which emerged from the work of many investigators. The basic structural element is referred to as the elementary fibril, and it consists of cellulose molecules oriented parallel to the fibril axis with discrete crystalline and amorphous regions along its length. A single cellulose molecule can pass through several crystalline regions (micelles) which comprise the major fraction of the elementary fibril. Although the theory was first conceived in 1930,[25] many researchers continue to support it[20,26-29] over more recent postulates.

In contrast to the fringed-micelle theory, it has been proposed that the elementary fibril is completely crystalline with the exception of molecules at crystallite surfaces and in distorted crystalline regions.[22,30-32] According to this model, the least ordered regions occur at strain-distorted segments along the fibril. The crystallite surface chains are considered to be slightly less ordered than the chains within the crystalline regions but not as reactive as those at the surfaces of the distorted crystalline regions. Thus, this concept does not allow for completely disordered regions (i.e., amorphous) as does the fringed-micelle concept. However, both concepts involve regions of less than perfect crystalline order, and these regions are thought to be the primary sites of attack during alkaline,[7,11,19] acidic,[18,22,30-35] and enzymatic degradation.[34-36] The inherent ability of a particular medium to penetrate and swell the elementary fibril[17] and the size of the reactant molecule[34,35] also reportedly influence the extent of attack on the cellulose molecules. Either concept would adequately explain these observations, but the distorted crystalline regions would be expected to react at slower rates than the amorphous regions of a fringed-micelle structure.

The folded-chain concept[37] is another recent development in the ongoing effort to elucidate the details of cellulose physical structure. Cellulose molecules are thought to be arranged in regular folds forming a flat ribbon with a width of 8 monomer units. Secondary folding of this structure causes the cellulose molecules to be oriented parallel to the axis of the protofibril, which is the equivalent of the elementary fibril in the fringed-micelle structure. The folded-chain concept was originally proposed on the basis of electron microscopic observations and later received additional support from methanolysis experiments.[38,39] According to this theory, cellulose is completely crystalline

with the exception of the monomer units at the primary folds of the protofibril. Degradative attack can therefore occur only at the primary folds. Thus, the levelling-off degree of polymerization (DP) obtained during the methanolysis treatment (DP = 8) was said to equal the primary fold length.

Ahmed and Rapson[40] recognized that the orientation of cellulose molecules in the fringed-micelle structure could not account for the marked shrinkage of cotton fibers when placed in 16% sodium hydroxide (mercerization).[41] In addition, their observation that cellulose hydroxyl accessibility decreased during extensive acid hydrolysis was thought to be inconsistent with the folded-chain concept. Since the folded-chain accounts for the shrinkage phenomenon and the existence of less ordered (more accessible) regions explains the decrease in accessibility, they postulated a folded- or helical-chain structure with intermittent regions of disorder.

However, the basic concept of a folded-chain structure has been criticized for several reasons.[20] Although the structure is considered to be at least partially crystalline, the relatively small size of the crystallites makes it difficult to rationalize the existence of discrete x-ray interferences. This objection arises from the fact that relatively small crystalline domains are presumably not detectable in x-ray diffraction patterns.[42] Other objections to the folded-chain concept involve discrepancies in the modulus of elasticity, density, and appearance of the basic structural unit.[43]

Studies involving Raman and solid-state carbon-13 nuclear magnetic resonance (^{13}C-NMR) spectroscopy, in conjunction with x-ray diffractometry, have provided a great deal of new information regarding the molecular conformation and crystalline packing of cellulose chains.[44-46] The two polymorphs of

primary interest are cellulose I, usually thought of as the native form, and cellulose II, which is produced by mercerization or regeneration of native fibers. Historically, the primary difference between polymorphic forms was thought to be the difference in lattice packing. However, recent results indicate that the two structural forms have different conformations of the basic anhydrocellobiose repeating units and as a result, exhibit distinct crystalline lattices.[44-46] In addition, the ^{13}C-NMR difference spectrum for cotton linters, before and after extensive acid hydrolysis, was similar to the spectrum for an amorphous sample (ball-milled Whatman CF-1), thus indicating that regions of three-dimensional disorder do exist in cellulose and were removed during the hydrolytic treatment.[46]

Since conformational differences can account for the contraction of the unit cell in the chain direction upon conversion of cellulose I to cellulose II,[44,45] a folded-chain structure is not required to explain the associated fiber shrinkage. Furthermore, it is unclear whether the regions of three-dimensional disorder removed during acid hydrolysis were completely amorphous or imperfect crystalline regions.[46] Although the results of those studies do not eliminate the possibility that the folded-chain concept is valid, they do provide support for the existence of regions of three-dimensional disorder, consistent with both the fringed-micelle structure and a crystalline fibril with distorted crystalline regions. Thus, all of these concepts are considered as possible morphological models in the interpretation of the results of the present study, despite the fact that a previous alkaline degradation study did support the fringed-micelle structure.[7]

ALKALINE REACTIONS OF CELLULOSE

During alkaline pulping, cellulose undergoes several processes, including alkaline swelling, dissolution of low DP molecules, random cleavage of glycosidic linkages, stepwise elimination of monomer units from the reducing end ("peeling"), and rearrangement of the reducing end group to make it stable to peeling ("chemical stopping").[1,2] In addition, an inaccessibility mechanism ("physical stopping") for peeling termination has been postulated.[7,11,19]

Diffusion of the alkaline pulping liquor into cellulose fibers results in the solvation of significant numbers of the hydroxyl groups, thereby causing the fibers to swell.[2] The alkali concentration in a typical kraft cook is ca. 4% sodium hydroxide,[2] and the degree of swelling of wood and cotton fibers does not change significantly in the range of 0-10% sodium hydroxide.[47] Since higher concentrations (ca. > 10% sodium hydroxide) are required to disrupt a significant portion of the cellulose I crystalline regions,[48] it follows that swelling during an alkaline cook is essentially limited to the highly accessible (i.e., disordered) regions of the fiber. If a cellulose chain is accessible over its entire length and its DP is sufficiently low (ca. DP < 10), the molecule may be brought into solution.[2] In addition, both swelling and dissolution are influenced by changes in physical structure and molecular size, resulting from alkaline degradation.

The peeling reaction is primarily responsible for cellulose yield losses during alkaline pulping.[1,2,49] Since the reaction proceeds rapidly even at relatively low temperatures (< 100°C), most of the readily degradable carbohydrate material is lost during the heat-up period of the cook.[4,9] The diagram in Fig. 2 illustrates the mechanism for peeling. In general, the

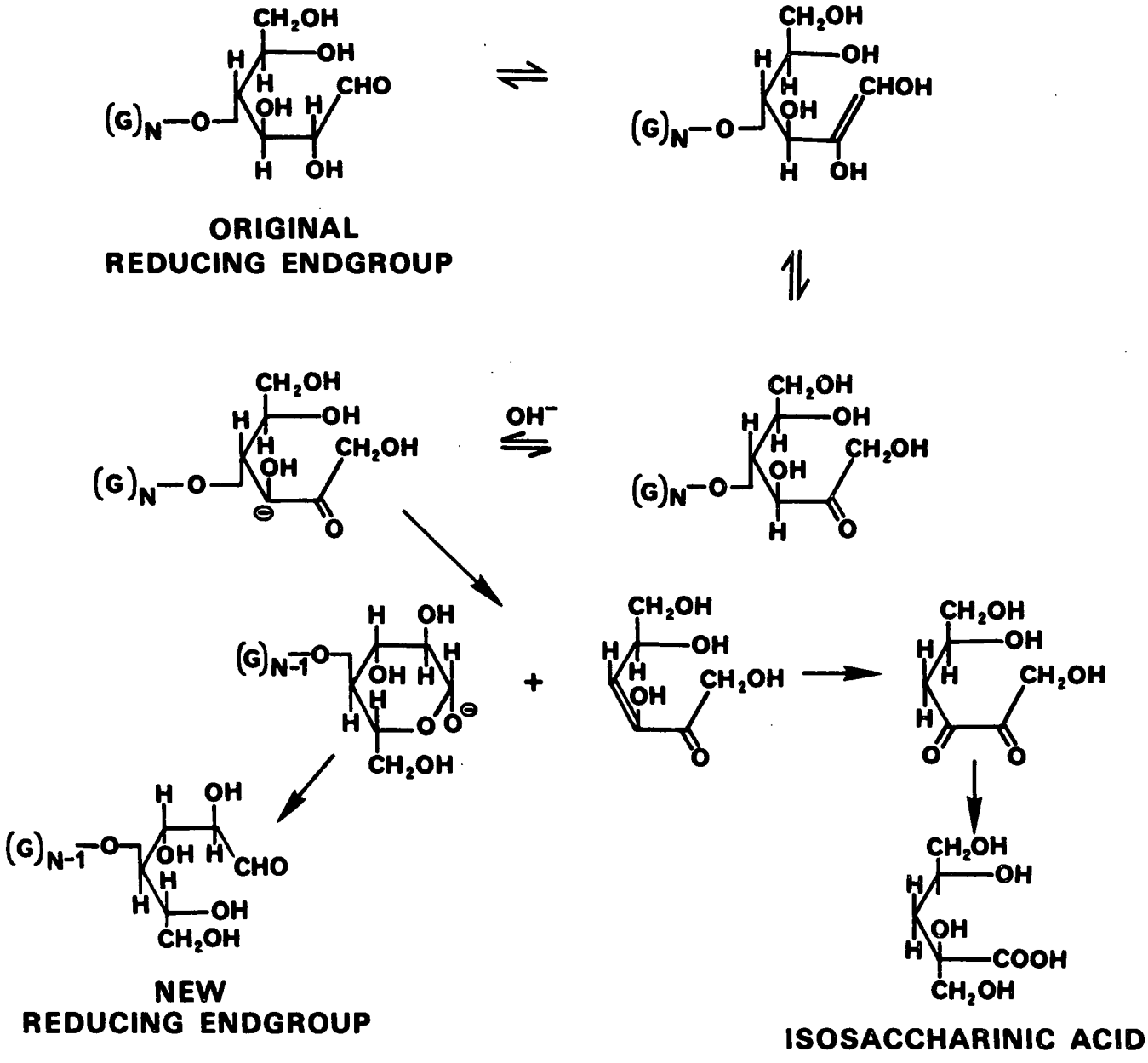

Figure 2. The peeling reaction.[50]

reaction involves isomerization of the aldose end unit (reducing end group) to a ketose, followed by elimination of the rest of the chain, and rearrangement of the original end unit to an isosaccharinic acid.[50] As a result, a new reducing end group is formed, and peeling continues in a stepwise fashion until the reducing end group is stabilized or the entire chain is depolymerized.

The cellulose molecule is rendered stable to peeling by a competing mechanism, referred to as chemical stopping.[1,2,49] In this reaction, the aldose end unit does not isomerize but instead undergoes elimination of the C-3 hydroxyl group and subsequent rearrangement to form a metasaccharinic acid end group (Fig. 3).[51] Although this appears to be the dominant acidic end group, significant quantities of alkali-stable, 2-C-methylglyceric acid end units have also been found.[8,52] The proposed mechanism for the formation of 2-C-methylglyceric acid end groups is shown in Fig. 4.[52] Regardless of the specific type of acidic end group formed, chemical stopping typically occurs at a much slower rate than peeling. As a result, many monomer units are peeled-off before a reducing end group is stabilized.

The ratio of the rates of peeling and chemical stopping, often referred to as the average degradable chain length, is influenced to a great extent by the alkaline reaction conditions[7,11,53] and the physical structure of the cellulose substrate.[10,19,54,55]

At temperatures ranging from 65 to 132°C, the degradable chain length was reported to decrease from 1000 to 140 monomer units.[7] Replacing the sodium hydroxide with calcium, strontium, or barium hydroxide has also been reported to drastically reduce the degradable chain length.[11] Furthermore, increasing the alkali concentration up to ca. 2M sodium hydroxide caused no significant change

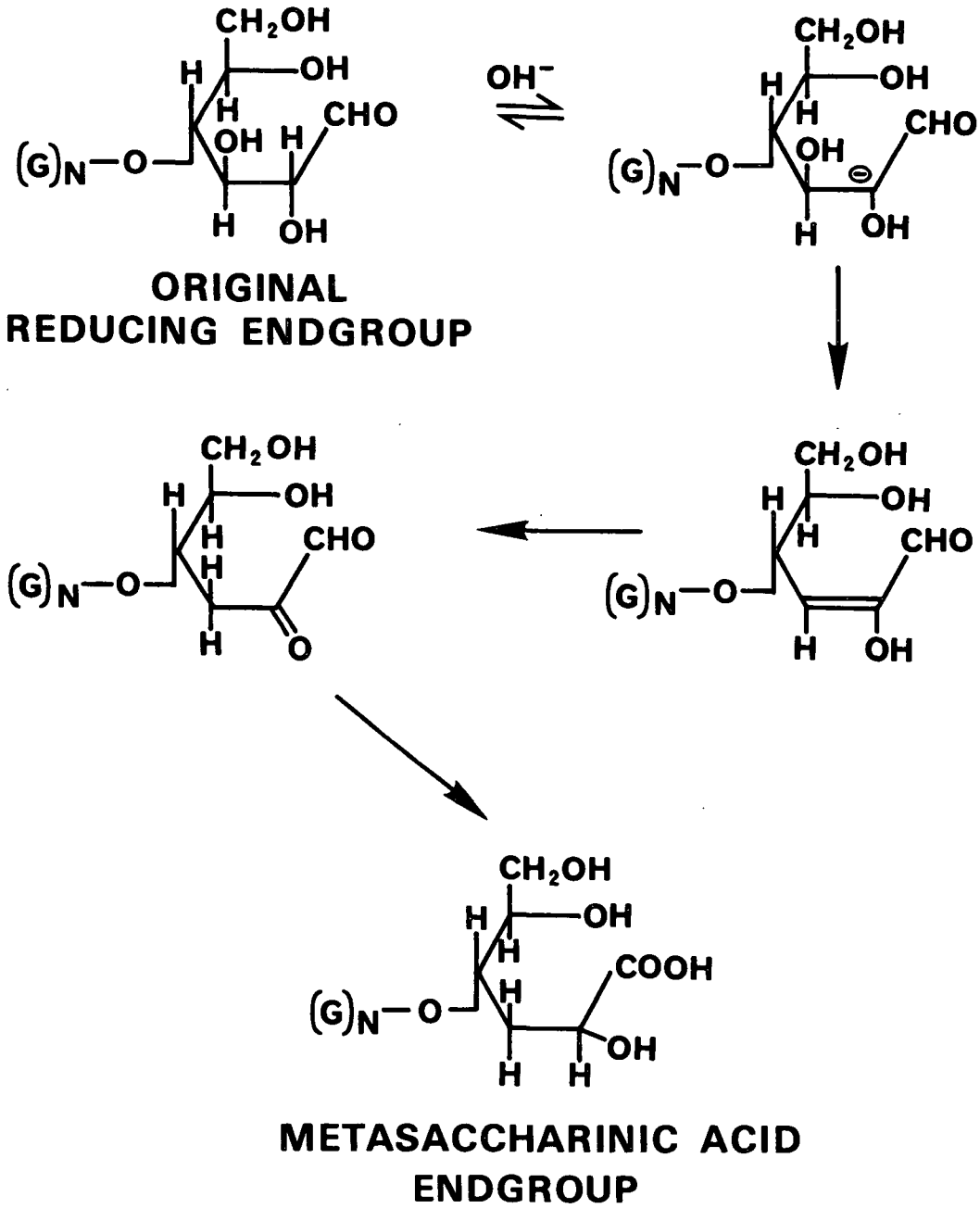

Figure 3. Chemical stopping reaction involving formation of metasaccharinic acid end group.[51]

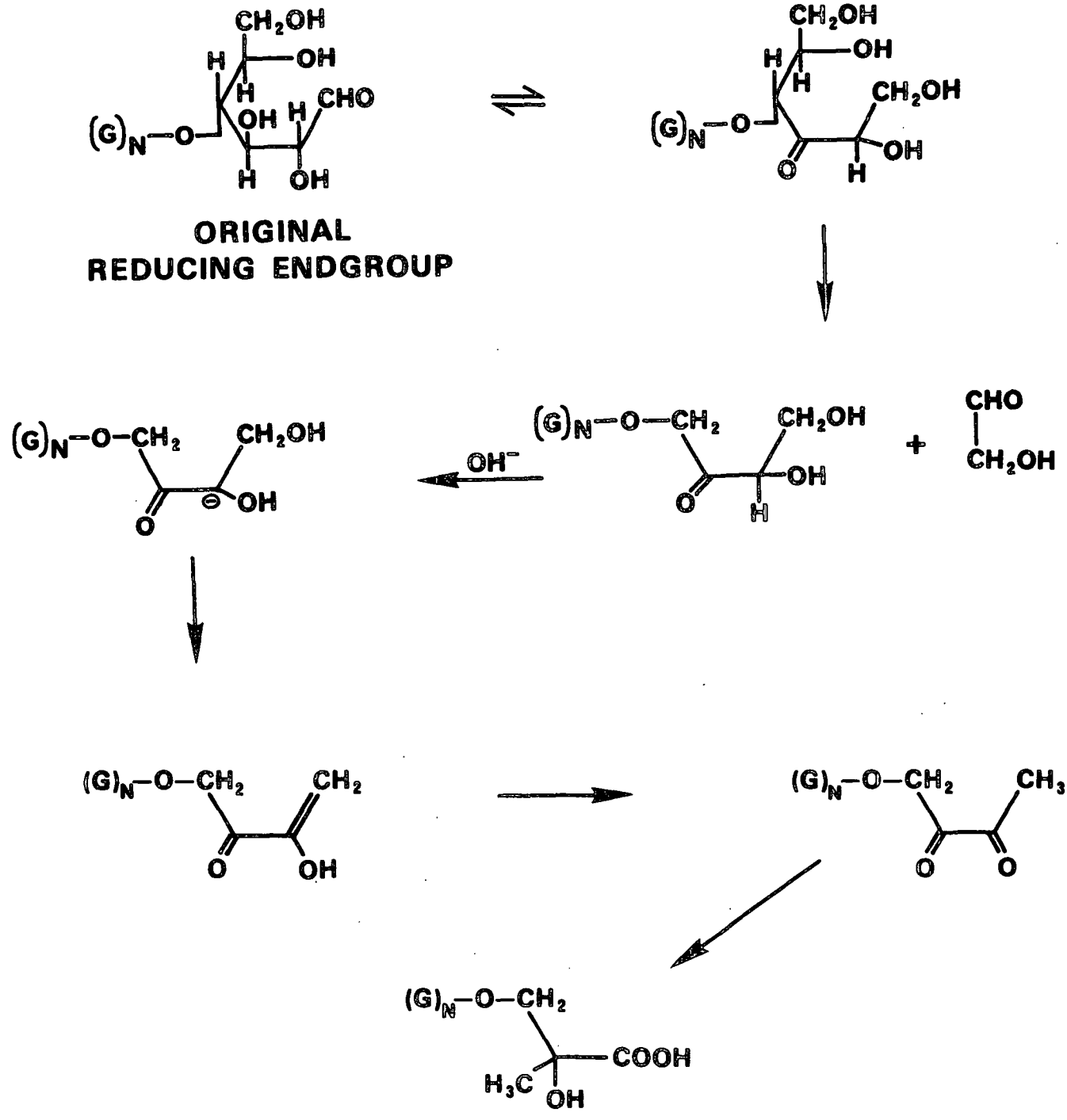

Figure 4. Chemical stopping reaction involving formation of 2-C-methylglyceric acid end group.[52]

in the average degradable chain length, while the value was substantially decreased over the range of 4.3 to 18.6M sodium hydroxide.[53] Since the cellulose structure was considered completely swollen at the higher concentrations, it was concluded that chemical stopping was enhanced by increasing the alkali concentration within that range.

Other studies have shown that the degradable chain length for mercerized cellulose is less than for native cellulose.[10,19,54,55] Although the effect is not clearly understood, it appears that chemical stopping is preferred in a cellulose II versus a cellulose I structure. However, it is also possible that the two polymorphs form different relative amounts of metasaccharinic acid (Fig. 3) and 2-C-methylglyceric acid (Fig. 4) end groups. This could be due to differences in the ability of the two mechanisms to operate in the different structural environments.

During the high temperature (> 150°) portion of an alkaline cook, cellulose also undergoes random cleavage of glycosidic linkages.[1,2,49] If severe enough, this type of degradation can cause a deterioration in pulp strength by lowering the cellulose DP. In addition, it also generates new reducing end groups which can undergo secondary peeling and chemical stopping.[56] However, even at high temperature, the random chain cleavage reaction occurs at a much slower rate than the endwise degradation and stabilization reactions.

The mechanisms for random chain cleavage in cellulose have not been firmly established due to the simultaneous occurrence of the other alkaline reactions and the resultant difficulty in characterizing the entire reaction system. However, Brandon, et al.[12] found that several mechanisms were involved in the alkaline degradation of 1,5-anhydro-cellobiitol (subject to chain

cleavage only). In addition, they suggested that the mechanism(s) for chain cleavage in cellulose depend(s) to some extent upon molecular mobility restrictions imposed by the physical structure. In a separate study it was shown that mercerized cellulose underwent a higher rate of chain cleavage than native cellulose.[10] Glycosidic linkages in cellulose II are presumably less strained than in a cellulose I structure.[44,45] Thus, it is possible that the chain cleavage mechanisms and rates are dictated by the molecular mobility and conformation within a particular cellulose physical structure.

Unfortunately, the manner in which cellulose physical structure influences its ability to undergo alkaline reactions has not been extensively clarified. Haas, et al.[7] have proposed a mechanism for the participation of the physical structure in the peeling reaction. Cotton hydrocellulose was degraded anaerobically with 5% sodium hydroxide at temperatures ranging from 65 to 132°C. Under these conditions, it was assumed that the crystalline (cellulose I) regions were essentially inert toward the reaction medium. Assuming a fringed-micelle structure, reducing end groups at the crystalline-amorphous interfaces were considered to be stabilized toward peeling by their inaccessibility to hydroxide ion ("physical stopping"). In fact, the kinetic analysis showed that physical stopping, and not acidic end group formation, was the dominant stabilization mechanism. The ratios of physical to chemical stopping rates ranged from 13.9 at 65°C to 1.9 at 132°C. However, the kinetic model and analytical methods involved some inherent assumptions that require further clarification.

The most significant of these assumptions were that random chain cleavage was negligible, no cellulose molecules were completely peeled or dissolved, and accessible reducing end group reactivity remained constant throughout the time interval studied.[7] The first assumption is reasonable based on all of the

available information regarding the random chain cleavage reaction. However, the failure to directly measure accessible and inaccessible reducing end groups during degradation makes the last two assumptions questionable. Cellulose chains which might have peeled completely or dissolved were treated as though they were physically stopped. In addition, the latter assumption caused the kinetic model to predict accessible reducing end group contents which were directly proportional to the rate of peeling. Thus, reducing end groups detected in the initial hydrocellulose could only be abruptly stopped, chemically or physically. Since only the chemically stopped end groups were measured and accessible reducing end group contents were dictated by the kinetic model, the balance of the molecules were automatically assumed to have been physically stopped. Furthermore, data presented in Appendix IV indicate that the analytical method used to determine initial accessible reducing end group contents is unreliable. Consequently, the importance of physical stopping relative to peeling and chemical stopping may have been overstated by their results.

In a more recent study of alkaline cellulose degradation, Johansson and Samuelson[8] reported that chemical stopping was the only stabilization mechanism. Acidic and reducing end groups were determined directly, and the net reduction in the total number of end groups was attributed to the loss of entire cellulose chains. However, this involves the inherent assumption that the reducing end group analysis (borohydride reduction/hydrolysis/chromatography) was capable of detecting end groups which were inaccessible to the alkali. Thus, cellulose molecules which may have been physically stopped were assumed to have been completely peeled.

Although neither study[7,8] can conclusively confirm or deny the existence of physical stopping, it was felt that the concept was reasonable and therefore warranted further investigation. Consequently, this study was designed to directly test its validity and to furnish additional information regarding the effect of cellulose physical structure on the rates of peeling, chemical stopping, and random chain cleavage.

THESIS OBJECTIVE

Cellulose is known to undergo random chain cleavage, peeling, and chemical stopping in oxygen-free alkaline media. The mechanisms of these reactions have been studied extensively using alkali-soluble cellulose models. In general, reaction paths derived from model experiments are consistent with the results obtained in experiments with cellulose fibers (native and mercerized cotton). However, native (cellulose I) and mercerized (cellulose II) cellulose reportedly exhibit different reactivities toward the alkaline reactions. In addition, physical stopping of peeling by crystalline domains is thought to be a major peeling stabilization mechanism.

Assessment of the role of physical structure in the alkaline reactions of cellulose fibers is made difficult by the fact that the inherent reactivity of the cellulose molecule and the effects of physical structure on reactivity are essentially inseparable. Alkali-soluble cellulose models either lack a polymeric structure or differ from cellulose in some aspect of their molecular structure. Therefore, differences in reactivity between such models and cellulose fibers would not necessarily be due to physical structure effects alone.

The objectives of this study were to determine how cellulose physical structure affects the alkaline reaction rates of the cellulose molecule and to evaluate the validity of the concept of physical stopping. A fibrous hydrocellulose and an amorphous hydrocellulose with similar molecular structures were selected as the substrates. The fibrous hydrocellulose has a highly ordered physical structure, and the amorphous hydrocellulose has a completely disordered (i.e., noncrystalline) physical structure. Thus, differences in reactivity between the two substrates can be attributed to differences in their physical structures.

RESULTS AND DISCUSSION

EXPERIMENTAL APPROACH

This thesis is a comparative study of the alkaline degradations of fibrous and amorphous hydrocelluloses in 1.0M sodium hydroxide at 60 and 80°C. The fibrous hydrocellulose is predominantly crystalline (cellulose I). Therefore, physical structure would be expected to play a major role in its alkaline reactions. In contrast, the amorphous hydrocellulose is noncrystalline. Consequently, the amorphous substrate would be expected to undergo alkaline reactions without the substantial interference which is believed to result from a highly ordered physical structure.

The peeling reaction was characterized by losses in cellulose yield. Formation of carboxylic acid end groups gave the measure of chemical stopping. The reactive species for these reactions (accessible reducing end groups) were determined directly on the cellulose samples. By converting portions of the samples to completely accessible forms (i.e., regenerating from DMSO-PF solutions), detection of total reducing end groups, including accessible and inaccessible (physically stopped) species, was facilitated. In addition, random chain cleavage was characterized by changes in total end group content (acidic and total reducing end groups).

The physical structures of the fibrous and amorphous hydrocelluloses were characterized during the degradations. Thus, changes in the hydrocellulose physical structures and differences in the physical structures of the two substrates could be used to assess the effects of physical structure on the alkaline reactions.

CELLULOSE SUBSTRATES

Cotton fibers were selected as the source of cellulose because they are a relatively pure form of cellulose and, hence, the purification treatment is simpler than for wood fibers.[57] Consequently, the cellulose molecular structure is less subject to modification during purification, and the resulting fibers contain minimal amounts of impurities in comparison to purified wood fibers (i.e., holocellulose).[58,59]

Alkaline degradations were conducted at relatively low temperatures (60 and 80°C) to facilitate the study of peeling and stopping reactions. However, many of the cellulose reducing end groups were converted to acidic end groups during the alkaline purification. In order to ensure the presence of sufficient reducing end groups to study peeling and stopping, the purified cotton fibers were first subjected to a mild acid hydrolysis. The fibrous hydrocellulose was then freeze-dried to minimize drying stresses which are known to drastically influence cellulose reactivity.[35]

Amorphous* hydrocellulose was prepared from the fibrous hydrocellulose for the purpose of comparing the alkaline reactivity of the amorphous and fibrous substrates. To prepare the amorphous hydrocellulose, fibrous hydrocellulose was first dissolved in the dimethylsulfoxide-paraformaldehyde (DMSO-PF) solvent.[60,61] This solvent system dissolves the cellulose through formation of the methylol derivative. The hydrocellulose was then regenerated from its methylol derivative under anhydrous conditions, thoroughly washed to remove impurities, and freeze-dried. The degree of methylol substitution of the regenerated hydrocellulose

*The term amorphous refers to the lack of crystallinity or three-dimensional order in cellulose and does not imply a completely random structure as may be possible with other polymers.

was ca. 0.006, which corresponds to approximately one methylol group per cellulose molecule. Thus, the regeneration was essentially complete. In addition, the ash contents of the fibrous and regenerated hydrocelluloses were ca. 0.02%, indicating that additional inorganic contaminants were not introduced into the regenerated hydrocellulose. The fibrous and regenerated hydrocelluloses were then characterized as to physical structures, end group compositions, and number-average degrees of polymerization ($\overline{DP}_n$).

Cellulose hydroxyl accessibility was measured as the percentage of hydroxyl groups deuterated in liquid deuterium oxide. This technique provides a practical measure of the fraction of cellulose molecules accessible to the alkaline degradation medium. The accessibility values obtained for the fibrous and regenerated hydrocelluloses were 51.4 ± 0.8% and 99.2 ± 1.0%, respectively. The accessibility of the fibrous hydrocellulose is greater than its disordered fraction, since the hydroxylic protons of both the disordered regions and the crystalline surfaces are exchanged.[42,62] The regenerated hydrocellulose which is completely accessible must not contain any crystalline domains which would have been inaccessible to the deuterium oxide.

X-ray diffraction was used to assess the crystalline characteristics of the hydrocelluloses. X-ray diffractograms of the fibrous and regenerated hydrocelluloses, and a ball-milled Whatman CF-1 cellulose (amorphous standard)[44-46] are shown in Fig. 5. The diffractogram of the fibrous sample contains well-defined reflectances of the 002, $10\overline{1}$, and 101 planes of the cellulose I crystalline lattice, indicating a relatively high degree of cellulose I crystallinity.[42,62] In contrast, the regenerated hydrocellulose exhibits a diffuse scattering pattern similar to that obtained for the ball-milled cellulose, and characteristic of amorphous or noncrystalline cellulose.[63]

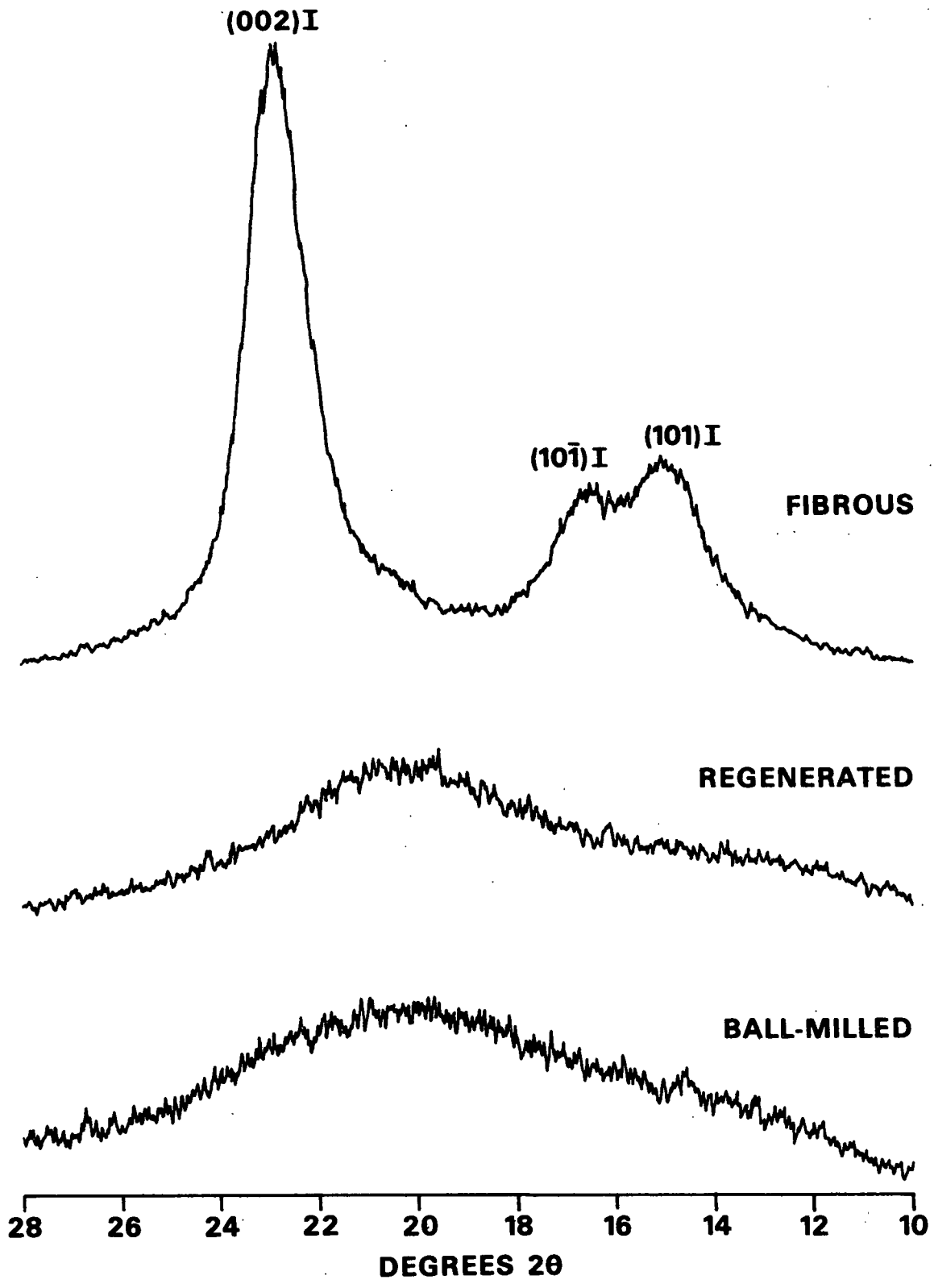

Figure 5. X-ray diffractograms of fibrous hydrocellulose, regenerated hydrocellulose, and ball-milled Whatman CF-1 cellulose.

The molecular conformations associated with the different cellulose crystalline lattices produce distinct signals in Raman[44,45] and solid-state ^{13}C-NMR[46,63] spectra. The solid-state ^{13}C-NMR resonances and the low frequency (250-650 cm^{-1}) Raman bands characteristic of particular cellulose polymorphs (i.e., cellulose I and II) become more intense as the ratio of crystalline to amorphous components increases. Therefore, both spectral methods were utilized to further characterize the physical structures of the hydrocellulose substrates.

Raman spectra of the fibrous, regenerated, and ball-milled samples are shown in Fig. 6. The fibrous hydrocellulose spectrum has relatively intense cellulose I bands, indicating that the molecules are predominantly in the cellulose I conformation. This is best illustrated by the intense signal at 378 cm^{-1}. In contrast, the Raman spectra of the regenerated and ball-milled samples exhibit broad bands indicative of irregular sequences of conformations along the cellulose chains.[45]

The solid-state ^{13}C-NMR spectra of the fibrous, regenerated, and ball-milled samples are shown in Fig. 7. The spectrum of the fibrous hydrocellulose contains a set of sharp resonances indicative of the cellulose I polymorph.[46,64] In addition, the broader resonances appearing slightly upfield of the sharper C-4 and C-6 resonances are thought to be the C-4 and C-6 resonances associated with three-dimensional regions of disorder and crystallite surfaces. The analogous components of the C-1 and C-2,3,5 resonances are overlapped by the corresponding sharper resonances and are therefore not evident in the spectrum. However, the sharper C-4 and C-6 resonances are more intense than the corresponding broader resonances, indicating a relatively high content of the cellulose I polymorph. In contrast, the regenerated and ball-milled spectra

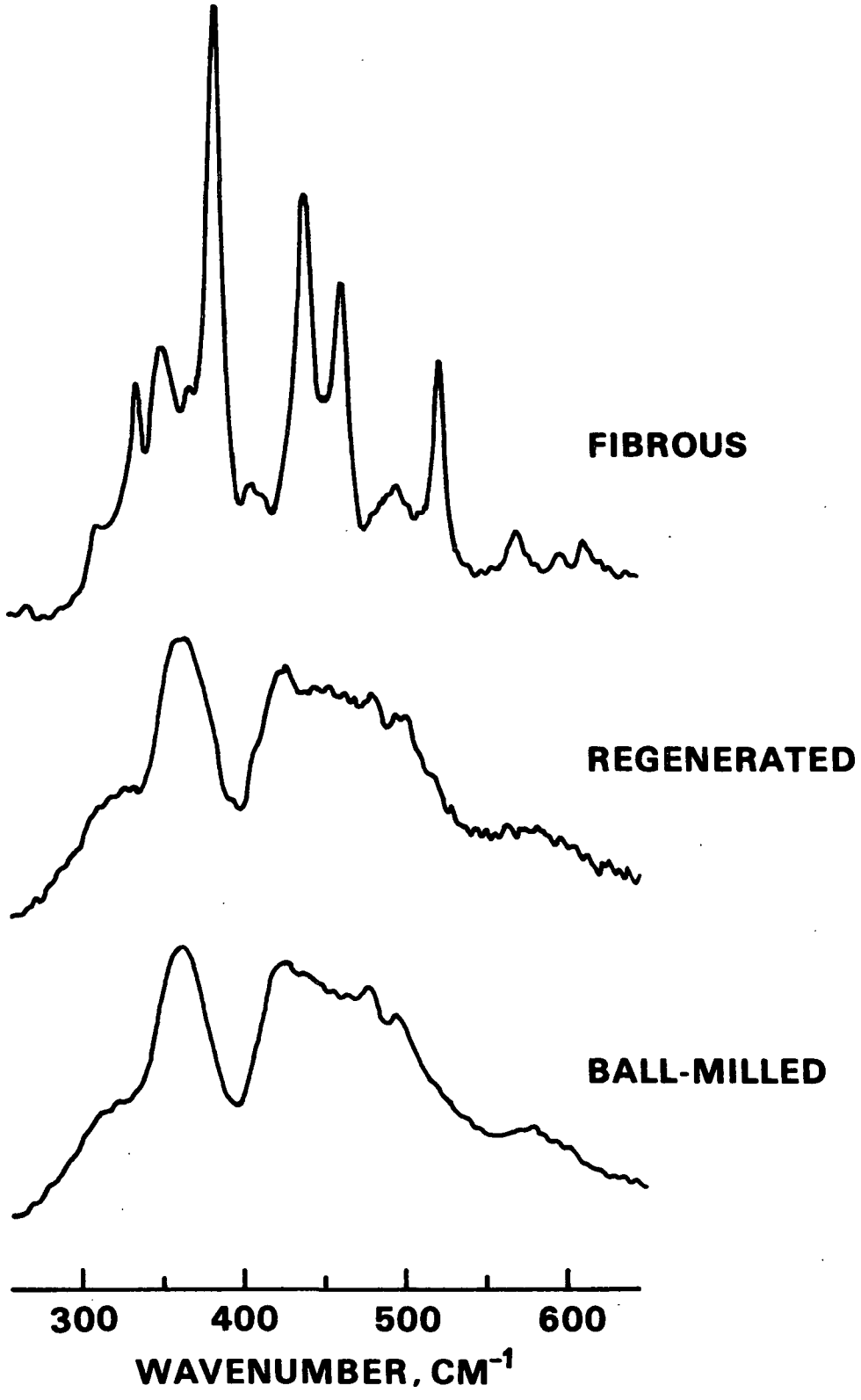

Figure 6. Raman spectra of fibrous hydrocellulose, regenerated hydrocellulose, and ball-milled Whatman CF-1 cellulose.

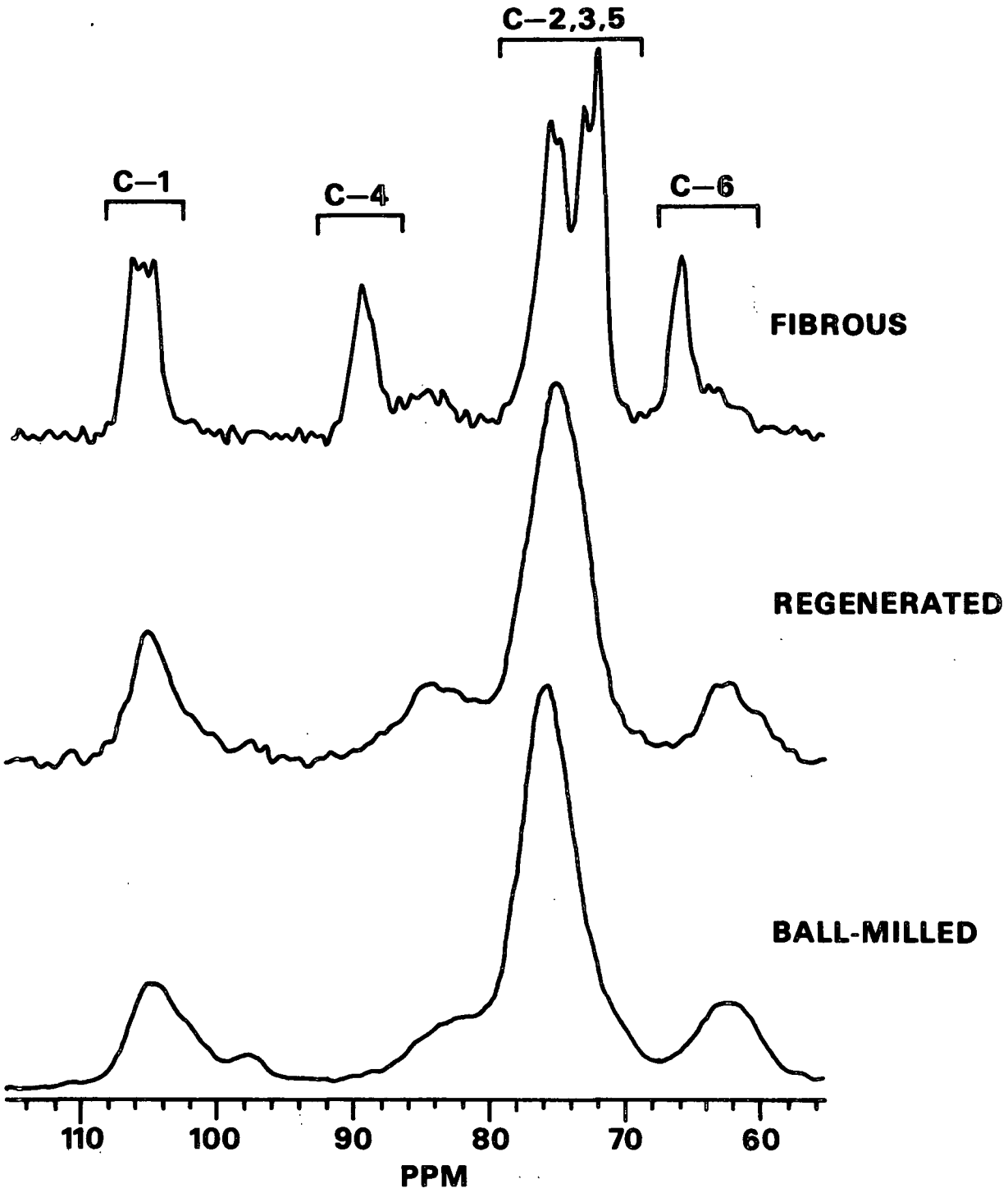

Figure 7. Solid-state ^{13}C-NMR spectra of fibrous hydrocellulose, regenerated hydrocellulose, and ball-milled Whatman CF-1 cellulose.

exhibit only broadened C-4 and C-6 resonances, and the C-1 and C-2,3,5 multiplets are not resolved. This observation reinforces the finding of no significant structural order (i.e., crystallinity) in the regenerated and ball-milled celluloses by x-ray diffraction and Raman spectroscopy.

In summary, the fibrous hydrocellulose consists predominantly of cellulose I as shown by x-ray diffraction, and Raman and solid-state ^{13}C-NMR spectroscopy. The cellulose I crystalline regions comprise the inaccessible fraction, and the accessible fraction is apparently composed of disordered regions and cellulose I crystallite surfaces. In contrast, the regenerated hydrocellulose is amorphous and completely accessible.

The original objective of this study was to compare the alkaline degradations of fibrous and amorphous hydrocelluloses with similar molecular sizes and end group compositions. When small quantities of the fibrous hydrocellulose (ca. 2 g) were regenerated, the end group composition and $\overline{DP}_n$ were not significantly altered. However, when larger quantities of the amorphous hydrocellulose (ca. 20 g) were prepared for kinetic studies, the cellulose underwent some degradation during the scaled-up regeneration process.

Differences in the molecular structures of the fibrous and amorphous substrates are illustrated in Table 1. The lack of a significant change in acidic end groups and the large increase in total reducing end groups are consistent with chain cleavage causing the lower $\overline{DP}_n$ values of the amorphous hydrocellulose. Reducing end groups which were inaccessible in the fibrous hydrocellulose were made accessible by the regeneration process. In addition, the relatively small fraction of inaccessible reducing end groups in the fibrous hydrocellulose suggests that end groups are typically located in or very close

to disordered regions of the structure. This is reasonable because an end group located within a crystalline domain would distort the crystalline lattice, thereby introducing a disordered region into the crystalline domain. The validity of the end group values is supported by the close agreement of the $\overline{DP}_n$ values obtained from the total end group contents and gel permeation chromatography (GPC) of the cellulose carbanilate derivatives.[65] Thus, to demonstrate differences in reactivity of the hydrocelluloses toward the peeling and stopping reactions (due to the dissimilar physical structures), the different reducing end group contents are taken into account (see Peeling and Stopping Reactions).

Table 1. End group and $\overline{DP}_n$ data[a] for hydrocellulose substrates.

	Fibrous Hydrocellulose	Amorphous Hydrocellulose
Acidic end groups[b,c]	1.10 ± 0.08	0.99 ± 0.07
Accessible reducing end groups[b]	1.16 ± 0.06	3.42 ± 0.07
Inaccessible reducing end groups[b]	0.11 ± 0.10	0.02 ± 0.06
Total reducing end groups[b]	1.26 ± 0.06	3.45 ± 0.04
$\overline{DP}_n$ (end groups)[c,d]	422 ± 4	225 ± 3
$\overline{DP}_n$ (GPC)[e]	464 ± 21	249 ± 15

[a]Mean values for three determinations.
[b]End group values expressed as mole fractions of total monomer units x 10^3.
[c]Includes carboxylic acid groups of pectic materials.
[d]$\overline{DP}_n$ = total end groups^{-1}.
[e]$\overline{DP}_n$ determined by GPC analysis of tricarbanilate derivatives.[65]

Both substrates contained pectic materials which were not removed during the purification or regeneration processes. The carboxyl groups of the pectic materials accounted for ca. 25% of the acidic functional groups in the hydrocellulose substrates. Since chemical stopping is characterized by the formation of acidic end groups, and pectic material which contains acidic groups was

removed during the alkaline degradations (see Appendix I), the removal of pectic material was taken into account in the assessment of the chemical stopping reaction.

ALKALINE REACTIONS

General

The fibrous and amorphous hydrocelluloses were degraded in 1.0M sodium hydroxide under anaerobic conditions. The reaction mixtures were heated to 60 or 80°C, maintained at the desired temperature for up to 168 hours, cooled to 20°C, and neutralized with 1M hydrochloric acid. Since the heat-up (ca. 14 min) and cool-down (ca. 3 min) times were significant compared to the shorter reaction periods, zero-time samples of both substrates at 60 and 80°C were prepared by limiting the reaction period to ca. 1 minute. Thus, the degraded samples differed from the zero-time samples only in the duration of the alkaline treatment at the reaction temperature.

The degraded hydrocelluloses were thoroughly washed, and yields were determined after freeze-drying. The samples were then analyzed for acidic end groups, accessible and inaccessible reducing end groups, and hydroxyl accessibility. In addition, x-ray diffractograms, and Raman and solid-state ^{13}C-NMR spectra were acquired for selected samples.

The following discussion of the results obtained in this investigation is divided into three major parts. The first part deals with the characterization of the hydrocellulose physical structures during degradation. Based on the behavior of the physical structures and the alkaline reaction data, possible morphological models for the hydrocellulose substrates are proposed.

In the second part of this section, the peeling and stopping reactions of the hydrocelluloses are discussed. The roles of cellulose physical structure in peeling, chemical stopping, and physical stopping are assessed by kinetic analysis of the reaction data.

Finally, the third part of this section deals with complete peeling and random chain cleavage. Complete peeling is discussed in qualitative terms only. Random chain cleavage results are presented, and a kinetic analysis is used to quantify the results. Possible effects of cellulose physical structure on random chain cleavage are discussed.

Changes in Physical Structure

To assess the effects of the hydrocellulose physical structures on the alkaline reaction rates, morphological changes in the hydrocelluloses were monitored during the alkaline degradations. Hydroxyl accessibility was determined on all degradation samples (Tables 17 and 18, Appendix II). In addition, x-ray diffractograms, and Raman and solid-state ^{13}C-NMR spectra were obtained for selected 80°C reaction samples.

The hydroxyl accessibility of the fibrous hydrocellulose was initially 51.4 ± 0.8%. Exposure of the fibrous substrate to the alkaline medium caused the accessibility to decrease slightly to 50.7 ± 1.0% and 49.1 ± 1.2% at 60 and 80°C, respectively, but the accessibilities did not change significantly with time (0-168 hours).

In contrast, the initial hydroxyl accessibility of the amorphous hydrocellulose was 99.2 ± 1.0%. As illustrated in Fig. 8, the accessibility decreased substantially during the alkaline treatments. The accessibilities of the 60 and 80°C zero-time samples were *ca.* 95 and 90%, respectively. Since the

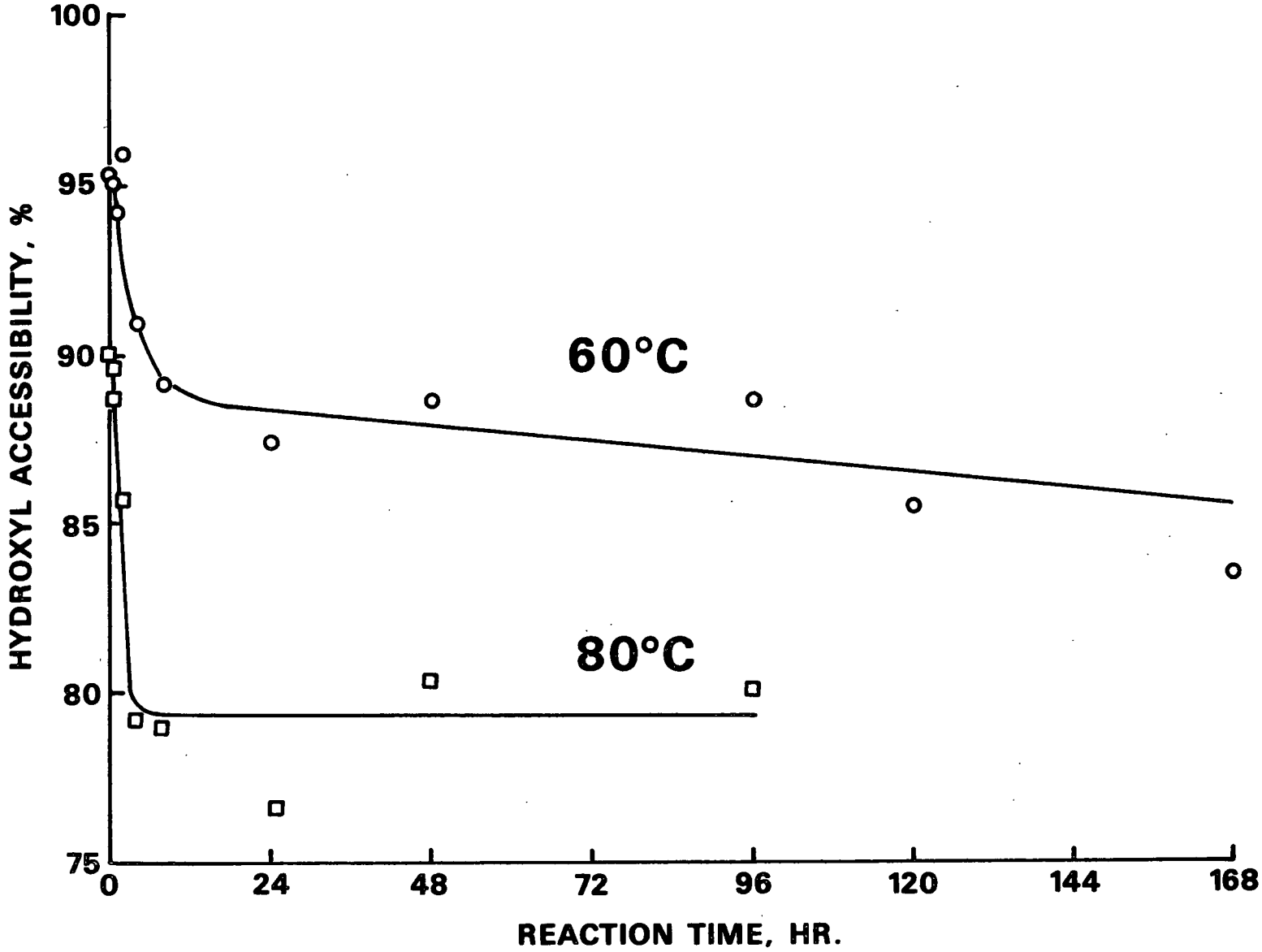

Figure 8. Hydroxyl accessibility of the amorphous hydrocellulose during degradation in 1.0M sodium hydroxide.

initial substrate was completely accessible, partial recrystallization apparently occurred upon exposure of the amorphous hydrocellulose to the alkaline medium. Accessibility decreased throughout the 60°C reaction to ca. 85% at 168 hours, while the accessibility of the 80°C amorphous degradation samples decreased to ca. 80% at 4 hours and remained relatively constant through the remainder of the reaction.

X-ray diffractograms of the initial substrate, zero-time sample, and 48-hour sample for the 80°C degradation of the fibrous hydrocellulose are shown in Fig. 9. All three diffractograms exhibit characteristic 002, $10\bar{1}$, and 101 reflectances of the cellulose I crystalline lattice.[42,62] Although there appears to be a slight increase in peak intensity going from the fibrous substrate to the zero-time sample, no significant differences are observed in the diffractograms of the zero-time and 48-hour degradation samples. Thus, the x-ray diffractograms also indicate no significant changes in the physical structure of the fibrous hydrocellulose during degradation.

X-ray diffractograms of the initial substrate, zero-time sample, and 48-hour sample from degradation of the amorphous hydrocellulose at 80°C are shown in Fig. 10. The diffractogram of the zero-time sample exhibits a set of weak reflectances corresponding to the 002, $10\bar{1}$, and 101 planes of the cellulose II crystalline lattice.[42,62] This indicates that the initial decrease in hydroxyl accessibility was primarily due to the formation of cellulose II crystalline regions. The diffractogram of the 48-hour sample exhibits slightly more intense cellulose II reflectances, indicating a further small increase in the cellulose II fraction during the reaction period. The latter change may be due to selective removal of amorphous material and/or additional recrystallization.

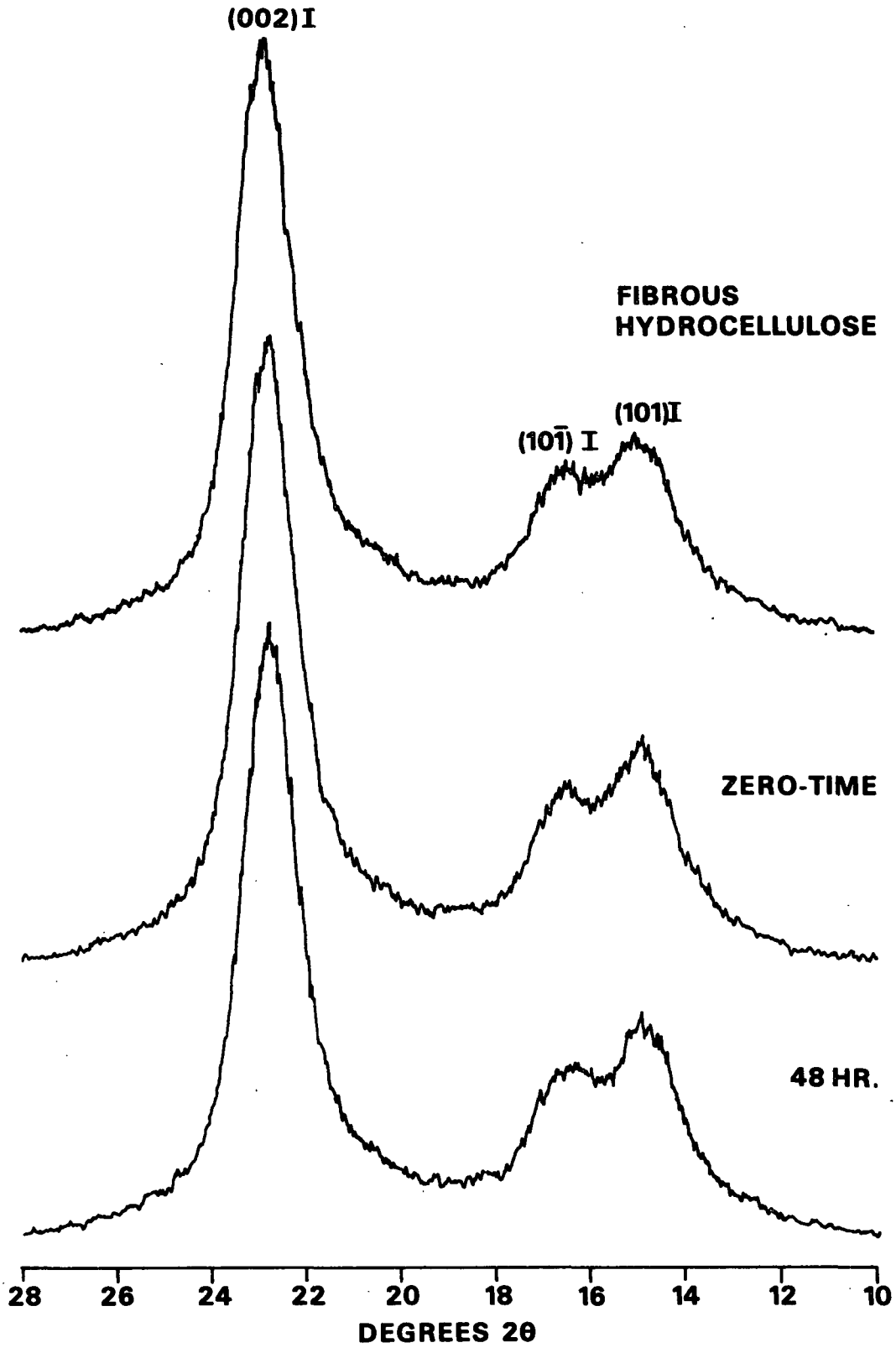

Figure 9. X-ray diffractograms of the fibrous hydrocellulose during degradation in 1.0M sodium hydroxide at 80°C.

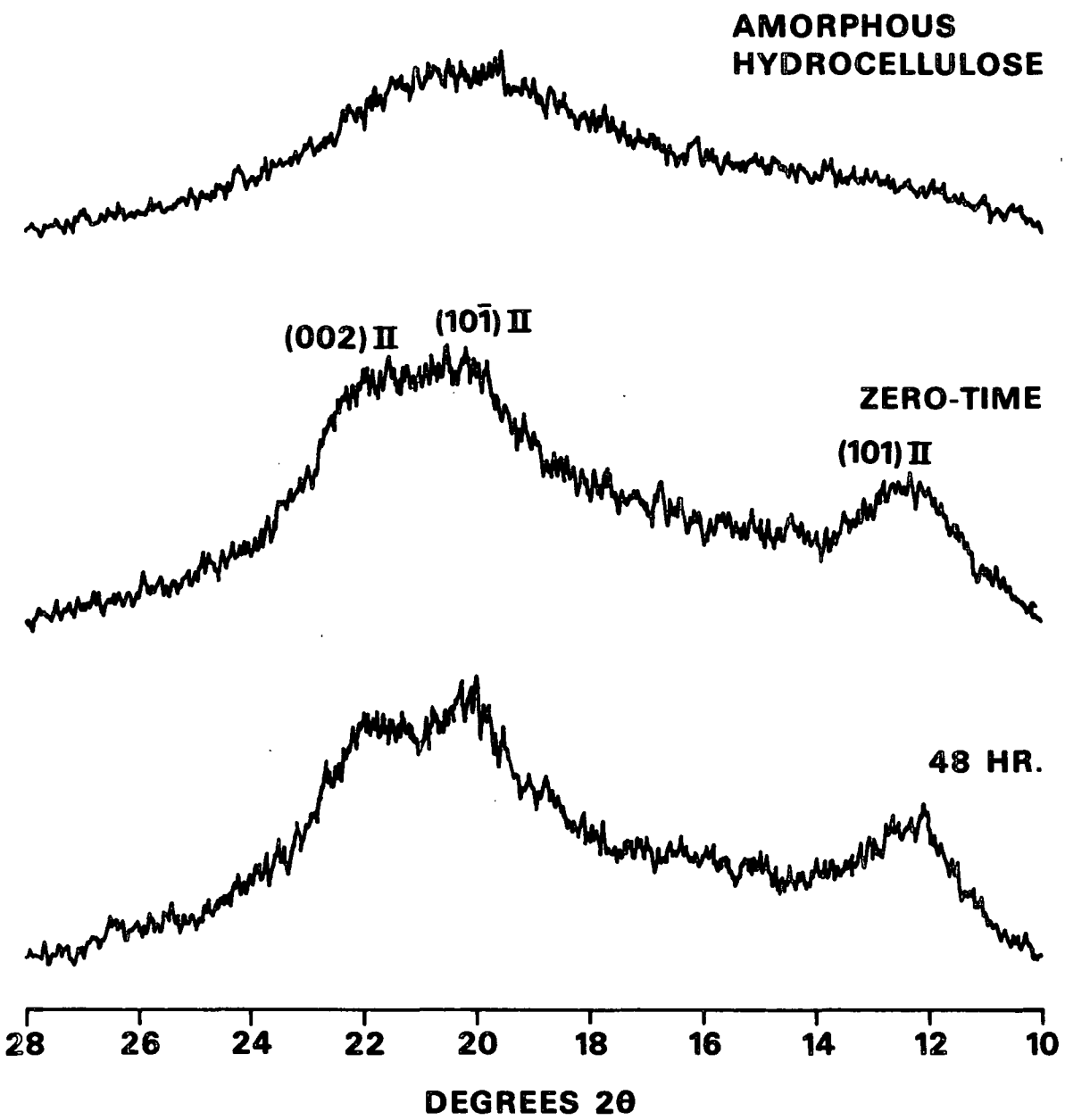

Figure 10. X-ray diffractograms of the amorphous hydrocellulose during degradation in 1.0M sodium hydroxide at 80°C.

Partial Raman spectra of the initial substrate, zero-time sample, and 48-hour sample from the 80°C degradation of the fibrous hydrocellulose are shown in Fig. 11. All three spectra contain characteristic cellulose I bands with similar intensities.[44,45] This is consistent with no significant changes occurring in the physical structure of the fibrous hydrocellulose during alkaline degradation.

Partial Raman spectra of the initial substrate, zero-time sample, and 48-hour sample from degradation of the amorphous hydrocellulose at 80°C are shown in Fig. 12. The intensities of the Raman bands increase significantly going from the initial substrate to the zero-time sample. This effect is best demonstrated by the emergence of the characteristic cellulose II band at 355 cm^{-1}.[44,45] The spectrum of the 48-hour sample exhibits slightly more intense bands than the zero-time sample, thus confirming the slight increase in cellulose II character during the degradation as indicated by x-ray diffraction.

Solid-state ^{13}C-NMR spectra of the initial substrate, zero-time sample, and 48-hour sample from the 80°C degradation of the fibrous hydrocellulose are illustrated in Fig. 13. All three spectra contain the sharp resonances associated with the cellulose I polymorph and the broader C-4 and C-6 resonances indicative of regions of three-dimensional disorder and crystallite surfaces.[46,64] However, the differences between the spectra are small and do not indicate a significant change in the relative amounts of crystalline and disordered material during degradation. This is best demonstrated by the lack of significant differences in the relative intensities of the sharp and broad resonances of C-4 and C-6.

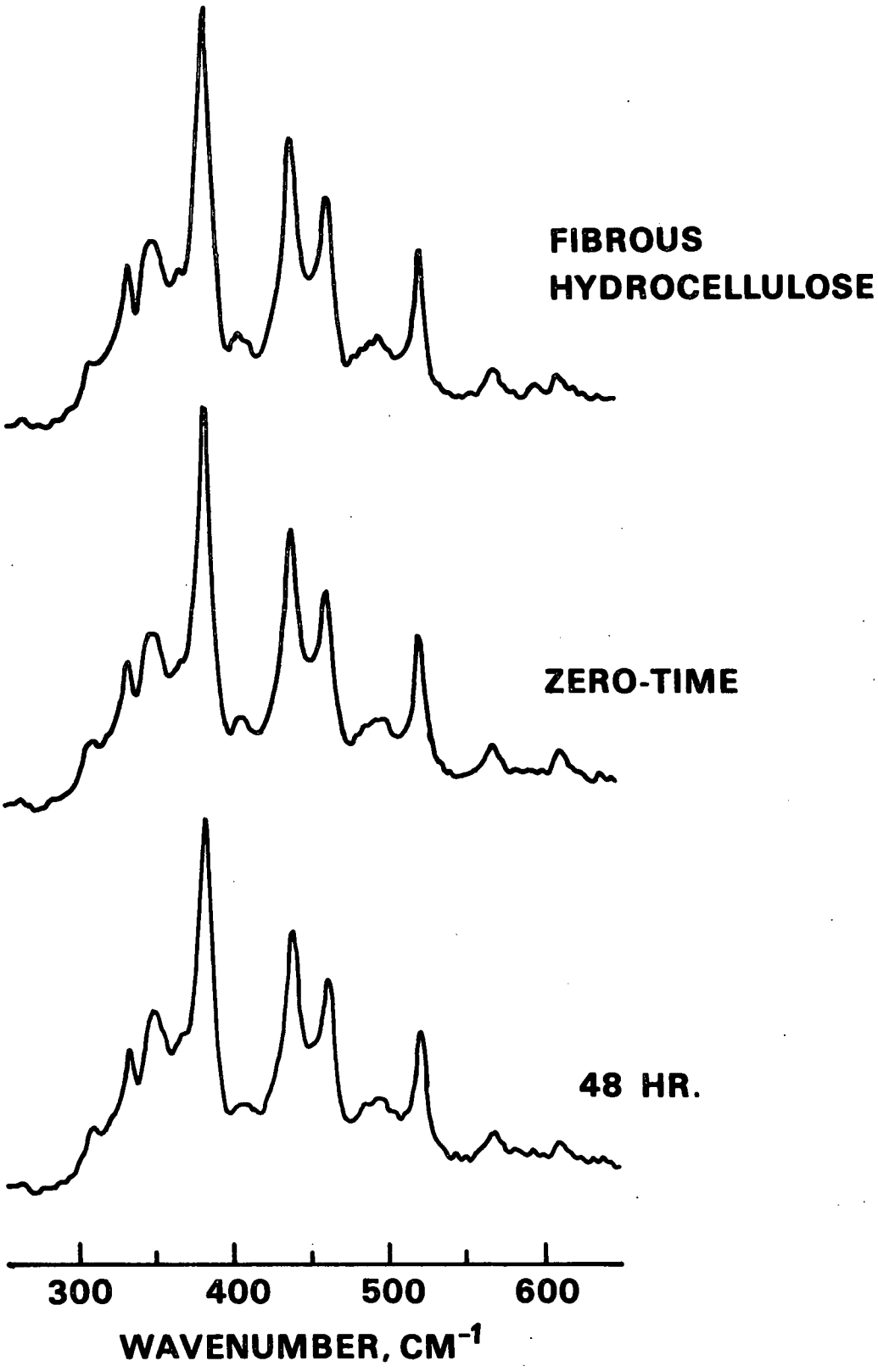

Figure 11. Raman spectra of the fibrous hydrocellulose during degradation in 1.0M sodium hydroxide at 80°C.

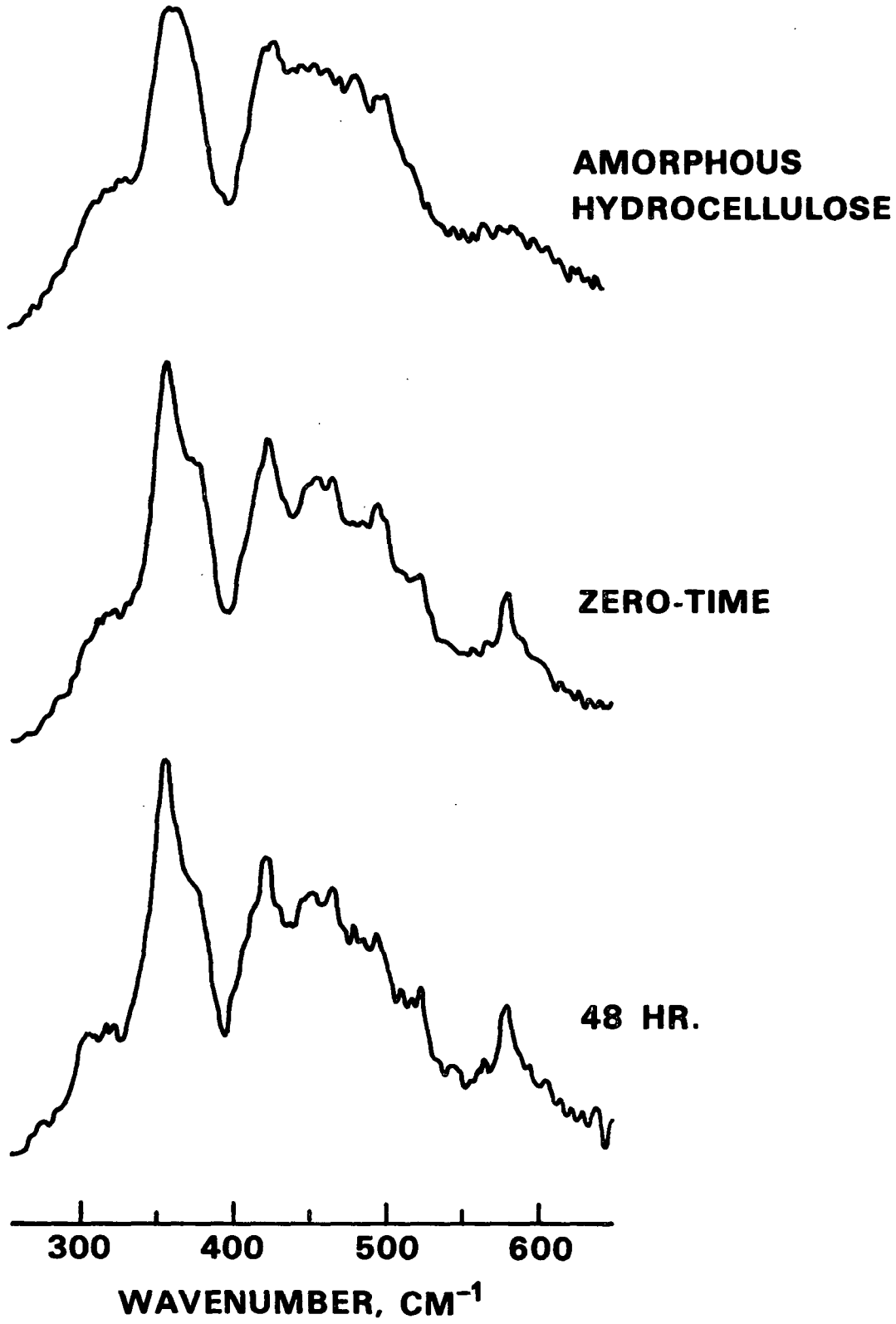

Figure 12. Raman spectra of the amorphous hydrocellulose during degradation in 1.0M sodium hydroxide at 80°C.

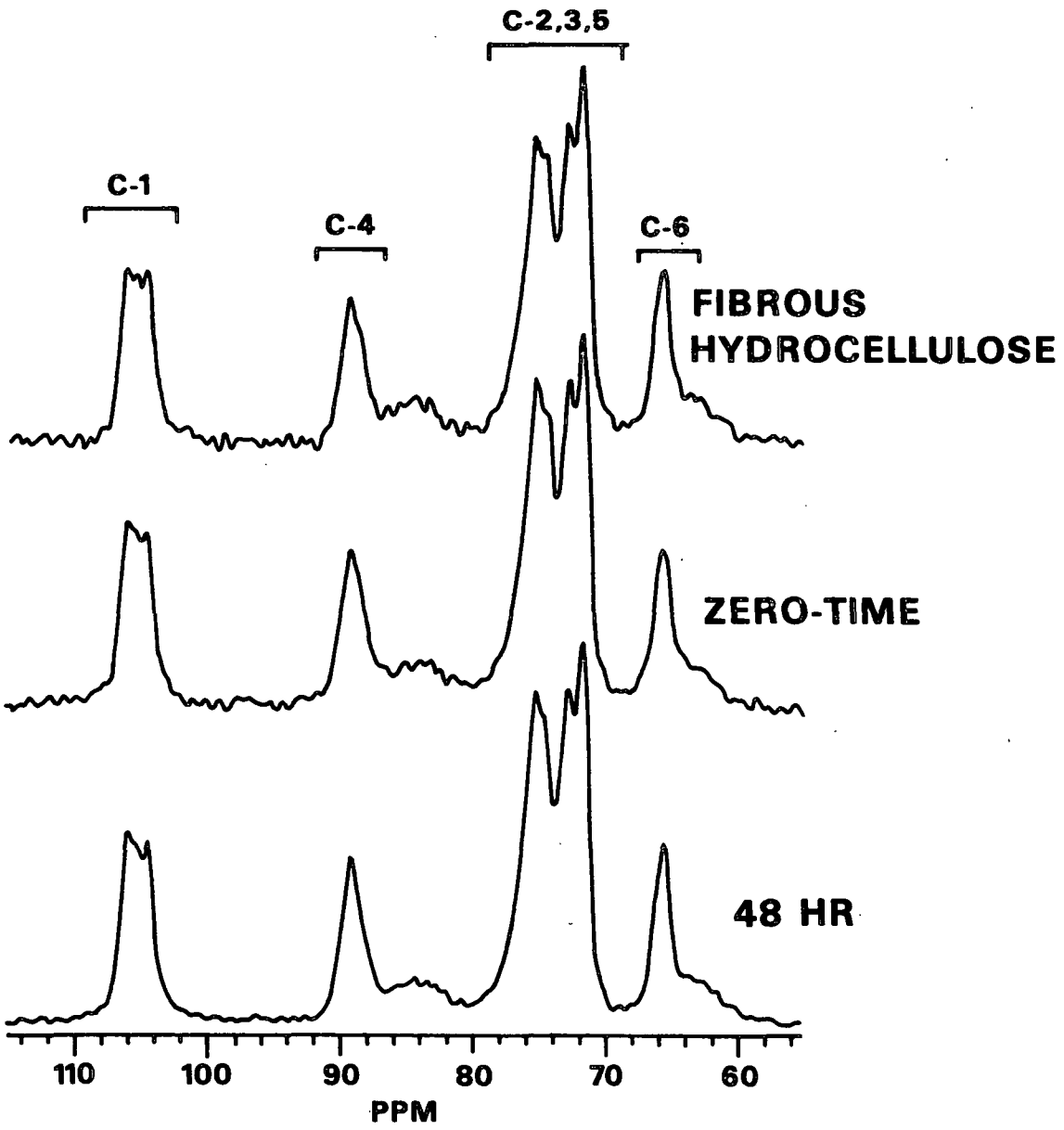

Figure 13. Solid-state ^{13}C-NMR spectra of the fibrous hydrocellulose during degradation in 1.0M sodium hydroxide at 80°C.

Solid-state ^{13}C-NMR spectra of the initial substrate, zero-time sample, and 48-hour sample from degradation of the amorphous hydrocellulose at 80°C are shown in Fig. 14. In comparison to the ^{13}C-NMR spectra of the fibrous samples (Fig. 13), changes in the spectra of the amorphous degradation samples are more substantial. The C-1 resonance for the zero-time sample is more intense than for the initial substrate and is clearly resolved into a doublet for the 48-hour sample. The broad C-4 resonance for the initial substrate decreases in intensity for the zero-time and 48-hour samples, respectively. In addition, a sharper C-4 resonance, not apparent for the initial substrate, appears at *ca.* 88 ppm for the zero-time sample and is further resolved into a doublet for the 48-hour sample. The C-2,3,5 resonance for the initial substrate exhibits shoulders for the zero-time sample and is resolved into a triplet for the 48-hour sample. Finally, the C-6 resonance becomes sharper going from the initial substrate to the zero-time and 48-hour samples, respectively. The resonance frequencies and multiplicities for the zero-time and 48-hour samples are characteristic of the cellulose II polymorph.[46,64] The most striking differences between the spectra of the two polymorphs are that the C-6 resonance is shifted further upfield for cellulose II, and the C-2,3,5 cluster is a triplet for cellulose II as opposed to a quartet for cellulose I. Thus, the significant increase in the cellulose II content of the amorphous hydrocellulose during alkaline degradation indicated by x-ray diffraction and Raman spectroscopy is also indicated by the solid-state ^{13}C-NMR spectra.

In summary, the fibrous hydrocellulose, consisting predominantly of the cellulose I polymorph, exhibited no significant change in the relative amounts of crystalline and disordered material during the reaction periods. The amorphous hydrocellulose, however, underwent partial recrystallization (cellulose II) and possibly selective peeling of amorphous material.

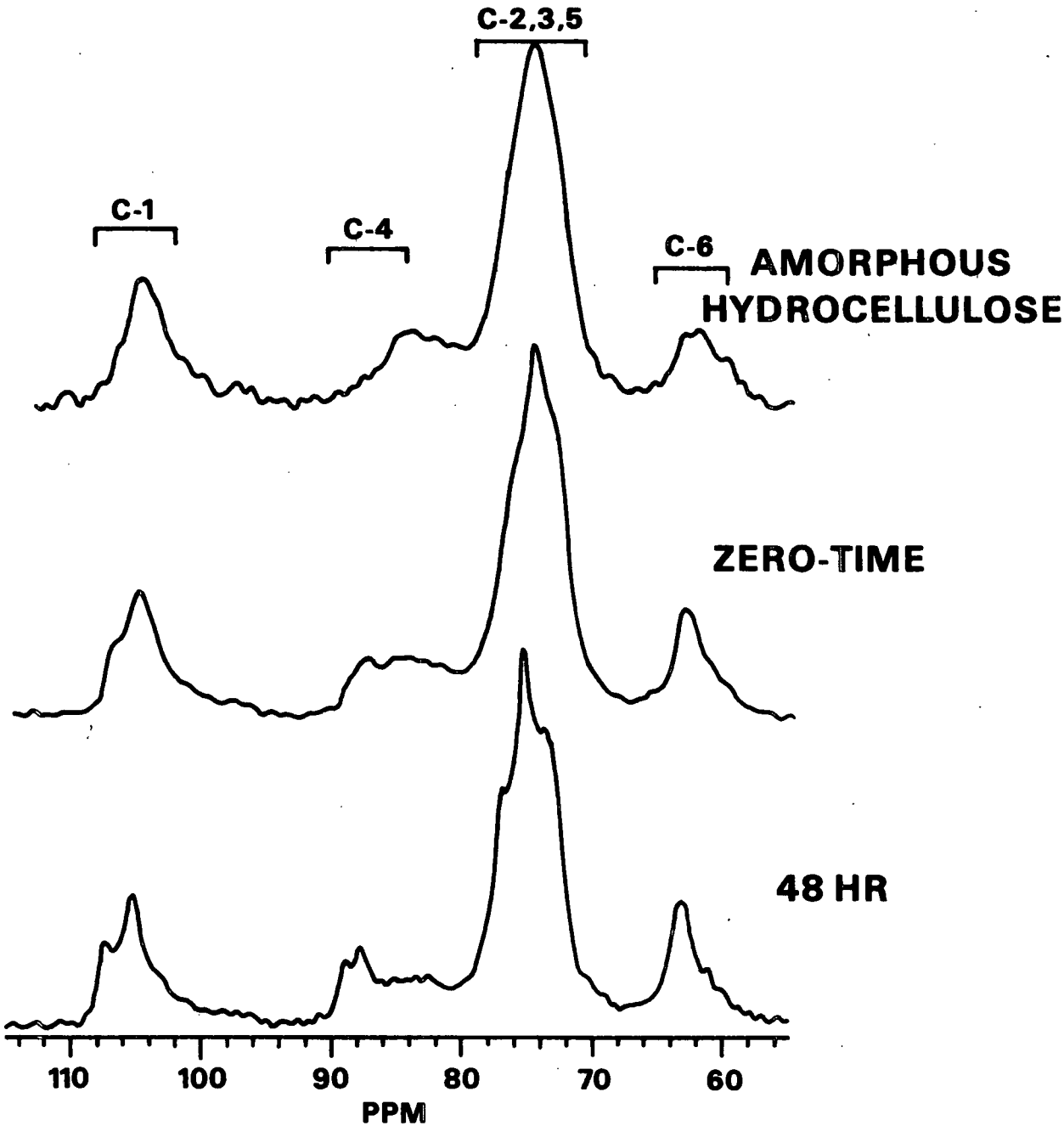

Figure 14. Solid-state ^{13}C-NMR spectra of the amorphous hydrocellulose during degradation in 1.0M sodium hydroxide at 80°C.

Since the alkaline reaction data presented in the following section indicate that the reactivity of the fibrous substrate (toward peeling and chemical stopping) decreased during the reaction periods, it appears that the reactions were occurring in increasingly ordered regions of the structure. Thus, selective peeling in the disordered regions of a fringed-micelle (amorphous domains) or folded chain (primary folds of protofibril) structure should have produced a net decrease in the disordered fraction. Although the maximum yield losses for the fibrous substrate were 7.5 and 9.7% at 60 and 80°C, respectively, it is possible that such losses of disordered material are not detectable by the applied methods. Alternatively, selective removal of amorphous material could have been offset by a comparable amount of decrystallization of cellulose I domains. However, neither explanation is completely consistent with the alkaline reaction data.

The lack of changes in physical structure and the reaction data are consistent with the fibrous hydrocellulose having a crystalline elementary fibril with slightly distorted crystalline domains (Fig. 15). This type of structure had previously been postulated on the basis of changes in the relative accessibilities of C-2, C-3, and C-6 hydroxyl groups during acid hydrolysis.[22,30-32] In its original form, the model included strain distorted, tilt and twist segments along the fibril, but only the surface molecules along those segments were thought to comprise the disordered regions. As depicted in Fig. 15, the distorted crystalline segments are the most disordered at the surface and are increasingly ordered progressing toward the elementary fibril core. This model is more reasonable than the original,[22,30-32] since twisting or bending a rigid rod composed of parallel, thinner rods would be expected to produce a three-dimensional distortion in the structure and not only affect the

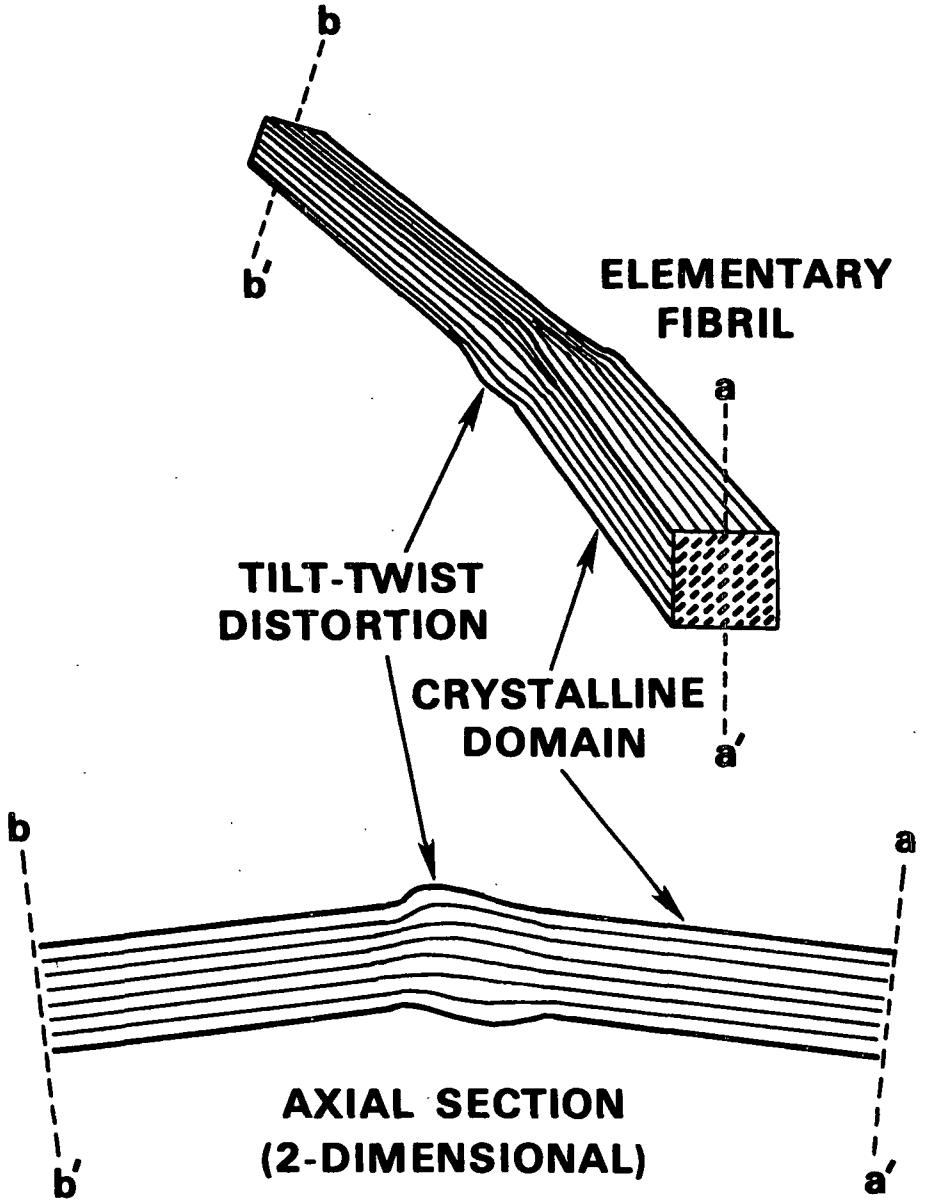

Figure 15. Diagram of crystalline elementary fibril with distorted crystalline region.

surface components. However, since the distortions are not severe enough to completely disrupt the parallel arrangement of cellulose molecules, the molecules would probably display some of the conformational and crystalline properties of cellulose I.

Preferential removal (peeling) of a portion of the molecular segments from the distorted crystalline regions would not cause a significant increase in the cellulose I fraction because the material removed would exhibit both crystalline and disordered characteristics. Peeling of crystallite surface chains would result in the exposure of adjacent molecules, creating a new surface component. In addition, the reported loss of disordered material during extensive acid hydrolysis[46] can be attributed to more substantial losses of distorted crystalline material than occurred in this study under the milder alkaline conditions.

According to this model, disordered regions of the fibrous hydrocellulose would exhibit more structural order than amorphous regions of the amorphous substrate. This is consistent with the fibrous hydrocellulose having lower rates of peeling and chemical stopping than the amorphous hydrocellulose (see Peeling and Stopping Reactions). The occurrence of random chain cleavage only in the amorphous hydrocellulose (see Complete Peeling and Random Chain Cleavage) also supports the existence of less mobile and accessible molecules in the disordered regions of the fibrous hydrocellulose. In addition, physical stopping of ca. 50% of the original degradable molecules (with accessible reducing end groups) in the fibrous hydrocellulose (see Peeling and Stopping Reactions) can be attributed to cessation of peeling as it progresses from the distorted to perfect crystalline domains of this model.

In contrast, both the structural and reaction data for the amorphous hydrocellulose are consistent with the formation of cellulose II crystallites and selective removal of amorphous material. Since the hydroxyl accessibility of the amorphous substrate decreased throughout the 60°C reaction and during the initial period of the 80°C reaction, significant losses of amorphous material must have occurred only during those intervals. This coincides with the periods during which the amorphous hydrocellulose underwent more rapid peeling and chemical stopping, and exhibited the most significant rates of random chain cleavage and physical stopping. Reductions in its reactivity during those periods and particularly in the later period of the 80°C reaction indicate decreases in the amounts of degradable amorphous material. Thus, increasing proportions of the reactions were apparently occurring in the cellulose II domains.

From a structural standpoint, both the cellulose I domains of the fibrous hydrocellulose and the cellulose II domains that formed in the amorphous hydrocellulose are highly resistant to alkaline reactions under the relatively mild alkaline conditions employed. However, the disordered regions of the fibrous hydrocellulose are apparently more structurally ordered and therefore more resistant to the alkaline reactions than the noncrystalline domains of the amorphous hydrocellulose.

Peeling and Stopping Reactions

Peeling and stopping reactions can only occur if a cellulose molecule has a reducing end group which is accessible to the alkaline medium. Therefore, it was necessary to quantify accessible (reactive) and inaccessible (nonreactive) reducing end groups. Since the ionic radii of hydroxide and borohydride-^{3}H ions

are approximately 3.5 Å[83] and 2.8 Å,[84] respectively, the accessibility of a reducing end group to both species is essentially equal. Thus, cellulose reducing end groups which are reduced by borohydride-^{3}H are classified as accessible reducing end groups (see Reducing End Groups), the reactive species for peeling and stopping reactions. Reducing end groups which react with borohydride-^{3}H only after the hydrocellulose has been made completely accessible (by regeneration under nondegradative conditions) are classified as inaccessible reducing end groups (see Reducing End Groups) and are considered nonreactive.

As illustrated in Table 1 (Cellulose Substrates), the two substrates had different initial accessible reducing end group contents. This makes direct comparison of peeling and stopping rates of the hydrocelluloses invalid because the apparent reaction rates are based on different numbers of reactive molecules. Therefore, the kinetic model used by Haas, et al.[7] was employed to provide a means for direct comparison of reaction rates of molecules within the two substrates. This model [notation modified from Haas[7]] consists of pseudo-first-order rate expressions for peeling [Eq. (1)], chemical stopping [Eq. (2)], and physical stopping [Eq. (4)]. In all three rate expressions, the reaction rates are related to the number of accessible reducing end groups by pseudo-first-order rate coefficients. Thus, differences in the rate coefficients would be expected to reflect differences in the reactivity of accessible reducing end groups occupying different structural environments. Effects of cellulose physical structure on hydroxide ion reactivity and mobility are inherent in the rate coefficients. Consequently, the term "accessible reducing end group reactivity" includes all effects of cellulose physical structure on the particular reaction.

Plots of yield (relative to average yield of duplicate zero-time samples) *versus* reaction time for the fibrous and amorphous hydrocelluloses at 60 and 80°C are shown in Fig. 16. The data are presented in Tables 13-16 (Appendix II). The amorphous hydrocellulose underwent more rapid and extensive yield loss than the fibrous hydrocellulose at both 60 and 80°C. However, in contrast to the 60°C reactions in which yield loss continued throughout the time interval studied (168 hr), the yield of both substrates leveled off after *ca.* 48 hours at 80°C.

Although peeling is characterized by yield loss, a portion of the yield loss could have been due to dissolution of cellulose molecules. However, the majority of dissolution probably occurred during the heat-up periods. Therefore, dissolution effects are considered insignificant after zero-time. In addition, both substrates underwent losses of pectic material during the initial periods of the reactions, but these losses were estimated to be insignificant compared to the yield losses due to peeling (see Appendix I).

Since the yield losses were predominantly due to peeling, the pseudo-first-order rate expression for peeling [notation modified from Haas[7]] is given by:

$$d[Y_L]/dt = k_p[ARE_t] \qquad (1)$$

where $[Y_L]$ = yield loss expressed as the mole fraction of monomer units at zero-time.

t = time, hr

k_p = pseudo-first-order rate coefficient for peeling, hr^{-1}

$[ARE_t]$ = accessible reducing end group content at time "t" expressed as the mole fraction of monomer units at zero-time.

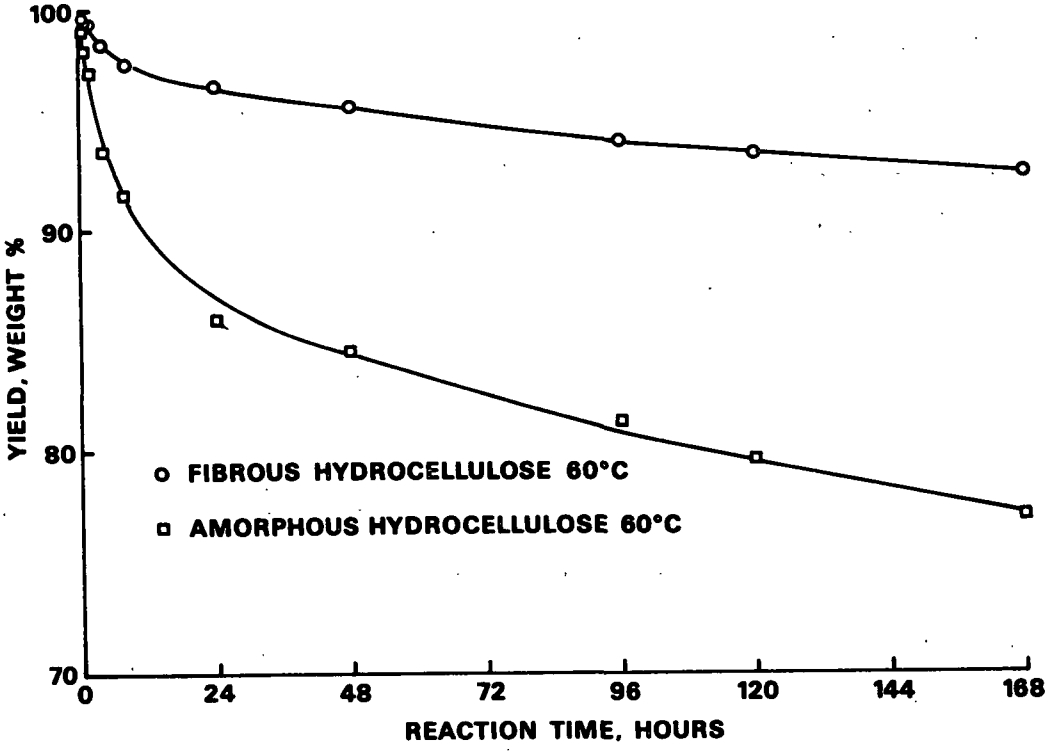

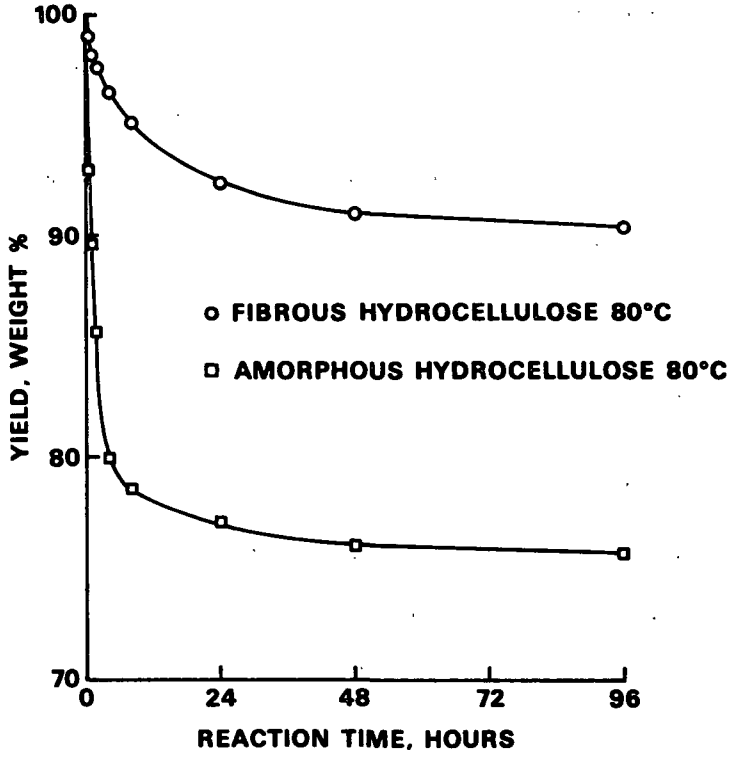

Figure 16. Hydrocellulose yield during degradation in oxygen-free 1.0M sodium hydroxide.

The differential term in Eq. (1) was evaluated at the experimental sampling times by measuring the slopes of plots of yield loss versus reaction time. Using the corresponding accessible reducing end group contents (Tables 13-16, Appendix II), the pseudo-first-order rate coefficients for peeling (k_p) were calculated with Eq. (1). Selected k_p values are listed in Table 2, and complete lists of the k_p values are presented in Tables 19-22 (Appendix III).

Table 2. Rate coefficients for peeling.[a]

Reaction Time, hr.	60°C		80°C	
	Fibrous	Amorphous	Fibrous	Amorphous
0	4.1	6.2	28	40
2	3.3	5.5	8.9	14
4	2.7	4.2	8.1	6.2
48	0.5	0.6	1.4	0.2
96	0.4	0.5	0.6	0.1

[a] k_p, hr^{-1}.

In all cases, the rate coefficients for peeling decreased with reaction time. This indicates that the accessible reducing end groups were more reactive toward peeling initially because the end groups occupied less ordered regions of the substrates. As the less ordered material was removed the accessible reducing end groups occupied increasingly ordered regions of the substrates and were therefore less reactive.

The amorphous hydrocellulose exhibited higher k_p values than the fibrous hydrocellulose throughout the 60°C reaction and during the initial period of the 80°C reaction. The periods during which the reactivity of accessible reducing end groups in the amorphous hydrocellulose was greater coincide with the periods of decreasing hydroxyl accessibility (Fig. 8, Changes in Physical Structure). This indicates that the higher rate of peeling of the amorphous hydrocellulose

was due to the less ordered structure of the degrading molecules relative to that in the fibrous hydrocellulose. Consequently, the amorphous hydrocellulose underwent significant decreases in the number of highly accessible, amorphous molecules. This is also consistent with molecules in the amorphous hydrocellulose being completely peeled in the early stages of the reactions (see Complete Peeling and Random Chain Cleavage).

During the later period of the 80°C reaction, the amorphous hydrocellulose exhibited a lower k_p value than the fibrous hydrocellulose. Since this corresponds to the period during which the hydroxyl accessibility of the amorphous hydrocellulose had leveled off (Fig. 8, Changes in Physical Structure), the majority of degradable amorphous chains had apparently reacted. Consequently, peeling was probably occurring close to cellulose II domains where it was drastically inhibited. In contrast, the reactivity of the fibrous hydrocellulose at 80°C decreased more gradually than the reactivity of the amorphous hydrocellulose and continued to decrease significantly throughout the reaction period. This indicates that peeling progressed more slowly through the disordered regions of the fibrous substrate than the amorphous regions of the amorphous substrate. Thus, both the lower reactivity of molecules in disordered regions of the fibrous substrate and the more gradual progression of peeling through those regions support the hypothesis that the disordered regions are slightly distorted crystalline domains rather than amorphous regions (see Changes in Physical Structure). In addition, the magnitude of the decreases in k_p for both substrates during the 60 and 80°C reactions indicates that peeling is substantially inhibited by both cellulose I (fibrous hydrocellulose) and cellulose II (amorphous hydrocellulose) crystalline domains.

Chemical stopping of the peeling reaction was characterized by the formation of carboxylic acid end groups. The acidic end group data (not corrected for losses of pectic material) are presented in Tables 13-16 (Appendix II). Losses of pectic material containing significant numbers of acidic functional groups occurred during the initial periods of the reactions. The quantities of the acidic groups lost were estimated (Table 12, Appendix I), and corrected values of the carboxylic acid end group contents of the hydrocelluloses during the initial periods were obtained (Table 11, Appendix I).

Both hydrocelluloses underwent significant chemical stopping during the reaction periods (Table 3). At 60°C, about half of the initial molecules with accessible reducing end groups terminated to carboxylic acid end groups in the amorphous hydrocellulose. In contrast, only one-fifth of the reactive molecules in the fibrous hydrocellulose underwent chemical stopping. At 80°C, the fractions of molecules chemically stopped increased for both substrates, but the amorphous hydrocellulose still underwent substantially more chemical stopping than the fibrous hydrocellulose. The apparent increase in importance of chemical stopping with increasing temperature is primarily due to the more extensive reaction of the hydrocelluloses at 96 hours in the 80°C reactions than at 168 hours in the 60°C reactions. This is evidenced by the fact that yield essentially leveled off during the later periods of the 80°C reactions, while significant yield loss due to peeling continued to occur at 168 hours in the 60°C reactions (Fig. 16). Thus, more of the initial reactive molecules would have undergone chemical stopping at 60°C if the reaction times were extended beyond 168 hours. More specific detail of chemical stopping is presented in the following kinetic analysis.

Table 3. Percentages of initial reactive molecules stabilized by chemical stopping.

Reaction	Time, hr	% Chemically Stopped[a]
Fibrous 60°C	168	20
Amorphous 60°C	168	50
Fibrous 80°C	96	38
Amorphous 80°C	96	87

[a]100% x carboxylic acid end groups formed/ accessible reducing end group content at zero-time.

In the case of chemical stopping, the rate of formation of carboxylic acid end groups is also proportional to the number of accessible reducing end groups. The pseudo-first-order rate expression [notation modified from Haas[7]] is given by:

$$d[AE]/dt = k_{cs}[ARE_t] \qquad (2)$$

where [AE] = carboxylic acid end group content expressed as the mole fraction of monomer units at zero-time.

k_{cs} = pseudo-first-order rate coefficient for chemical stopping, hr^{-1}.

The differential term in Eq. (2) was evaluated graphically from plots of carboxylic acid end groups versus reaction time. Due to the losses of acidic functional groups associated with pectic material, the estimated carboxylic acid end group contents of the substrates during the initial periods (Table 11, Appendix I) were used in evaluating d[AE]/dt for those periods. Selected k_{cs} values are listed in Table 4, and complete lists of the k_{cs} values are presented in Tables 19-22 (Appendix III).

Table 4. Rate coefficients for chemical stopping.[a]

Reaction Time, hr.	60°C		80°C	
	Fibrous	Amorphous	Fibrous	Amorphous
0	1.4	3.0	11	26
2	1.1	2.7	3.4	11
4	0.9	2.0	3.1	8.1
48	0.2	0.6	1.2	2.3
96	0.1	0.6	0.7	2.1

[a] $k_{cs} \times 10^2$, hr^{-1}.

Similar to peeling, the rate coefficients for chemical stopping decreased with time for both substrates. Thus, as the accessible reducing end groups occupied progressively more ordered regions of the structures, their reactivity decreased toward chemical stopping as well as peeling.

The amorphous hydrocellulose exhibited higher k_{cs} values than the fibrous hydrocellulose throughout both the 60 and 80°C reactions. During the early period of the 80°C reaction and throughout the 60°C reaction, when the amorphous substrate also exhibited higher k_p values (Table 2), its higher k_{cs} values can be primarily attributed to the less ordered structure occupied by the accessible reducing end groups. However, during the later period of the 80°C reaction peeling was apparently occurring close to the cellulose II domains of the amorphous hydrocellulose and was drastically inhibited. Simultaneously, peeling was more gradually approaching the cellulose I domains of the fibrous substrate. The higher k_{cs} values for the amorphous hydrocellulose are therefore indicative that chemical stopping is less inhibited by cellulose II than by cellulose I crystalline domains. In contrast, peeling is strongly inhibited by both crystalline types.

Further clarification of this effect is provided by comparing the relative rates of peeling and chemical stopping for the two substrates. The relationship is described by Eq. (3), obtained by dividing Eq. (1) by Eq. (2).

$$d[Y_L]/d[AE] = k_p/k_{cs} \quad (3)$$

Average values of k_p/k_{cs}, obtained by measuring the slopes of plots of yield loss versus carboxylic acid end groups using linear regression analysis, are presented in Table 5.

Table 5. Relative rates of peeling and chemical stopping.

Reaction	k_p/k_{cs}
Fibrous 60°C (0-168 hr)	291
Fibrous 80°C (0-96 hr)	264
Amorphous 60°C (0-48 hr)	204
(48-168 hr)	84
Amorphous 80°C (0-4 hr)	154
(4-96 hr)	23

At both 60 and 80°C, the fibrous hydrocellulose exhibited higher values of k_p/k_{cs} than the amorphous hydrocellulose. Since k_p/k_{cs} remained constant throughout the fibrous hydrocellulose reactions, the relative reactivity of its accessible reducing end groups toward both reactions did not change as the reactions proceeded from regions of lower to higher structural order. This is consistent with the less ordered regions exhibiting some cellulose I character, such as would be the case with slightly distorted cellulose I domains and crystallite surfaces (see Changes in Physical Structure). Furthermore, the decrease in k_p/k_{cs} for the amorphous hydrocellulose in the later periods of the reactions indicates that peeling was significantly more inhibited than chemical stopping as the cellulose II domains were approached. Since a portion of the

accessible reducing end groups must have resided close to cellulose II domains during the early periods of the reactions, the lower k_p/k_{cs} values for the amorphous hydrocellulose can also be attributed to preferential inhibition of peeling by cellulose II crystallites during the early reaction periods.

These findings support the contention that cellulose II domains do not hinder chemical stopping as effectively as cellulose I domains, while both crystalline polymorphs are highly resistant to peeling. Thus, peeling is apparently inhibited by the physical presence of crystalline domains retarding the progression of peeling along the cellulose chain. On the other hand, both the degree of structural order and the specific conformational environment of the accessible reducing end group dictate its reactivity toward chemical stopping. This is consistent with results of previous studies in which the rate of peeling relative to chemical stopping was reported to be greater for native cellulose (cellulose I) than for mercerized cellulose (cellulose II).[10,19,54,55]

In addition, the decrease in k_p/k_{cs} for both substrates with increasing temperature indicates that chemical stopping becomes more important relative to peeling with increasing temperature. This is consistent with chemical stopping having a higher activation energy than peeling in hydrocellulose, as previously reported.[7]

Besides undergoing chemical stopping, cellulose molecules also reportedly terminate to reducing end groups which are incapable of peeling due to their inaccessibility to the alkaline medium.[7,11,19] This phenomenon does not merely involve a reduction in reactivity of the accessible reducing end group toward peeling (and chemical stopping) as was demonstrated earlier in this section. Instead, so-called "physical stopping" occurs when the reducing end group

becomes inaccessible to the alkaline medium, causing it to be nonreactive. This probably occurs by collapse of adjacent molecules around the reducing end group at or close to the edge of a crystalline domain. Thus, a molecule must have an accessible reducing end group in order to undergo peeling to a point in the physical structure where physical stopping can occur.

Inaccessible reducing end group contents of the hydrocelluloses are listed in Tables 13-16 (Appendix II). As shown in Table 6, physical stopping accounted for the stabilization of significant percentages of the initial reactive molecules in both substrates. The fibrous hydrocellulose underwent physical stopping of about half of its reactive molecules at both 60 and 80°C. In contrast, significantly smaller fractions of the reactive molecules in the amorphous substrate underwent physical stopping. Surprisingly, the percentages of molecules physically stopped did not increase significantly with increasing temperature as was the case with chemical stopping.

Table 6. Percentages of initial reactive molecules stabilized by physical stopping.

Reaction	Time, hr	% Physically Stopped[a]
Fibrous 60°C	168	45
Amorphous 60°C	168	26
Fibrous 80°C	96	49
Amorphous 80°C	96	21

[a]100% x inaccessible reducing end groups formed/ accessible reducing end group content at zero-time.

The greater fractions of molecules chemically stopped at 80°C were primarily attributed to the greater extent of the reactions relative to the

60°C cases. Therefore, both substrates must have contained limited numbers of potential physical stopping sites, depending upon the particular physical structures. As demonstrated by the data in Table 6, this number is significantly greater for the fibrous hydrocellulose. Thus, more extensive physical stopping in the fibrous hydrocellulose can be attributed to its larger crystalline fraction relative to that of the amorphous hydrocellulose after partial recrystallization.

Since physical stopping can only occur if a molecule contains an accessible reducing end group initially, the pseudo-first-order rate expression for physical stopping [notation modified from Haas[7]] can be written:

$$d[IRE]/dt = k_{ps}[ARE_t] \qquad (4)$$

where [IRE] = inaccessible reducing end group content expressed as the mole fraction of monomer units at zero-time.

k_{ps} = pseudo-first-order rate coefficient for physical stopping, hr^{-1}.

The differential term in Eq. (4) was evaluated graphically from plots of inaccessible reducing end groups versus reaction time. Selected k_{ps} values are listed in Table 7, and complete lists of the k_{ps} values are presented in Tables 19-22 (Appendix III).

The rate coefficients for physical stopping decreased with reaction time for both hydrocelluloses. This is primarily due to the decreasing rate of peeling, resulting from the decrease in reactivity of accessible reducing end groups occupying increasingly ordered regions of the physical structures. However, the complete cessation of physical stopping later in the 80°C reactions indicates that the maximum numbers of potential physical stopping sites had been

filled. This is consistent with the observation that the extent of physical stopping was not significantly influenced by the more extensive reaction of the substrates at 80°C relative to 60°C (Table 6).

Table 7. Rate coefficients for physical stopping.[a]

Reaction Time, hr	60°C		80°C	
	Fibrous	Amorphous	Fibrous	Amorphous
0	4.1	1.4	36	15
2	2.2	1.4	8.1	7
4	1.6	1.3	5.4	2
48	0.3	0.2	0	0
96	0.3	0.2	0	0

[a] $k_{ps} \times 10^2$, hr^{-1}.

At both 60 and 80°C, the fibrous hydrocellulose exhibited higher k_{ps} values than the amorphous hydrocellulose. Thus, the higher rate of physical stopping indicates that more molecules in the fibrous hydrocellulose extended into crystalline domains. This is in agreement with the higher percentages of reactive molecules physically stopped in the fibrous hydrocellulose (Table 6). Furthermore, more extensive physical stopping in the fibrous hydrocellulose may be partially due to the greater inhibition of chemical stopping by cellulose I than by cellulose II crystallites, allowing more molecules to peel to a point where physical stopping could occur.

To compare the relative importance of the two stopping modes, the percentages of stable end groups formed by chemical and physical stopping are presented in Table 8. At both 60 and 80°C, physical stopping was the dominant stabilization mechanism in the fibrous hydrocellulose, while chemical stopping dominated in the amorphous hydrocellulose. As previously stated, this is primarily due to the larger crystalline fraction of the fibrous hydrocellulose and the

lesser inhibition of chemical stopping by both the disordered and ordered (cellulose II) regions of the amorphous hydrocellulose. The increase in importance of chemical stopping and decrease in importance of physical stopping for both substrates with increasing temperature is due to several factors. These include the greater extents of the 80°C reactions, the higher activation energy of chemical stopping relative to peeling, and the filling of all potential physical stopping sites at 80°C.

Table 8. Percentages of stable end groups formed by chemical and physical stopping.

Reaction	Time, hr	% Chemically Stopped[a]	% Physically Stopped[b]
Fibrous 60°C	168	30	70
Amorphous 60°C	168	66	34
Fibrous 80°C	96	43	57
Amorphous 80°C	96	80	20

[a]100% x carboxylic acid end groups formed/carboxylic acid end groups plus inaccessible reducing end groups formed.
[b]100% x inaccessible reducing end groups formed/carboxylic acid end groups plus inaccessible reducing end groups formed.

Complete Peeling and Random Chain Cleavage

The total number of cellulose molecules, or total end group content, does not change during alkaline degradation unless molecules undergo dissolution, complete peeling, or random chain cleavage. Dissolution can involve molecules with reducing end groups or carboxylic acid end groups. However, since the majority of dissolution probably occurred during the heat-up periods, dissolution is considered insignificant during the reaction periods. Complete peeling results in the loss of a reducing end group, while random chain cleavage generates a reducing end group. Thus, decreases in the total end group content

are indicative of complete peeling, and increases in the total number of end groups can be used to monitor random chain cleavage. Unfortunately, the simultaneous occurrence of the two processes can make the quantitative assessment of both processes difficult.

Partial lists of the total end group contents of the hydrocelluloses (corrected for losses of pectic material) are presented in Table 9. Complete lists of total end group contents (not corrected for losses of pectic material) are presented in Tables 13-16 (Appendix II), and the estimated numbers of carboxylic acid groups associated with the pectic material are listed in Table 12 (Appendix I).

Table 9. Total end group contents of hydrocelluloses.[a]

Reaction Time, hr	60°C		80°C	
	Fibrous	Amorphous	Fibrous	Amorphous
0	1.94 ± 0.02	4.13 ± 0.04	1.88 ± 0.04	4.51 ± 0.03
1	1.94	3.57	1.90	4.28
2	1.92	3.44	1.96	4.35
8	2.04	3.52	1.96 ± 0.02	4.44 ± 0.02
24	1.95 ± 0.02	3.59 ± 0.02	1.89	4.96
48	1.92	3.65	1.89 ± 0.01	5.05 ± 0.08
96	1.86	3.76	1.90	5.35
168	1.89	4.09	--	--

[a]Expressed as 10^3 x mole fraction of total monomer units at zero-time.

The total end group content of the fibrous hydrocellulose remained relatively constant throughout the reaction periods, indicating no significant complete peeling or random chain cleavage. In contrast, both processes were evident in the reactions of the amorphous hydrocellulose. Initial decreases in the total numbers of end groups indicate that complete peeling occurred primarily during the early reaction periods. In the later periods, total end groups

increased because the number of molecules generated by random chain cleavage was greater than the number lost by complete peeling. Random chain cleavage must also have occurred during the initial periods but was not apparent due to the more substantial effects of complete peeling on the total end group contents.

The amorphous substrate underwent the most rapid decreases in hydroxyl accessibility during the same periods in which complete peeling was found to occur (Fig. 8, Changes in Physical Structure). This indicates that complete peeling primarily involved molecules existing entirely within amorphous regions and became insignificant once the majority of highly accessible chains had been removed or chemically stopped. In contrast, the fibrous substrate underwent no significant reductions in total end groups or in hydroxyl accessibility (Table 17, Appendix II). This suggests that none of the molecules in the fibrous hydrocellulose were capable of being completely peeled due to extensive involvement in the cellulose I crystalline regions. Therefore, the higher rate coefficients for peeling for the amorphous substrate during the initial reaction periods (Table 2, Peeling and Stopping Reactions) were at least partially due to complete peeling of highly accessible molecules.

Since complete peeling had apparently become insignificant during the later periods of the amorphous hydrocellulose reactions, it was possible to kinetically analyze the total end group data for random chain cleavage. Unfortunately, it was not possible to quantitatively assess either process during the initial periods due to their simultaneous occurrence.

The rate of chain cleavage, defined as the rate of increase in the total number of end groups, is considered to be proportional to the number of glycosidic linkages in the cellulose sample. Since the total number of monomer units

or yield is essentially equal to the number of glycosidic linkages, the pseudo-first-order rate expression for random chain cleavage can be written:

$$d[TE]/dt = k_{cc}[Y_t] \qquad (5)$$

where [TE] = total end group content expressed as the mole fraction of monomer units at zero-time.

k_{cc} = pseudo-first-order rate coefficient for random chain cleavage, hr^{-1}.

$[Y_t]$ = yield at time "t" expressed as the mole fraction of monomer units at zero-time.

The differential term in Eq. (5) was evaluated graphically from plots of total end groups versus reaction time. Rate coefficients for random chain cleavage were calculated with Eq. (5) for the experimental sampling times following the periods of significant complete peeling. Selected values of k_{cc} are listed in Table 10, and complete lists of k_{cc} values are presented in Tables 21 and 22 (Appendix III).

Table 10. Rate coefficients for random chain cleavage.[a]

Reaction Time, hr	60°C		80°C	
	Fibrous	Amorphous	Fibrous	Amorphous
0	0	ND	0	ND
2	0	ND	0	58
8	0	8.4	0	53
48	0	8.4	0	8.2
96	0	8.3	0	4.9
168	0	7.5	--	--

[a] $k_{cc} \times 10^6$, hr^{-1}.
ND - not determined.

This kinetic treatment is similar to those employed for the peeling and stopping reactions (see Peeling and Stopping Reactions). The rate coefficient for random chain cleavage functions as an index of reactivity of the glycosidic

linkages toward the reaction. As with the endwise reactions, reactivity includes the effects of physical structure on both the glycosidic linkages and the hydroxide ion. Thus, the decreases in the k_{cc} values with reaction time are indicative that the physical structure of the amorphous hydrocellulose rendered the glycosidic linkages less susceptible to chain cleavage as the reactions progressed. At 60°C, the k_{cc} values decreased gradually from 8 to 168 hours. The decrease in k_{cc} occurred more rapidly between 2 and 48 hours in the 80°C reaction, followed by a more gradual decrease up to 96 hours. This was apparently due to the greater reduction in accessibility of the amorphous hydrocellulose at 80°C (Fig. 8, Changes in Physical Structure). Therefore, it can be concluded that chain cleavage was more inhibited by the larger cellulose II fraction that formed in the amorphous substrate during the 80°C reaction.

The lack of chain cleavage in the fibrous hydrocellulose indicates that even molecules in disordered regions were less susceptible to chain cleavage than those in amorphous regions of the amorphous hydrocellulose. This further implies that the disordered regions of the fibrous hydrocellulose were more structurally ordered than the amorphous regions of the amorphous hydrocellulose. Thus, the resistance of the fibrous hydrocellulose to chain cleavage is consistent with the disordered regions being composed of slightly distorted crystalline domains and crystallite surfaces (see Changes in Physical Structure).

Mercerized cellulose (cellulose II) is reportedly more susceptible to random chain cleavage than native cellulose (cellulose I).[10] This suggests that the disordered regions associated with the two crystalline polymorphs display different degrees of structural order, giving rise to differences in

reactivity. Thus, the predominant molecular conformation apparently influences the susceptibility of a particular cellulose substrate to the random chain cleavage reaction. In addition, molecules in both cellulose I and II crystalline domains are highly resistant to chain cleavage.

CONCLUSIONS

Alkaline peeling and chemical stopping occur more rapidly in amorphous hydrocellulose than in the disordered regions of fibrous cotton hydrocellulose (predominantly cellulose I). In addition, random chain cleavage at 60 and 80°C occurs only in amorphous hydrocellulose. These results indicate that the reducing end groups and glycosidic linkages in disordered regions of cotton hydrocellulose are less reactive than those occupying amorphous regions. Therefore, it is proposed that the disordered regions of cotton hydrocellulose consist of molecules in slightly distorted crystalline domains and at crystallite surfaces, as previously suggested.[22,30-32]

Peeling is drastically inhibited to similar extents by celluloses I and II crystalline polymorphs, due to crystalline domains retarding the progression of peeling along the cellulose molecule. Chemical stopping is more inhibited by cellulose I than by cellulose II, such that the degree of structural order and the particular molecular conformation dictate the reactivity of a reducing end group toward chemical stopping. This is consistent with the higher rate of chemical stopping typically reported for mercerized cellulose relative to native cellulose.[10,19,54,55] In addition, chemical stopping increases in importance relative to peeling with increasing temperature, consistent with the findings of Haas, et al.[7]

Physical stopping occurs when peeling proceeds to a point in the cellulose structure where the reducing end group is inaccessible to the alkaline medium. Both cellulose I and cellulose II crystalline domains are effective in physical stopping of peeling. The extent of physical stopping increases with the number of molecules involved in crystalline domains and is limited by the number of

potential physical stopping sites present in a given cellulose structure. In addition to the formation of nonreactive reducing end groups by physical stopping, accessible reducing end groups can exist at the edge of a crystalline domain but react at extremely low rates in comparison to those in disordered regions. This finding refutes the report by Haas, et al. that cellulose molecules maintain constant reactivity toward peeling and chemical stopping unless physical stopping occurs.

EXPERIMENTAL

GENERAL ANALYTICAL PROCEDURES

Moisture contents were determined by heating cellulose samples at 105°C under vacuum until a constant weight was obtained.

Ash contents were measured by first charring oven-dry cellulose samples at 300°C (ca. 1 hr), and then heating at 575°C in an oxidizing atmosphere (ca. 1 hr).[66]

Infrared spectra were collected on a Nicolet 7199C Fourier transform spectrophotometer. Solution spectra were obtained with a Wilks calcium fluoride liquid cell with a 0.05 mm path length. Spectra of solids were obtained using a diffuse reflectance attachment supplied with the instrument.

X-ray diffractograms were determined on a Norelco diffraction unit with a wide range goniometer. The x-ray tube was operated at 35 kv and 20 ma, using nickel-filtered CuKα radiation. A 0.5° divergence slit defined the primary beam, while a 0.006-inch receiving and a 0.5° scatter slit defined the diffracted beam. Diffraction spectra were recorded at 2θ from 10 to 28°. Cellulose samples (0.05 g) were pressed into pellets using a Perkin-Elmer evacuable die (2000 psig).

Raman spectra were acquired on a Jobin Yvon Raman spectrometer utilizing an argon laser operated at 100 mw as the exciting source. Spectra were recorded from 200 to 1600 wavenumbers (cm^{-1}) using the sample pellets prepared for x-ray diffraction.

Solid-state ^{13}C-NMR spectra were obtained on General Electric S-100 instruments, which employ the combined techniques[46] of proton-carbon cross polarization, high power proton decoupling, and magic-angle sample spinning. The spectrometer was operated at 4.4 tesla with ^{13}C and proton decoupling frequencies of 25.2 and 100.2 MHz, respectively. Cross polarization times were 2 ms and the magic-angle sample spinning frequencies ranged from 2500 to 2800 MHz. Spectra were recorded from 0 to 160 ppm. Spectra of the hydrocellulose substrates and degraded samples were acquired by Dr. T. Early of GE-NMR Instruments Co., Inc. (255 Fourier Ave., Fremont, CA 94539), and the spectrum of the ball-milled Whatman CF-1 cellulose (supplied by Dr. R. H. Atalla) was acquired by Dr. L. W. Amos of Weyerhaeuser Co. (Tacoma, WA 98477).

SOLUTIONS AND REAGENTS

Anhydrous Pyridine

Calcium hydride (ca. 5 g) was mixed with reagent grade pyridine (1.5 L). After one week, the mixture was refluxed for 4 hours and then fractionally distilled.[67] The first 100 mL of distillate was discarded, and the next 1000 mL was collected and stored under dry nitrogen.

Purified Tetrahydrofuran

Reagent grade tetrahydrofuran (1.6 L) was fractionally distilled from lithium aluminum hydride.[67] The first 50 mL of distillate was discarded. The next 1000 mL was collected in a 2-L round bottom flask and used within 48 hours of preparation.

Potassium Acid Phthalate

Reagent grade potassium acid phthalate was dried under vacuum at 105°C and stored in vacuo over phosphorus pentoxide.

Strontium Hydroxide

Chemically pure grade strontium hydroxide (Amend Drug and Chemical Co., 50 g) was dissolved in boiling distilled water (1.2 L). The hot solution was filtered through Whatman No. 1 filter paper and cooled to ca. 10°C. The resulting strontium hydroxide crystals were dried to constant weight at 40°C under vacuum and stored in a tightly sealed Teflon bottle.

Due to the limited solubility of strontium hydroxide in water at room temperature, the required 1.0M solutions could not be prepared and added to the reactors in the same manner as the 1.0M sodium hydroxide solutions. However, it is possible to prepare 1.0M strontium hydroxide solutions at 100°C, the temperature at which the degradations were conducted in strontium hydroxide (see Appendix IV). Therefore, the hydrated strontium hydroxide crystals were standardized, and the appropriate quantities of strontium hydroxide and oxygen-free water were added separately to the reactors.

Portions of the recrystallized strontium hydroxide (0.200 g) were mixed with oxygen-free water (100 mL) and titrated with 1.0M hydrochloric acid to the phenolphthalein end point. The crystals gradually dissolved at room temperature as the acid was added in small increments. The formula weight of the hydrated strontium hydroxide crystals was calculated with Eq. (6).

$$W_f = 2\ W_c/V_a C_a \qquad (6)$$

where W_f = formula weight of strontium hydroxide crystals, g mol^{-1}

W_c = weight of strontium hydroxide crystals titrated, g

V_a = volume of hydrochloric acid consumed, L

C_a = concentration of hydrochloric acid, mol L^{-1}

Using the formula weight (251.8 g mol^{-1}), the weight of the strontium hydroxide crystals (10.072 g) required to prepare 40 mL of a 1.0M solution was calculated with Eq. (7).

$$W_r = W_f C_r V_s \tag{7}$$

where W_r = weight of strontium hydroxide crystals required for a reaction, g

C_r = concentration of strontium hydroxide required for a reaction, mol L^{-1}

V_s = volume of strontium hydroxide solution required for a reaction, L

Since the crystals contained bound water, the quantity of water (34.8 mL) required to prepare 40 mL of a 1.0M strontium hydroxide solution was calculated with Eq. (8).

$$V_w = V_s - [V_s C_r (W_f - W_m)/\rho_w] \tag{8}$$

where V_w = volume of water required for a reaction, L

W_m = molecular weight of strontium hydroxide, 121.6 g mol^{-1}

ρ_w = density of water, g L^{-1}

Sodium Methoxide-Isopropoxide Solution

A 1M sodium methoxide solution was prepared by slowly adding clean sodium (80.5 g) in small amounts to reagent grade methanol (3.5 L) under a nitrogen atmosphere. The solution was filtered through Whatman GF/C glass microfiber pads, and diluted with methanol (5.25 L) and isopropanol (8.75 L). The resulting 0.2M sodium methoxide-isopropoxide solution was stored under nitrogen in tightly stoppered flasks in the dark.

Oxygen-Free Water

Filtered, deionized water was treated with activated charcoal prior to distillation in a Corning MP-12 Pyrex laboratory still. The distilled water was boiled for about 30 minutes, transferred to a 1-L Teflon bottle, and purged with nitrogen while cooling in an ice bath. The water was stored under a nitrogen atmosphere in the tightly sealed Teflon bottle and used within 24 hours of preparation.

Stock Sodium Hydroxide Solution

Reagent grade sodium hydroxide (450 g) was dissolved in oxygen-free water (900 mL) under a nitrogen atmosphere. After cooling, the solution was stored in a tightly sealed, paraffin-lined reagent bottle. Two aliquots (ca. 0.36 g) of the stock solution were accurately weighed into 100-mL volumetric flasks and diluted to volume with oxygen-free water. The concentration of the stock solution (32.44% w/w) was determined by titrating the diluted solutions against potassium acid phthalate to the phenolphthalein end point.

20% Sodium Hydroxide Solution

Reagent grade sodium hydroxide (250 g) was dissolved in distilled water (950 mL). After cooling, the stock solution was transferred to a tightly stoppered, paraffin-lined reagent bottle. Two aliquots (ca. 0.5 g) of the solution were accurately weighed into 100-mL volumetric flasks and diluted to volume with distilled water. The concentration of the stock solution was determined by titrating the diluted solutions against potassium acid phthalate to the phenolphthalein end point. Distilled water was added in small increments to the stock solution, and the titrations were repeated until a 6.094M (20% w/w) sodium hydroxide concentration was obtained.

Diethylenetriaminepentaacetic Acid (DTPA) Solution

Reagent grade DTPA (6.0 g) was dissolved in 0.15% (w/v) sodium hydroxide (3 L), and the resulting solution was adjusted to pH 9 with concentrated hydrochloric acid.

Diethylbarbituric Acid Buffer Solution

5,5-Diethylbarbituric acid (1.151 g) was dissolved in distilled water (500 mL), 1.0M sodium hydroxide (4.0 mL) was added, and the solution was diluted to 1 L with distilled water.[68]

Standard Potassium Dichromate Solution

Reagent grade potassium dichromate (primary standard) was dried at 150°C for 2 hours and cooled under vacuum. After cooling, the potassium dichromate (4.9037 g) was carefully weighed into a volumetric flask, dissolved in distilled water (ca. 750 mL), and diluted to 1 L with distilled water to give a 0.1N (0.0167M) solution.

Standard Ferrous Ammonium Sulfate Solution

Reagent grade ferrous ammonium sulfate (19.8 g) was dissolved in distilled water (ca. 750 mL) and diluted to 1 L with distilled water in a volumetric flask. Two aliquots (50 mL) of the solution were each combined with phosphoric acid (5 mL) and diphenylaminesulfonate redox indicator (2 drops), and titrated to a purple end point with standard 0.1N potassium dichromate solution.[69] The flask containing the standard 0.0498N ferrous ammonium sulfate solution was flushed with nitrogen, tightly stoppered, and stored for no more than 24 hours before use.

Standard Methylene Blue Solution

Certified grade methylene blue chloride (0.77 g) was mixed with distilled water (1 L) and stirred overnight. The resulting solution was filtered through a Whatman GF/C glass microfiber pad and stored in a tightly sealed polypropylene bottle. The concentration of the methylene blue stock solution (1.97 ± 0.02 mM) was determined by mixing aliquots (50 mL) of the dye solution with standard 0.100N potassium dichromate solution (25 mL) and titrating the excess potassium dichromate with standard 0.0498N ferrous ammonium sulfate solution.[70] Concentrated phosphoric acid (5 mL) was added to the titration to produce a sharper end point (purple to green) with the sodium diphenylaminesulfonate redox indicator (3 drops).[69]

PREPARATION OF CELLULOSE SUBSTRATES

Purified Cotton Fiber

Raw cotton fiber cut in ca. 0.25 inch lengths was obtained from the Southern Regional Research Center of the United States Department of Agriculture (New Orleans, LA). The cotton fibers (100 g) were alternately soaked in chloroform (2 L) for 9 hours and filtered dry a total of four times. The procedure was then repeated using seven 12-hour extractions with 95% ethanol (2 L).[71] Finally, the ethanol was removed by repeatedly washing the fibers with distilled water.

The solvent-extracted fibers were placed in a 6-L, insulated stainless steel beaker fitted with a Teflon lid and a perforated Teflon plate which was positioned about 2 inches beneath the lid. The vessel was continuously flushed with nitrogen while boiling 1% (w/v) sodium hydroxide solution (6 L) was introduced from the bottom of the beaker. The resulting slurry was maintained at

100°C and stirred with a Teflon-coated magnetic stir bar. At 30-minute intervals, the extraction medium was displaced by introducing fresh solution (6 L) from the bottom of the beaker. A total of four hot alkali and four hot distilled water extractions were conducted in this manner.[72] The purified cotton fibers were then rinsed with cold distilled water (7 L), 0.5% (w/v) acetic acid (7 L), and distilled water (20 L).

The wet fibers (ca. 60 g o.d.) were further purified by alternately soaking in 0.2% (w/v) DTPA solution (3 L) for 1 hour and thoroughly rinsing with distilled water, a total of three times. The fibers were then rinsed with 0.1M sodium hydroxide (6 L), 0.1M hydrochloric acid (10 L), and distilled water (10 L), and stored wet at ca. 0°F.

Fibrous Hydrocellulose

Purified cotton fibers (ca. 60 g o.d.) were combined with 1.0M hydrochloric acid (6 L) in a 6-L Erlenmeyer flask, and the slurry was maintained at 40°C for 20 hours by immersing the flask in a constant temperature water bath. The resulting fibrous hydrocellulose was rinsed with distilled water (until neutral), freeze-dried, and stored in vacuo over phosphorus pentoxide.

Amorphous Hydrocellulose

A stirred mixture of fibrous hydrocellulose (7.0 g) and reagent grade dimethylsulfoxide (700 mL) was heated to 125°C. Paraformaldehyde (35 g) was added, and stirring was continued until a clear solution formed and most of the excess formaldehyde had bubbled off (ca. 10 min).[60,61] The resulting methylol cellulose solution was cooled, diluted to 3.5 L with dimethylsulfoxide (DMSO), and filtered through Whatman GF/C glass microfiber pads.

The methylol cellulose solution (0.2%, w/v, cellulose/DMSO) was regenerated by dropwise addition to a mechanically stirred 0.2M sodium methoxide-isopropoxide solution (14 L). The resulting precipitate was divided equally into 20 portions (ca. 0.35 g cellulose), and each portion was washed with 0.2M sodium methoxide-isopropoxide (175 mL) and methanol (3 x 150 mL) by centrifugation and decantation. The dissolution/regeneration process was repeated twice, and the resulting cellulose/methanol slurries were combined.

The slurry was divided equally into 32 portions (ca. 0.65 g cellulose), and each portion was washed with methanol (150 mL), 0.1M hydrochloric acid (2 x 150 mL), and distilled water (3 x 150 mL) by centrifugation and decantation. The portions were recombined, freeze-dried, and stored *in vacuo* over phosphorus pentoxide (18.9 g amorphous hydrocellulose, ca. 90% yield).

PROCEDURES FOR DEGRADATION STUDIES

Reactors

Alkaline degradations were conducted in cylindrical 316 stainless steel pressure vessels with internal volumes of ca. 50 mL (Fig. 17). The inner cap was sealed by compressing a Teflon sealing ring (replaced every other run) with a heat-treated bolt threaded through the outer cap. The vessels were equipped with 1/8 inch I.D. thermocouple wells fabricated from Supelco 304 stainless steel chromatographic grade tubing and 316 stainless steel Swagelok fittings. The reactor parts were rinsed with acetone, washed with soapy water, thoroughly rinsed with distilled water, and dried at 105°C prior to each run.

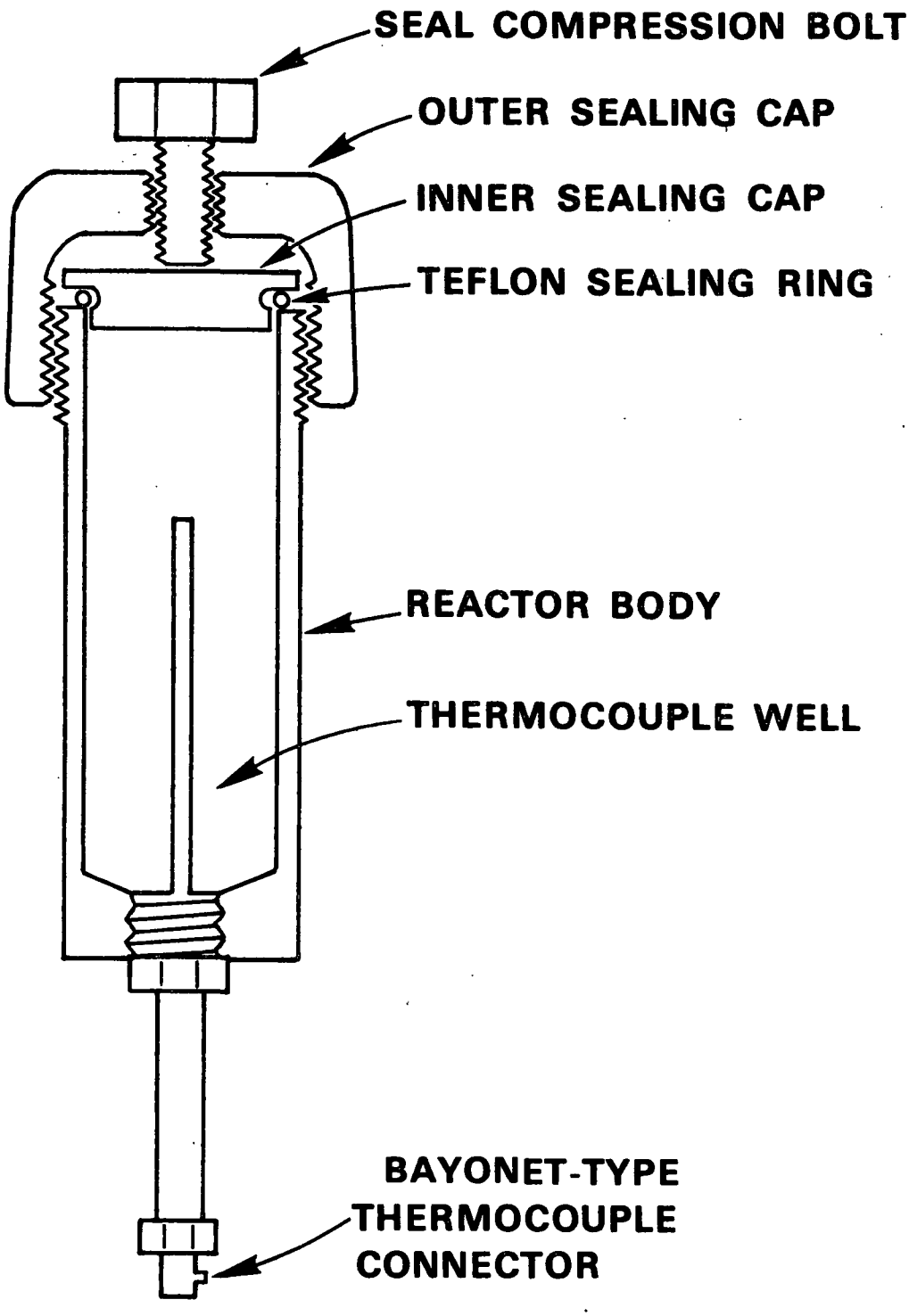

Figure 17. Reactor.

The sealed reactors were attached to a rotating rack which was submersed in a constant temperature oil bath. Bayonet-type, iron constantan thermocouple probes were inserted into the thermocouple wells, and the reactors were turned end-over-end (ca. 3 rpm) during the degradation process. Thermocouple leads were connected through a slip-ring assembly on the end of the rotating shaft to an Omega 199 digital temperature readout with a strip chart recorder. The bath temperature was maintained by circulating heat transfer oil through a Chromalox heat exchanger controlled by a Honeywell digital control programmer.

Sodium Hydroxide Solutions

Stock sodium hydroxide solution (123.3 g) was weighed into a 1-L volumetric flask and diluted with oxygen-free water inside a glove box which had been flushed with nitrogen for ca. 1 hour. A portion of the dilute alkali (ca. 50 mL) was titrated against potassium acid phthalate to the phenolphthalein end-point. The remaining solution (1.00M sodium hydroxide) was transferred to a tightly sealed polypropylene bottle and stored in the glove box under a slight positive nitrogen pressure.

Degradations

The freeze-dried cellulose substrates (fibrous and amorphous hydrocellulose) were dried to constant weight under vacuum in a desiccator containing phosphorus pentoxide. The desiccator and reactors were placed in the glove box with the standardized 1.00M sodium hydroxide. Prepurified nitrogen (Matheson Scientific Co.) was passed through traps containing calcium sulfate and phosphorus pentoxide before entering the glove box. The desiccator was opened after the glove box had been purged with nitrogen for 30 minutes. After an additional 30 minutes, the exit port of the glove box was closed, and a slight positive nitrogen pressure was maintained.

Cellulose substrate (0.4000 g) was weighed into the reactors, and 1.00M sodium hydroxide (40.0 mL, determined volumetrically) was added. The reactors were sealed and removed from the glove box through a rubber diaphragm. This was necessary in order to maintain the nitrogen atmosphere in the glove box, since several samples were typically loaded on the same day. When 1.0M strontium hydroxide was used as the degradation medium, the strontium hydroxide crystals (10.072 g) and oxygen-free water (34.8 mL) were added separately to the reactor.

The reactors were then placed in the constant temperature oil bath, the thermocouples were attached, and the reactors were rotated. Temperatures inside the reactors were recorded during the heat-up and cool-down cycles. The desired reaction temperatures (60-100°C) were attained in 14 ± 1 minutes, apparently due to a combination of the temperature differences between the reaction mixtures and the oil bath, and the heat transfer characteristics of the reactors. The reaction mixtures were cooled to 20°C in an ice bath, and the cool-down periods were controlled to 3 ± 0.2 minutes by agitating the reactors as necessary in the ice bath. The reaction mixtures were maintained at the desired temperatures for up to 168 hours. In addition, zero-time samples were prepared for both substrates at 60 and 80°C by running the reaction mixtures through the heat-up and cool-down cycles, and limiting the time at the reaction temperature to ca. 1 minute.

SUBSTRATE ANALYSIS

Yield

The cooled reaction mixture was transferred to a polyethylene bottle and neutralized with 1.0M hydrochloric acid. The degraded hydrocellulose was filtered on a Whatman GF/C glass microfiber pad in a sintered glass filter

funnel (coarse) and slowly rinsed with 0.1M hydrochloric acid (5 x 60 mL) and distilled water (5 x 60 mL). The sample was transferred to a tared, 50-mL Erlenmeyer flask, freeze-dried, and dried *in vacuo* over phosphorus pentoxide to constant weight.

Acidic End Groups

The methylene blue acidic end group analysis was calibrated according to the TAPPI Standard Method.[68] Standard methylene blue solution (2,3,4,5,6,7,8,9,10 mL) was added by autopipette to nine 100-mL volumetric flasks, each containing diethylbarbituric acid buffer solution (10 mL). The solutions were diluted to volume with distilled water. An aliquot of each solution (1.0 mL) was added to a 10-mL volumetric flask containing 0.1M hydrochloric acid (1.0 mL) and then diluted to volume with distilled water. Absorbances of the solutions at 620 nm were measured with a Perkin-Elmer 320 spectrophotometer using silica cells (1.0 cm pathlength) and a distilled water reference. Methylene blue concentration (first set of dilutions) was plotted *versus* absorbance (Fig. 18). A linear calibration [Eq. (9)] was obtained with a 0.9995 correlation coefficient.

$$[MB] = (A_{620} + 0.008)/4.548 \qquad (9)$$

where [MB] = methylene blue concentration (first set of dilutions), mmol L^{-1}

A_{620} = absorbance at 620 nm

The TAPPI Standard Method for carboxylic acids[68] was modified to accommodate smaller samples with a wide range of carboxyl contents. Glass vials (4-mL) used for the methylene blue absorption method were coated with a 3% (w/w) solution of Dow Corning 200 silicone oil in carbon tetrachloride and heated at 275°C for 2 hours.[68] The vial caps were lined with Teflon. These steps were taken to prevent significant dye absorption by the glass vials.

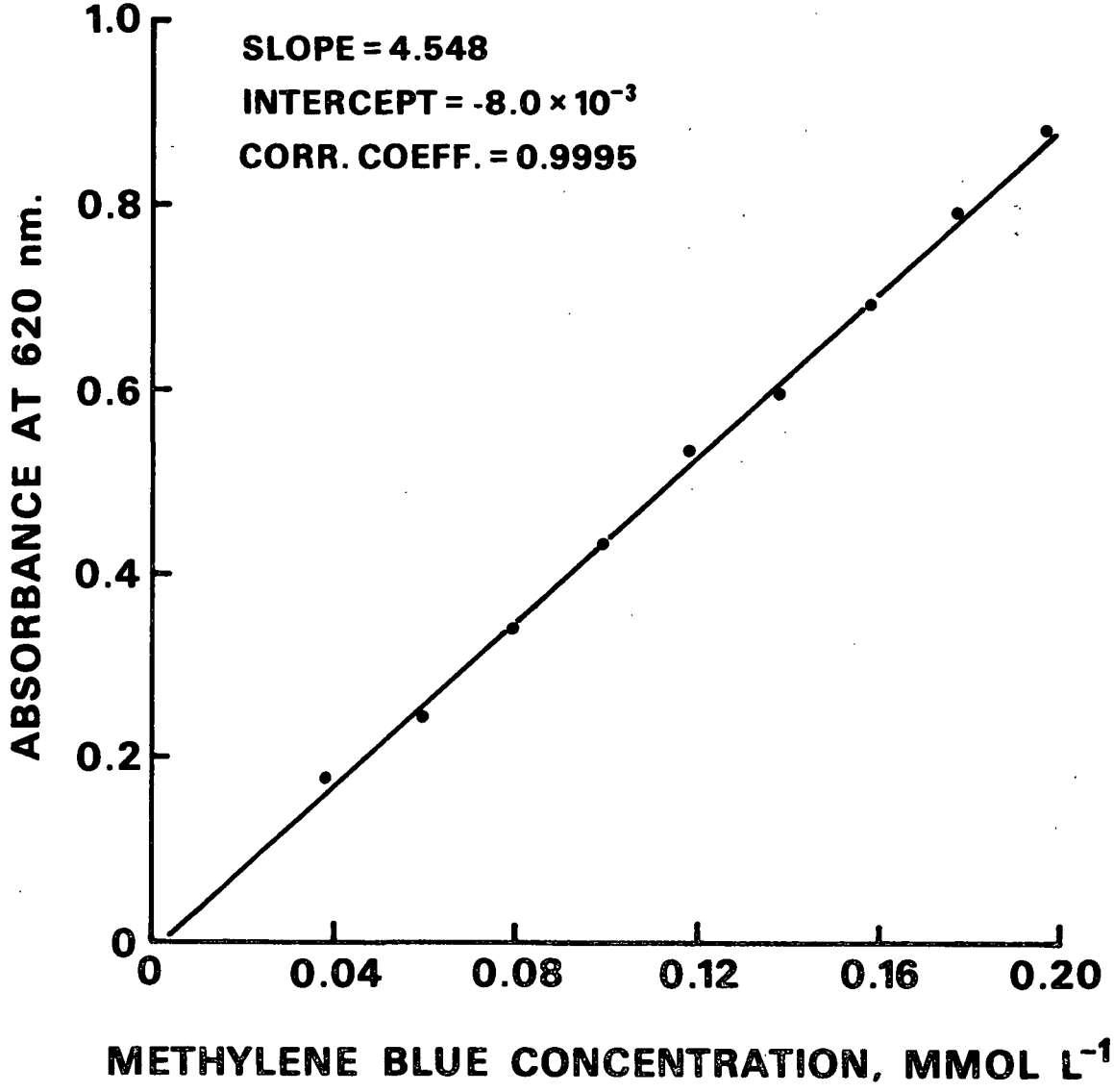

Figure 18. Methylene blue calibration plot.

A methylene blue-buffer solution was prepared by combining standard methylene blue solution (10 mL) and diethylbarbituric acid buffer solution (10 mL) in a 100-mL volumetric flask, and diluting to volume with distilled water. Two different quantities of each cellulose sample (5-20 mg) were carefully weighed into the coated vials, while simultaneously weighing parallel samples for moisture content determinations. Methylene blue-buffer solution (2.0 or 4.0 mL) was added to each sample. Sample weights and the volume of the methylene blue-buffer solution used were selected such that no more than 60% of the dye was consumed.

The vials were sealed and rotated end-over-end (ca. 30 rpm) for 16 hours. After centrifugation, an aliquot of the supernatant (0.50 mL) was transferred to a 5-mL volumetric flask containing 0.1M hydrochloric acid (0.50 mL) and diluted to volume with distilled water. The absorbance at 620 nm was measured, and the methylene blue concentration was calculated using Eq. (9). Since fresh methylene blue-buffer solution was prepared for each set of analyses, the initial methylene blue concentration was determined each time.

The percentage of methylene blue consumed was plotted against the oven-dry weight of sample. Using linear regression analysis, the quantity of sample which would consume exactly 50% of the dye was determined.[68] Acidic end group contents were then calculated using Eq. (10).

$$X_{ae} = V_{mb}\, W_m\, Y_s\, [MB]_o / 2\, W_s\, Y_z \qquad (10)$$

where X_{ae} = acidic end group content expressed as the mole fraction of monomer units at zero-time

V_{mb} = volume of methylene blue-buffer solution, L

W_m = molecular weight of anhydroglucose monomer unit, 162 g mol^{-1}

W_s = oven-dry sample weight that consumes 50% of the methylene blue, g

Y_s = degradation yield of sample, wt. %

Y_z = degradation yield of corresponding zero-time sample, wt. %

$[MB]_o$ = initial concentration of methylene blue, mol L^{-1}

Reducing End Groups

A portion of each cellulose sample (0.075 g) was stirred with dimethylsulfoxide (10 mL) and paraformaldehyde (0.5 g) in a 25-mL Erlenmeyer flask which was submersed in a 125°C oil bath. After a clear solution formed, additional dimethylsulfoxide (40 mL) was added, and the diluted methylol cellulose solution was filtered through a Whatman GF/C glass microfiber pad. After cooling, the cellulose was regenerated by dropwise addition of the methylol cellulose solution to a stirred 0.2M sodium methoxide-isopropoxide solution (200 mL). The precipitated cellulose was washed with 0.2M sodium methoxide-isopropoxide (100 mL), methanol (2 x 100 mL), 0.1M hydrochloric acid (150 mL), and distilled water (2 x 200 mL) by centrifugation and decantation.

Blanks for cellulose analyses were prepared by first mixing each substrate (0.05 g) with 0.25M sodium borohydride solution (50 mL) in a 125-mL polypropylene bottle. The bottle was mechanically shaken for 24 hours. Excess borohydride was decomposed by slowly adding 3M acetic acid (10 mL). The reduced cellulose was filtered on a Whatman GF/C glass microfiber pad, washed with 0.1M hydrochloric acid (50 mL) and distilled water (100 mL), and freeze-dried.

D-Glucose, D-glucitol, and cellulose samples (substrates, blanks, degraded samples, and regenerated degraded samples; 50 mg) were combined with distilled water (25 mL) in 125-mL polypropylene bottles. An aqueous solution (25 mL)

containing sodium borohydride (0.0189 g mL^{-1}) and sodium borohydride-^{3}H (New England Nuclear, 350 mCi $mmol^{-1}$, 0.007 mg mL^{-1}) was added, and the bottles were mechanically shaken for 24 hours.

The D-glucose reduction (D-glucitol was treated similarly as a blank) was terminated by adding IR-120 (H^{+}) resin (20 mL). After degassing overnight, the sample was filtered through a Whatman GF/C glass microfiber pad, concentrated to dryness on a rotary evaporator, and concentrated to dryness from methanol (20 mL) three times. The residue was dissolved in methanol (ca. 6 mL) and filtered through a glass microfiber pad. The filtrate was concentrated to ca. 0.5 mL on a rotary evaporator, dissolved in warm (60°C) absolute ethanol (ca. 6 mL), and concentrated in a rotary evaporator until crystallization started. Anhydrous ethyl ether (ca. 6 mL) was added to facilitate crystallization of the D-glucitol. The crystals were washed with anhydrous ethyl ether (2 x 6 mL), dried under vacuum, carefully weighed into 20-mL glass scintillation vials, and dissolved in distilled water (1.0 mL). Scintisol liquid scintillation cocktail (Isolab, Inc., 10 mL) was added, and the samples were analyzed for tritium content with a Beckman LS-100 scintillation system.

Cellulose reductions with sodium borohydride-borohydride-^{3}H were terminated by slowly adding 3M acetic acid (10 mL).[73] The radio-labelled, reduced cellulose was filtered on Whatman GF/C glass microfiber pads, washed with 0.1M hydrochloric acid (50 mL) and distilled water (100 mL), freeze-dried, and further dried in vacuo over phosphorus pentoxide.

The radio-labelled, reduced cellulose samples (ca. 50 mg) were soaked overnight in anhydrous trifluoroacetic acid (4 mL). The mixtures were refluxed until the cellulose was completely dissolved (ca. 15 min.). The solutions were

diluted with distilled water (1.5 mL), refluxed for 15 minutes, diluted with distilled water (12.4 mL), and refluxed for 30 minutes.[74] The resulting hydrolyzates were concentrated to dryness on a rotary evaporator, concentrated to dryness from distilled water (20 mL) three times, and transferred with distilled water (25 mL) to 125-mL polypropylene bottles. An aqueous solution (25 mL) of sodium borohydride (0.473 g) was added, and the bottles were mechanically shaken for 24 hours. The radio-labelled, reduced hydrolyzates were then isolated and analyzed for tritium content by the procedures used for D-glucose and D-glucitol.

The specific activities (counts min^{-1} mg^{-1}) of the samples were calculated, and the cellulose reducing end group contents were determined from Eq. (11), (12), and (13).

$$X_{are} = Y_c(A_c - A_{cb})/Y_z(A_g - A_{gb}) \quad (11)$$

$$X_{tre} = Y_c(A_{rc} - A_{cb})/Y_z(A_g - A_{gb}) \quad (12)$$

$$X_{ire} = X_{tre} - X_{are} \quad (13)$$

where X_{are} = accessible reducing end group content expressed as the mole fraction of monomer units at zero-time

X_{tre} = total reducing end group content expressed as the mole fraction of monomer units at zero-time

X_{ire} = inaccessible reducing end group content expressed as the mole fraction of monomer units at zero-time

Y_c = degradation yield of cellulose sample, wt. %

Y_z = degradation yield of corresponding zero-time sample, wt. %

A_c = specific activity of sugar from cellulose sample, counts min^{-1} mg^{-1}

A_{cb} = specific activity of sugar from cellulose blank, counts min^{-1} mg^{-1}

A_g = specific activity of reduced D-glucose, counts min^{-1} mg^{-1}

A_{gb} = specific activity of reduced D-glucitol (glucose blank), counts min^{-1} mg^{-1}

A_{rc} = specific activity of sugar from regenerated cellulose sample, counts min^{-1} mg^{-1}

Degree of Polymerization

Cellulose samples (31.3 mg) were weighed into 30-mL glass hypovials (Pierce Chemical Co.) and dried *in vacuo* over phosphorus pentoxide *ca.* 12 hours. Anhydrous pyridine (12.5 mL) and phenyl isocyanate (0.75 mL) were added to the vials, and the vials were flushed with nitrogen and sealed with Teflon-silicone septa using aluminum crimp caps (Pierce Chemical Co.). The vials were then placed in stainless steel pressure vessels which were rotated end-over-end at *ca.* 3 rpm in an 80°C oil bath for 48 hours.[65]

The reaction solutions were cooled, and methanol (0.35 mL) was added to react with excess phenyl isocyanate. The solutions were diluted with p-dioxane (35 mL), filtered through Whatman GF/C glass microfiber pads, and added dropwise to stirred methanol (200 mL) containing glacial acetic acid (1.25 mL). The precipitated cellulose carbanilates were washed with methanol (100 mL) containing acetic acid (0.625 mL), distilled water (100 mL) containing acetic acid (0.625 mL), and distilled water (2 x 200 mL) by centrifugation and decantation; transferred with distilled water (*ca.* 20 mL) to tared 50-mL Erlenmeyer flasks; and freeze-dried.[65]

The cellulose carbanilates (8 mg) and an internal reference, methyl N-phenylcarbamate (0.007 mg),[65] were dissolved in reagent grade tetrahydrofuran (5 mL). The resulting solutions were eluted on Styragel columns (Water Associates) having nominal exclusion limits of 10^3, 10^4, 10^5, 10^6, and 10^7 Å,

and capable of resolving polymers in the molecular weight range of 1×10^3 to $> 2 \times 10^7$. Freshly purified tetrahydrofuran[67] was pumped through the columns at 2.0 mL min^{-1} with a Waters 6000A pump. A Perkin-Elmer LC-55B spectrophotometer equipped with a flow cell and operating at 235 nm was used as the detector.

The Styragel columns were calibrated by a dispersion-compensated universal technique[75,76] using ten nearly monodisperse polystyrene standards with molecular weights ranging from 4.8×10^3 to 3.6×10^6. Mark-Houwink constants, K and α, used in the calibration were 1.18×10^{-2} cm^3 g^{-1} and 0.74, respectively, for polystyrene, and 2.01×10^{-3} cm^3 g^{-1} and 0.92, respectively for cellulose tricarbanilate.[77] The chromatograms were evaluated numerically by computer,[75,78] providing number- and weight-average DP values and plots of normalized molecular weight distributions.

Hydroxyl Accessibility

The analytical method was calibrated with 19 standard deuterium oxide-water solutions (0.05-1.00 mole % D) prepared by volumetric addition of deuterium oxide (99.8 mole % D) to sealed vessels containing distilled water. The infrared spectrum (obtained with the calcium fluoride liquid cell) of the distilled water was subtracted from the spectra of the standard solutions. The absorbance at 2773 cm^{-1} (baseline point) was subtracted from the absorbance at 2510 cm^{-1} (O-D stretching band) to obtain relative absorbance values. The plot of mole fraction deuterium (D/D+H) *versus* relative absorbance (Fig. 19) was linear [Eq. (14)] and had a correlation coefficient of 0.9996.

$$X_d = (A_r - 0.004905)/32.35 \qquad (14)$$

where X_d = mole fraction of deuterium (D/D+H)

A_r = relative absorbance

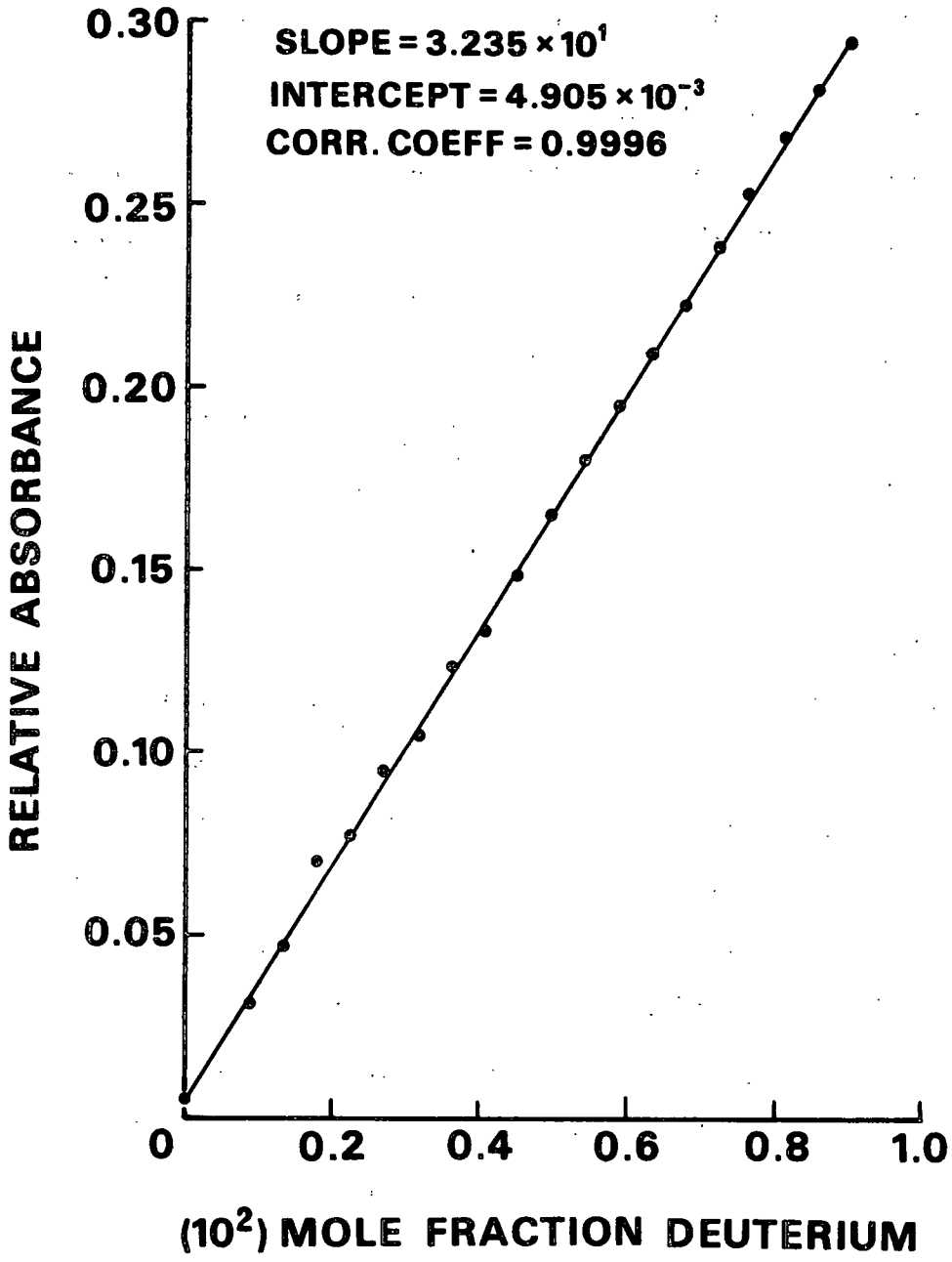

Figure 19. Deuterium oxide-water calibration plot.

The procedure of Rouselle and Nelson[79] was utilized with minor modifications to determine cellulose hydroxyl accessibility. Cellulose samples (50 mg) were carefully weighed into 4-mL glass vials which were sealed with Teflon-silicone septa (Pierce Chemical Co.), while parallel samples were weighed for moisture content determinations. Deuterium oxide (99.8 mole % D, 2 mL) was added to the vials by syringe. The vials were rotated end-over-end at ca. 30 rpm for 12 hours and then placed in a 60°C vacuum oven purged with dry nitrogen. The caps were removed from the vials, the oven door was quickly sealed, and the oven was evacuated. During the drying process, the oven was occasionally flushed with dry nitrogen to remove accumulated deuterium oxide vapor. After ca. 24 hours, the oven was filled with dry nitrogen, the oven door was opened, and the vials were quickly sealed as the oven was purged with dry nitrogen.

After cooling, 20% sodium hydroxide solution (2 mL) was added to the vials by syringe, and the vials were rotated end-over-end at ca. 30 rpm for 12 hours. After centrifugation, the supernatant (ca. 1 mL) was removed by syringe and distilled in a short-path distillation apparatus (Kontes K-548250) which had been purged with dry nitrogen. The distillates were quickly transferred to clean 4-mL glass vials, and the vials were sealed with Teflon-silicone septa (Pierce Chemical Co.). The infrared spectrum (obtained with the calcium fluoride liquid cell) of freshly distilled water was subtracted from the spectra of the distilled sample extracts. The mole fractions of deuterium in the sample extracts were then calculated using Eq. (14).

The percentage of cellulose hydroxyl groups deuterated is described by Eq. (15).

$$A_{OH} = 100\% \times (D/OH) \quad (15)$$

where A_{OH} = cellulose hydroxyl accessibility, %

D = deuterium content of sample extract, mol D

OH = hydroxyl content of cellulose sample, mol OH

The hydroxyl content of the cellulose sample can be calculated with Eq. (16).

$$OH = W_c F_c / M_{OH} \quad (16)$$

where W_c = cellulose sample wt., g

F_c = weight fraction of dry cellulose in sample

M_{OH} = weight of cellulose containing one mole of hydroxyl groups, 54 g cellulose/mol OH

The deuterium content of the sample extract is described by Eq. (17).

$$D = HX_D/(1-X_D) \quad (17)$$

where H = hydrogen content of sample extract, mol H

The hydrogen content of the sample extract can be calculated with Eq. (18).

$$H = H_N + H_P + H_M \quad (18)$$

where H_N = hydrogen content of 2 mL of 20% NaOH, 0.229 mol H

H_P = hydrogen ions displaced from hydroxyls of ca. 50 mg cellulose, 0.001 mol H

H_M = hydrogen content of moisture in initial cellulose sample, mol H

The hydrogen content of moisture (water) in the cellulose sample prior to deuteration is described by Eq. (19).

$$H_M = W_c F_w / (9\ g.H_2O/mol\ H) \quad (19)$$

where F_W = weight fraction of water in cellulose sample

Equation (20), obtained by combining Eq. (15) through (19), was then used to calculate cellulose hydroxyl accessibility.

$$A_{OH} = [5400\ X_d / W_c F_c (1-X_d)][0.2230 + (W_c F_w / 9)] \quad (20)$$

Degree of Methylol Substitution

The degree of methylol substitution of the regenerated (amorphous) hydrocellulose was determined by the chromotropic acid-formaldehyde analysis developed by the Analytical Department of The Institute of Paper Chemistry. The use of chromotropic acid to detect formaldehyde has been described by Walker.[80]

The analytical method was calibrated with 8 standard formaldehyde solutions (0-10 mg L^{-1}) prepared by volumetric addition of 37% (w/w) formaldehyde stock solution to sealed vessels containing distilled water. The standard solutions (25 mL) were mixed with 85% phosphoric acid (2.5 mL) and distilled. The distillate (ca. 16 mL) was collected in an ice-cooled volumetric flask containing distilled water (ca. 4 mL) and diluted to 25 mL with distilled water. An aliquot of the diluted distillate (0.5 mL) was mixed with 0.5% (w/v) chromotropic acid solution (0.4 mL) and 81% sulfuric acid (3.2 mL), and the resulting solution was heated at 60°C for 20 minutes in a constant temperature water bath. Absorbance of the solution at 570 nm was measured with a Perkin-Elmer 320 spectrophotometer using a silica cell (1.0 cm pathlength) and a reference solution consisting of distilled water (1.8 mL) and 81% sulfuric acid (6.4 mL). Formaldehyde concentration (standard solutions) was plotted versus absorbance (Fig. 20). A linear calibration [Eq. (21)] was obtained with a 0.9965 correlation coefficient.

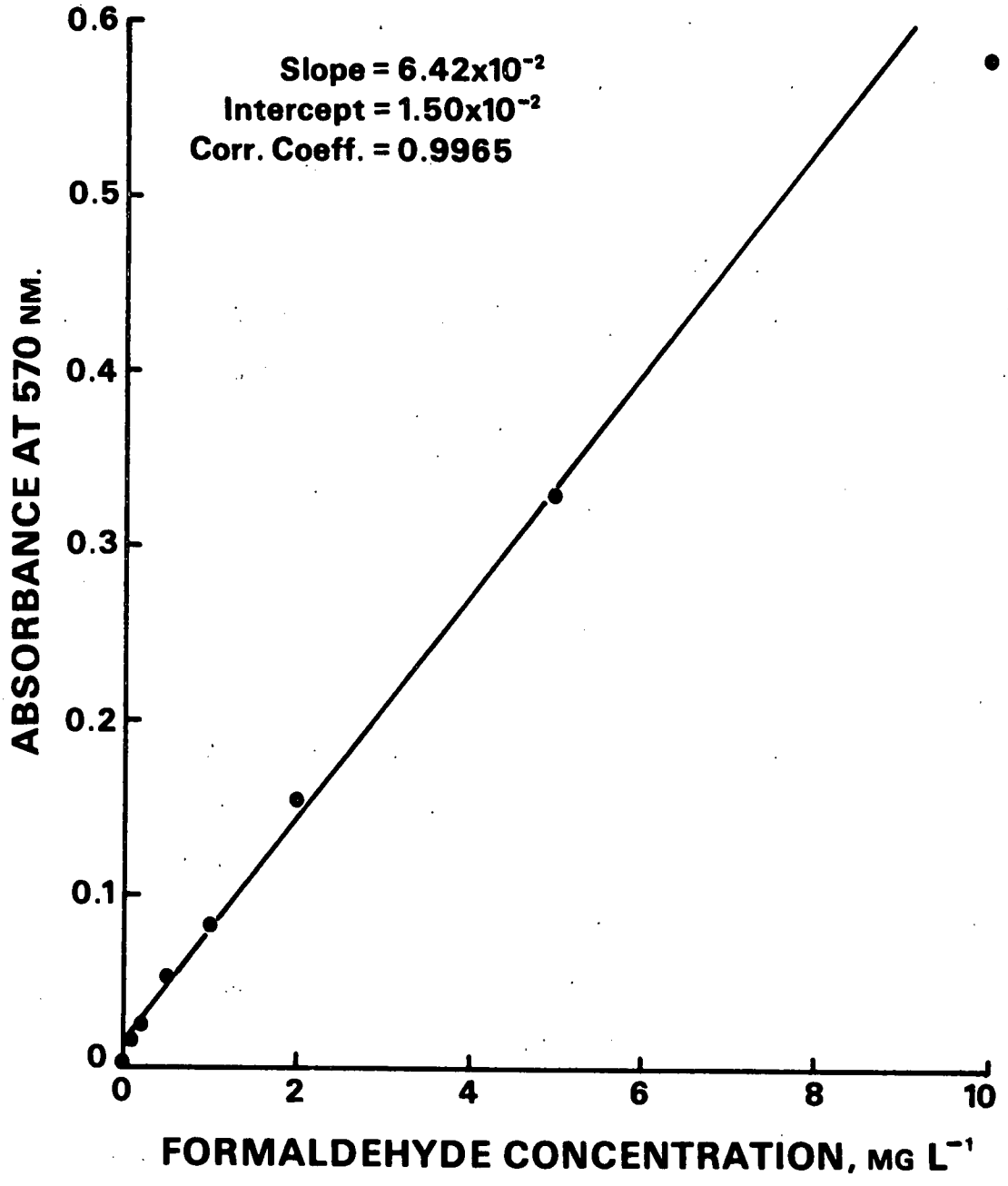

Figure 20. Formaldehyde calibration plot.

$$[F] = (A_{570} - 0.015)/0.0642 \quad (21)$$

where [F] = formaldehyde concentration (standard solutions), mg L^{-1}

A_{570} = absorbance at 570 nm.

Regenerated hydrocellulose (0.1 g) was combined with distilled water (12.5 mL) and 85% phosphoric acid (2.5 mL). The mixture was refluxed for 1 hour and then distilled. The first two portions of the distillate (ca. 8 mL) were collected in ice-cooled volumetric flasks containing distilled water and diluted to 10 mL with distilled water. Aliquots of the diluted distillates (0.5 mL) were mixed with 0.5% (w/v) chromotropic acid solution (0.4 mL) and 81% sulfuric acid (3.2 mL), and the resulting solutions were heated at 60°C for 20 minutes. The absorbance at 570 nm was measured, and the formaldehyde concentration was calculated using Eq. (21). The quantity of formaldehyde in the two portions of the distillate was calculated, and the degree of methylol substitution of the regenerated hydrocellulose was calculated using Eq. (22).

$$DS = M_f/M_n \quad (22)$$

where DS = degree of methylol substitution

M_f = total formaldehyde content of the two distillates, mol

M_n = number of monomer units in the cellulose sample (0.1 g), 6.17×10^{-4} mol

ACKNOWLEDGMENTS

The author gratefully acknowledges the assistance of his thesis advisory committee: Drs. L. R. Schroeder, R. H. Atalla, and N. S. Thompson. In particular, the author sincerely appreciates the encouragement, guidance, and dedication of his committee chairman, Dr. L. R. Schroeder.

The author wishes to thank Mrs. J. Swinford for her excellent skills and patience in typing and editing this manuscript. The author also acknowledges the many other faculty members, staff personnel, and fellow students for their valuable assistance and friendship during the course of this work.

The author recognizes and appreciates the financial support provided by The Institute of Paper Chemistry, made possible through contributions from the member companies.

For their continued love, prayers, encouragement, and personal guidance, the author expresses his sincere appreciation to his family and friends. In particular, the author extends his most sincere thanks to his wife, Carole, and son, Nicholas, for their love and sacrifices throughout the course of this research.

LITERATURE CITED

1. Bryce, J. R. G., In Casey's Pulp and paper chemistry and chemical technology. 3rd ed., Vol. I, p. 377, Wiley-Interscience, N.Y., 1980.

2. Rydholm, S. A., Pulping Processes, Interscience, New York, 1965.

3. Sanyer, N.; Chidester, G. H., In Browning's The chemistry of wood. p. 441, Interscience, N.Y., 1963.

4. Matthews, C. H., Svensk Papperstid. 17:629-35(1974).

5. Meller, A., Holzforschung 14(5):78-89(1960), and references cited therein.

6. Albertsson, U.; Samuelson, O., Svensk Papperstid. 24:1001-4(1962).

7. Haas, D. W.; Hrutfiord, B. F.; Sarkanen, K. V., J. Appl. Polymer Sci. 11:587-600(1967).

8. Johansson, M. H.; Samuelson, O., J. Appl. Polymer Sci. 19:3007-13(1975).

9. Sjostrom, E., Tappi 60(9):151-4(1977), and references cited therein.

10. Lai, Y.-Z.; Sarkanen, K. V., Cellulose Chem. Technol. 1:517-27(1967).

11. Colbran, R. L.; Davidson, G. F., J. Textile Inst. 52:T73-87(1961).

12. a) Brandon, R. E.; Schroeder, L. R.; Johnson, D. C., Cellulose Technology Research, ACS Symp. Ser. 10:125-46(1975).
b) Brandon, R. E. Alkaline degradation of 1,5-anhydrocellobiitol, Doctoral Dissertation, The Institute of Paper Chemistry, Appleton, WI, 1973.

13. Gilbert, F. A. Mechanisms of high temperature alkaline degradation of methyl α-D-glucopyranoside and 1,6-anhydro-β-D-glucopyranose, Doctoral Dissertation, The Institute of Paper Chemistry, Appleton, WI, 1975.

14. a) MacLeod, J. M.; Schroeder, L. R., J. Wood Chem. Technol. 2(2):187-205(1982).
b) MacLeod, J. M., Anaerobic alkaline degradation of D-glucose, cellobiose, and derivatives, Doctoral Dissertation, The Institute of Paper Chemistry, Appleton, WI, 1975.

15. Nault, J. J. Alkaline degradation of methyl β-D-glucopyranoside and methyl 2-O-methyl-β-D-glucopyranoside, Doctoral Dissertation, The Institute of Paper Chemistry, Appleton, WI, 1979.

16. Blythe, D. A. An investigation of the role of sodium sulfide in cellulosic chain cleavage during kraft pulping, Doctoral Dissertation, The Institute of Paper Chemistry, Appleton, WI, 1984.

17. Segal, L., In Bikales and Segal's Cellulose and cellulose derivatives. Part V, p. 719, Wiley-Interscience, N.Y., 1971.

18. Sharples, A., In Bikales and Segal's Cellulose and cellulose derivatives, Part V, p. 991, Wiley-Interscience, N.Y., 1971.

19. Machell, G.; Richards, G. N., Tappi 41(1):12-16(1958).

20. Colvin, J. R., In Bikales and Segal's Cellulose and cellulose derivatives. Part IV, p. 695, Wiley-Interscience, N.Y., 1971, and references cited therein.

21. Mark, H., In Ott and Spurlin's Cellulose. Part I, 2nd ed., p. 217, Interscience, N.Y., 1954, and references cited therein.

22. Rowland, S. P., In Rowell and Young's Modified cellulosics. Part III, p. 162, Academic Press, N.Y., 1978.

23. Frey-Wyssling, A., Submicroscopic Morphology of Protoplasm and its Derivatives, Elsevier, N.Y., 1948.

24. Hermans, P. H., J. Phys. Chem. 45:827-36(1941).

25. Herrman, K.; Gerngross, O.; Abitz, W., Z. Phys. Chem. B10:371-94(1930).

26. Scallan, A. M., Textile Res. J. 41:647-53(1971).

27. Lin, S., Fibre Sci. Technol. 5:303-14(1972).

28. Lewin, M.; Roldan, L., Text. Res. J. 45:308(1975).

29. Chadambareswaran, P.; Patil, N.; Sudaram, V., J. Appl. Polymer Sci. 20:2297-8(1976).

30. Jeffries, R.; Jones, D.; Roberts, J.; Selby, K.; Simmens, S.; Warwicker, J., Cellulose Chem. Technol. 3:255-74(1969).

31. Rowland, S.; Roberts, E.; Bose, J.; Wade, C., J. Polymer Sci. (A-1) 9:1623-33(1971).

32. Rowland, S.; Roberts, E., J. Polymer Sci. (A-1) 10:2447-61(1972).

33. McBurney, L. F., In Ott and Spurlin's Cellulose. Part I, 2nd ed., p. 130, Interscience, N.Y., 1954.

34. Phillip, B.; Dan, D. C.; Fink, H.-P., International Symposium on Wood and Pulping Chemistry, Stockholm, Sweden, June, 1981.

35. Sihtola, H.; Neimo, L., Symposium on Enzymatic Hydrolysis of Cellulose, Session 1, p. 16, Aulanko, Finland, March, 1975.

36. Philipp, B.; Jacopian, V.; Loth, F.; Hirte, W.; Schulz, G., ACS Advances in Chemistry Series 181, p. 127, 1979.

37. Manley, R. St. J., J. Polymer Sci. (A-2) 9:1025-59(1971), and references cited therein.

38. Chang, M. M. Y., J. Polymer Sci. (Polymer Chem. Ed.) 12:1349-74(1974).

39. Manley, R. St. J., J. Polymer Sci. (Polymer Phys. Ed.) 12:1347-54(1974).

40. Ahmed, A. V.; Rapson, W. H., J. Polymer Sci. (A-1) 9:2299-2304(1971).

41. Goldthwait, C. F., In Ward's Chemistry and chemical technology of cotton. p. 373, Interscience, N.Y., 1955.

42. Tripp, V. M., In Bikales and Segal's Cellulose and cellulose derivatives. Part IV, p. 305, Wiley-Interscience, N.Y., 1971.

43. Colvin, J. R., J. Polymer Sci. (Polymer Letters) 4:747-54(1966).

44. Atalla, R. H., Proceedings of the International Symposium on Wood and Pulping Chemistry, Vol. I, p. 57, Stockholm, June, 1981.

45. Atalla, R. H., J. Appl. Polymer Sci. (Appl. Polymer Symp.) 37:295-301 (1983).

46. VanderHart, D. L.; Atalla, R. H., Proceedings of the International Dissolving and Specialty Pulps Conference, p. 207, TAPPI Press, Atlanta, 1983.

47. Warwicker, J. O., In Bikales and Segal's Cellulose and cellulose derivatives. Part IV, p. 325, Wiley-Interscience, N.Y., 1971.

48. Dimick, B. E. The importance of the structure of alkali metal hydroxide solutions in decrystallizing cellulose I, Doctoral Dissertation, The Institute of Paper Chemistry, Appleton, WI, 1976.

49. Richards, G. N., In Bikales and Segal's Cellulose and cellulose derivatives. Part V, p. 1007, Wiley-Interscience, N.Y., 1971.

50. Machell, G.; Richards, G. N.; Sephton, H. H., Chem. and Ind. 467-9(1957).

51. Machell, G.; Richards, G. N., J. Chem. Soc. 4500-6(1957).

52. Johansson, M. H.; Samuelson, O., Carbohyd. Res. 34:33-43(1974).

53. Lai, Y.-Z.; Ontto, D. E., J. Appl. Polymer Sci. 23:3219-25(1979).

54. Franzon, O.; Samuelson, O., Svensk Papperstid. 60:872-7(1957).

55. Christofferson, K.; Samuelson, O., Svensk Papperstid. 65:517-20(1962).

56. Corbett, W. M.; Richards, G. N., Svensk Papperstid. 60:791-4(1957).

57. Ward, K., In Ott and Spurlin's Cellulose. 2nd Ed., Part I, p. 9, Interscience, N.Y., 1954.

58. Corbett, W. M., In Whistler's Methods in carbohydrate chemistry, Vol. III, p. 3, Academic Press, N.Y., 1963.

59. Green, J. W., In Whistler's Methods in carbohydrate chemistry, Vol. III, p. 9, Academic Press, N.Y., 1963.

60. a) Nicholson, M. D.; Johnson, D. C.; and Haigh, F. C., Appl. Polymer Symp. 28:931-43(1976).
b) Nicholson, M. D. Reactions of cellulose in the dimethylsulfoxide-paraformaldehyde (DMSO-PF) solvent, Doctoral Dissertation, The Institute of Paper Chemistry, Appleton, WI, 1975.

61. a) Baker, T. J.; Schroeder, L. R.; Johnson, D. C., Cellulose Chem. Technol. 15:311-20(1981).
b) Baker, T. J. Formation and reactions of methylol cellulose, Doctoral Dissertation, The Institute of Paper Chemistry, Appleton, WI, 1979.

62. Wadsworth, L. C.; Cuculo, J. A., In Rowell and Young's Modified cellulosics. Part III, p. 117, Academic Press, N.Y., 1978.

63. Howsmon, J. A.; Sisson, W. A., In Ott and Spurlin's Cellulose. Part I, 2nd Ed., p. 231, Interscience, N.Y., 1954.

64. Earl, W. L.; VanderHart, D. L., Macromolecules 14:570-4 (1981).

65. Schroeder, L. R.; Haigh, F. C., Tappi 62(10):103-5(1979).

66. TAPPI Standard Method T 211 M-58, Ash content of pulp, 1958.

67. Perrin, D. D.; Armarego, W. L. F.; Perrin, D. R., Purification of Laboratory Chemicals, Pergamon Press, N.Y., 1966.

68. TAPPI Standard Method T 237 su-63, Carboxyl content of cellulose, 1963.

69. Fritz, J. S.; Schenk, G. H., Quantitative Analytical Chemistry, Allyn and Bacon, Inc., Boston, 1968.

70. Davidson, G. F., J. Textile Inst. 38:T408-18(1947).

71. Corbett, W. M., In Whistler's Methods in carbohydrate chemistry. Vol. III, p. 3, Academic Press, N.Y., 1963.

72. Conrad, C. M., In Ward's Chemistry and chemical technology of cotton. p. 15, Interscience, N.Y., 1955.

73. Richards, G. N.; Whelan, W. J., Carbohyd. Res. 27:185-91(1973).

74. Fengel, D.; Wegener, G.; Heizmann, A.; Przyklenk, M., Holzforschung 31(3):65-71(1977).

75. a) Ring, G. J. F.; Stratton, R. A.; Schroeder, L. R., J. Liquid Chromat. 6(3):401-24(1983).
b) Ring, G. J. F. The molecular weight distributions of bacterial cellulose as a function of synthesis time, Doctoral Dissertation, The Institute of Paper Chemistry, Appleton, WI, 1980.

76. McCrackin, F. L., J. Appl. Polymer Sci. 21:191-8(1977).

77. Valtasaari, L.; Saarela, K., Paperi Puu 57:5-10(1975).

78. Arbin, F. L. A. The effect of oxygen and anthraquinone on the alkaline depolymerization of amylose, Doctoral Dissertation, The Institute of Paper Chemistry, Appleton, WI, 1980.

79. Rouselle, M. A.; Nelson, M. L., Textile Res. J. 41:599-604(1971).

80. Walker, J. F., Formaldehyde, 3rd Edition, p. 469, Robert E. Krieger Publishing Co., Inc., N.Y., 1975.

81. Lewis, H. F.; Ritter, G. J., In Ott and Spurlin's Cellulose. Part I, 2nd Ed., p. 443, Interscience, N.Y., 1954.

82. Huwyler, H. R.; Franz, G.; Meier, H., Planta 146(5):635-42(1979).

83. Dean, J. A., Ed. Lange's Handbook of Chemistry. 13th Ed., p. 5-5, McGraw-Hill Book Co., N.Y., 1985.

84. Weast, R. C., Ed., CRC Handbook of Chemistry and Physics. 56th Ed., p. F-209 and F-213, CRC Press, Inc., N.Y., 1975.

APPENDIX I

ESTIMATION OF PECTIC MATERIAL IN HYDROCELLULOSE SUBSTRATES

During the initial stages of degradation of the fibrous hydrocellulose in 1.0M sodium hydroxide at 60 and 80°C, the carboxylic acid contents (Tables 13-16, Appendix II) decreased. In addition, the carboxylic acid content remained relatively constant during the early periods of the amorphous hydrocellulose degradations. Since the number of carboxylic acids increased during the later periods of the degradations of both substrates, it was apparent that chemical stopping was occurring. Thus, chemical stopping must also have occurred during the initial periods, and the measure of chemical stopping (i.e., formation of acidic end groups) must have included a negative component due to simultaneous removal of pectic material which contains carboxylic acid groups.

In a study of alkaline cellulose degradation, Johansson and Samuelson[8] observed that pectic materials, which were not removed during purification, were removed during the initial stages of alkaline degradation. Since the pectic material in cotton fibers is thought to be composed of ca. 70-80% polygalacturonide,[80,81] removal of small quantities during alkaline degradation would cause a significant decrease in the carboxylic acid content of the fibers.

Losses of pectic material could interfere with the assessment of alkaline reactions in at least two ways. First, since yield loss gives the measure of peeling, the apparent rate and extent of peeling would be inflated. Second, losses of carboxylic acids associated with the pectic material would introduce a negative component into the measure of chemical stopping. The effect for chemical stopping would be the most significant, since monomer units in ca. 70-80% of the pectic material contain a carboxylic acid group. Assuming that this was

true, the kinetic model was used to predict the numbers of acidic functional groups associated with the pectic material during the early reaction periods.

According to Eq. (3), plots of yield loss versus acidic end groups should be linear, because peeling and chemical stopping are both dependent on the number of accessible reducing end groups. These plots are shown in Fig. 21 for both substrates at both reaction temperatures.

$$d[Y_L]/d[AE] = k_p/k_{cs} \qquad (3)$$

Using linear regression analysis, the linear portions of the plots in Fig. 21 (shown with heavy lines) were extended to zero-yield loss (shown with dashed lines). The experimentally determined yield loss values for the substrates during the initial periods were then used to calculate the corresponding acidic end group contents. The estimated acidic end group contents are presented in Table 11. By subtracting the estimated acidic end group contents from the experimentally determined acidic end group contents of the substrates during the early reaction periods (Tables 13-16, Appendix II), the numbers of carboxyl groups associated with the pectic material (Table 12) were determined. The degradation samples for the experimental sampling times following the last entries in Tables 11 and 12 were considered to have undergone complete removal of pectic material.

As would be expected, the estimated acidic end group contents of both substrates at zero-time are greater for the 80°C zero-time samples due to more extensive chemical stopping during the heat-up period. In addition, the estimated numbers of carboxyl groups associated with the pectic material at zero-time are similar in all cases. Thus, the estimation procedure appears to be valid.

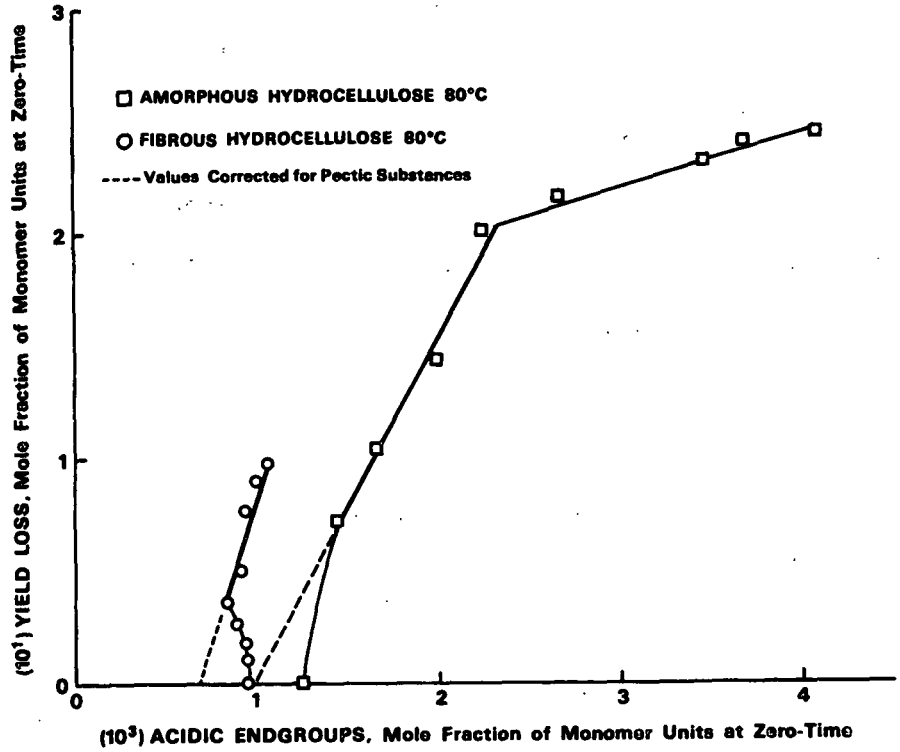

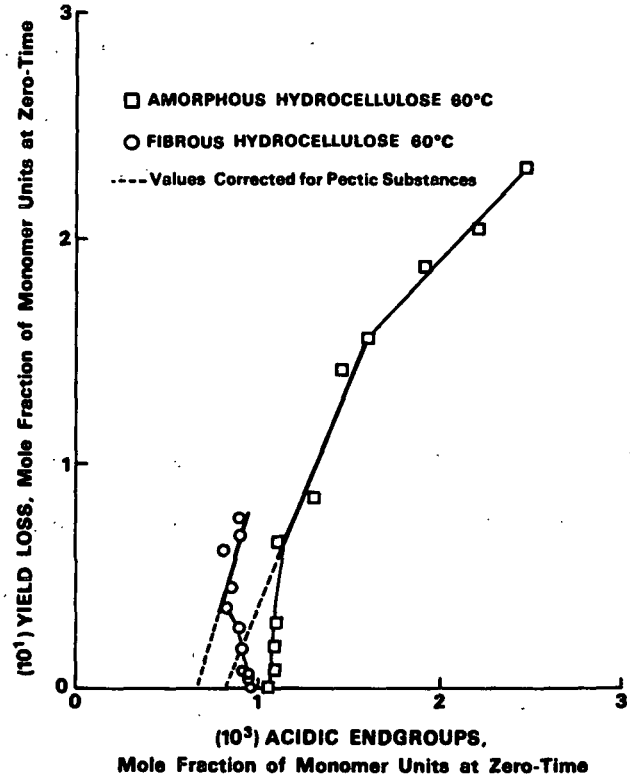

Figure 21. Yield loss [Y_L] versus acidic end groups [AE] during hydrocellulose degradation in 1.0M sodium hydroxide.

Table 11. Estimated acidic end group contents.[a]

Reaction Time, hours	Fibrous Hydrocellulose 60°C	Fibrous Hydrocellulose 80°C	Amorphous Hydrocellulose 60°C	Amorphous Hydrocellulose 80°C
0	0.66	0.68	0.83	0.98
0.5	0.68	0.72	0.87	--
1	0.68	0.75	0.92	--
2	0.69	0.78	0.96	--
4	0.72	--	--	--
8	0.75	--	--	--

[a]Values expressed as 10^3 x mole fraction of total monomer units at zero-time.

Table 12. Estimated carboxyl groups of pectic material.[a]

Reaction Time, hours	Fibrous Hydrocellulose 60°C	Fibrous Hydrocellulose 80°C	Amorphous Hydrocellulose 60°C	Amorphous Hydrocellulose 80°C
0	0.30	0.26	0.23	0.27
0.5	0.28	0.21	0.23	--
1	0.27	0.19	0.19	--
2	0.23	0.11	0.13	--
4	0.21	--	--	--
8	0.14	--	--	--

[a]Values expressed as 10^3 x mole fraction of total monomer units at zero-time.

Assuming that monomer units containing carboxyl groups comprised 70% of the total monomer units in the pectic material, the contributions of pectic material losses to the yield losses during the initial periods were determined. This was accomplished by dividing the total number of monomer units in the pectic material at zero-time by the yield loss (in monomer units) for the first degradation sample which contained no pectic material. The pectic material losses were found to comprise 0.5-1.2% of the total number of monomer units lost during the early reaction periods. Thus, it is concluded that pectic material

losses were insignificant compared to the yield losses due to peeling. However, to compensate for the substantial effects of pectic material losses on the acidic end group contents, the estimated acidic end group contents (Table 11) were used in place of the experimentally determined values for the substrates during the initial periods (Table 13-16, Appendix II).

APPENDIX II

EXPERIMENTAL DATA

This section contains the experimental data for the fibrous and amorphous hydrocelluloses during degradation in oxygen-free 1.0M sodium hydroxide at 60 and 80°C. Yield (relative to the average yield of duplicate zero-time samples), reducing end group contents (accessible, inaccessible, and total), acidic end group contents (not corrected for pectic material losses), and total end group contents (not corrected for pectic material losses) are presented in Tables 13-16. Hydroxyl accessibility values are presented in Tables 17 and 18.

Table 13. Yield[a] and end group[b] values for fibrous hydrocellulose during degradation in 1.0M sodium hydroxide at 60°C.

Reaction Time, hours	Yield	Accessible Reducing End Groups	Inaccessible Reducing End Groups	Total Reducing End Groups	Acidic End Groups	Total End Groups
0[c]	0.999	1.09	0.15	1.24	0.98	2.22
0[c]	1.001	1.19	0.12	1.31	0.94	2.25
0.5	0.996	1.15	0.17	1.32	0.95	2.27
1	0.994	1.00	0.26	1.26	0.95	2.21
2	0.993	1.08	0.15	1.23	0.92	2.15
4[c]	0.981	1.00	0.35	1.35	0.93	2.28
4[c]	0.987	1.00	0.24	1.24	0.93	2.17
8	0.974	1.01	0.28	1.29	0.90	2.19
24[c]	0.964	0.81	0.29	1.10	0.83	1.93
24[c]	0.967	0.76	0.37	1.13	0.84	1.97
48	0.955	0.71	0.37	1.08	0.85	1.93
96	0.939	0.64	0.40	1.04	0.82	1.86
120	0.933	0.51	0.56	1.07	0.90	1.97
168	0.925	0.35	0.66	1.01	0.89	1.90

[a]Yield values = mole fraction of total monomer units at zero-time.
[b]End group values = 10^3 x mole fraction of total monomer units at zero-time.
[c]Duplicate cooks.

Table 14. Yield[a] and end group[b] values for fibrous hydrocellulose during degradation in 1.0M sodium hydroxide at 80°C.

Reaction Time, hours	Yield	Accessible Reducing End Groups	Inaccessible Reducing End Groups	Total Reducing End Groups	Acidic End Groups	Total End Groups
0[c]	0.998	1.01	0.16	1.17	0.93	2.10
0[c]	1.002	1.07	0.15	1.22	0.97	2.19
0.5	0.989	0.93	0.19	1.12	0.94	2.06
1	0.982	0.75	0.40	1.15	0.94	2.09
2	0.975	0.73	0.45	1.18	0.88	2.06
4	0.963	0.55	0.52	1.07	0.83	1.90
8[c]	0.953	0.44	0.60	1.04	0.91	1.95
8[c]	0.947	0.44	0.62	1.06	0.91	1.97
24	0.923	0.27	0.68	0.95	0.94	1.89
48[c]	0.909	0.21	0.67	0.88	1.02	1.90
48[c]	0.910	0.20	0.71	0.91	0.97	1.88
96	0.903	0.16	0.66	0.82	1.07	1.89

[a]Yield values = mole fraction of total monomer units at zero-time.
[b]End group values = 10^3 x mole fraction of total monomer units at zero-time.
[c]Duplicate cooks.

Table 15. Yield[a] and end group[b] values for amorphous hydrocellulose during degradation in 1.0M sodium hydroxide at 60°C.

Reaction Time, hours	Yield	Accessible Reducing End Groups	Inaccessible Reducing End Groups	Total Reducing End Groups	Acidic End Groups	Total End Groups
0[c]	0.999	3.33	-0.01	3.32	1.09	4.41
0[c]	1.001	3.27	0.01	3.28	1.03	4.31
0.5	0.992	2.89	0.00	2.89	1.10	3.99
1	0.982	2.66	0.00	2.66	1.10	3.76
2	0.972	2.48	0.04	2.52	1.10	3.62
4[c]	0.932	2.29	0.00	2.29	1.11	3.40
4[c]	0.938	2.34	0.02	2.36	1.13	3.49
8	0.916	1.95	0.26	2.21	1.31	3.52
24[c]	0.861	1.58	0.55	2.13	1.45	3.58
24[c]	0.857	1.63	0.50	2.13	1.47	3.60
48	0.845	1.31	0.74	2.05	1.60	3.65
96	0.813	1.18	0.66	1.84	1.92	3.76
120	0.796	1.04	0.77	1.81	2.22	4.03
168	0.769	0.78	0.84	1.62	2.47	4.09

[a]Yield values = mole fraction of total monomer units at zero-time.
[b]End group values = 10^3 x mole fraction of total monomer units at zero-time.
[c]Duplicate cooks.

Table 16. Yield[a] and end group[b] values for amorphous hydrocellulose during degradation in 1.0M sodium hydroxide at 80°C.

Reaction Time, hours	Yield	Accessible Reducing End Groups	Inaccessible Reducing End Groups	Total Reducing End Groups	Acidic End Groups	Total End Groups
0[c]	1.001	3.53	-0.08	3.45	1.31	4.76
0[c]	0.999	3.60	0.02	3.62	1.20	4.82
0.5	0.928	2.81	0.05	2.86	1.43	4.29
1	0.896	2.16	0.47	2.63	1.66	4.29
2	0.857	1.96	0.41	2.37	1.98	4.35
4	0.799	1.37	0.74	2.11	2.24	4.35
8[c]	0.788	1.02	0.7	1.74	2.71	4.45
8[c]	0.783	1.11	0.69	1.80	2.63	4.43
24	0.769	0.82	0.68	1.50	3.46	4.96
48[c]	0.755	0.61	0.75	1.36	3.61	4.97
48[c]	0.766	0.62	0.75	1.37	3.76	5.13
96	0.757	0.53	0.76	1.29	4.07	5.36

[a]Yield values = mole fraction of total monomer units at zero-time.
[b]End group values = 10^3 x mole fraction of total monomer units at zero-time.
[c]Duplicate cooks.

Table 17. Hydroxyl accessibility of fibrous hydrocellulose during degradation in 1.0M sodium hydroxide.

Reaction Time, hours	Hydroxyl Accessibility, % 60°C	80°C
--[a]	52.2; 51.9; 50.6	—
0	51.5; 49.4[b]	49.7; 48.4[b]
0.5	50.8	47.8
1	51.8	49.1
2	51.3	48.8
4	50.2; 49.9[b]	48.9
8	50.6	50.7; 47.5[b]
24	51.8; 48.8[b]	49.5
48	51.3	48.6; 48.5[b]
96	51.9	51.6
120	50.8	
168	49.4	

[a]Fibrous hydrocellulose starting material.
[b]Single determinations on duplicate degradation samples.

Table 18. Hydroxyl accessibility of amorphous hydrocellulose during degradation in 1.0M sodium hydroxide.

Reaction Time, hours	Hydroxyl Accessibility, % 60°C	80°C
--[a]	100.2; 98.5; 98.2	—
0	96.5; 94.1[b]	90.7; 89.2[b]
0.5	95.0	88.7
1	94.2	89.6
2	94.1	85.7
4	92.2; 89.6[b]	79.2
8	89.1	79.2; 78.8[b]
24	87.2; 87.5[b]	76.7
48	88.6	79.6; 80.9[b]
96	88.6	80.1
120	85.5	—
168	83.5	—

[a]Amorphous hydrocellulose starting material.
[b]Single determinations on duplicate degradation samples.

APPENDIX III

KINETIC RATE COEFFICIENTS

This section contains the kinetic rate coefficients for the fibrous and amorphous hydrocelluloses during degradation in oxygen-free 1.0M sodium hydroxide. The rate coefficients for peeling (k_p), chemical stopping (k_{cs}), physical stopping (k_{ps}) and random chain cleavage (k_{cc}, amorphous substrate only), are presented in Tables 19-22.

Table 19. Degradation of fibrous hydrocellulose in 1.0M sodium hydroxide at 60°C.

Reaction Time, hours	k_p, hours^{-1}	k_{cs}, hours^{-1}	k_{ps}, hours^{-1}
0	4.1	0.014	0.041
0.5	4.1	0.014	0.033
1	4.0	0.014	0.033
2	3.3	0.011	0.022
4	2.7	0.009	0.016
8	1.4	0.005	0.003
24	0.8	0.003	0.003
48	0.5	0.002	0.003
96	0.4	0.001	0.003
120	0.3	0.001	0.003
168	0.3	0.001	0.003

Table 20. Degradation of fibrous hydrocellulose in 1.0M sodium hydroxide at 80°C.

Reaction Time, hours	k_p, hours^{-1}	k_{cs}, hours^{-1}	k_{ps}, hours^{-1}
0	28	0.11	0.36
0.5	14	0.053	0.18
1	12	0.044	0.14
2	8.9	0.034	0.081
4	8.1	0.031	0.054
8	5.8	0.022	0.019
24	3.5	0.017	0.000
48	1.4	0.012	0.000
96	0.6	0.007	0.000

Table 21. Degradation of amorphous hydrocellulose in 1.0M sodium hydroxide at 60°C.

Reaction Time, hours	k_p, hours^{-1}	k_{cs}, hours^{-1}	k_{ps}, hours^{-1}	k_{cc}, hours^{-1}
0	6.2	0.030	0.014	—
0.5	5.9	0.029	0.014	—
1	5.6	0.027	0.015	—
2	5.5	0.027	0.014	—
4	4.2	0.020	0.013	—
8	2.7	0.010	0.011	8.4×10^{-6}
24	0.9	0.007	0.006	8.7×10^{-6}
48	0.6	0.006	0.002	8.4×10^{-6}
96	0.5	0.006	0.002	8.3×10^{-6}
120	0.6	0.006	0.001	8.1×10^{-6}
168	0.6	0.006	0.002	7.5×10^{-6}

Table 22. Degradation of amorphous hydrocellulose in 1.0M sodium hydroxide at 80°C.

Reaction Time, hours	k_p, hours^{-1}	k_{cs}, hours^{-1}	k_{ps}, hours^{-1}	k_{cc}, hours^{-1}
0	40	0.26	0.15	—
0.5	32	0.21	0.14	—
1	17	0.11	0.14	—
2	14	0.11	0.070	5.8×10^{-5}
4	6.2	0.081	0.020	5.9×10^{-5}
8	1.7	0.042	0.002	5.3×10^{-5}
24	0.8	0.023	0.000	1.2×10^{-5}
48	0.2	0.021	0.000	0.8×10^{-5}
96	0.1	0.020	0.000	0.5×10^{-5}

APPENDIX IV

CELLULOSE DEGRADATION IN STRONTIUM HYDROXIDE

Colbran and Davidson[11] have shown that cellulose undergoes significantly less yield loss in strontium hydroxide than in sodium hydroxide. Therefore, since the carboxyl content of cellulose was found to increase more rapidly in strontium hydroxide, they concluded that the ratio of the rate of chemical stopping to peeling was higher during degradation in strontium hydroxide. Strontium hydroxide was thought to be capable of converting almost all of the reducing end groups to acidic end groups. Consequently, Haas, et al.[7] employed a strontium hydroxide treatment (1.0M strontium hydroxide, 100°C, 10 hours) to facilitate the measurement of reducing end groups in fibrous hydrocellulose. The reducing end group content of the initial substrate was said to equal the number of acidic end groups formed during the strontium hydroxide treatment.

In the present study, the fibrous and amorphous hydrocelluloses were degraded in 1.0M strontium hydroxide (oxygen-free) at 100°C for 10 hours.[7] The degraded hydrocelluloses were analyzed for yield, acidic end groups, and reducing end groups by the methods described in the Substrate Analysis section. In addition, reducing end group contents of the initial substrates were estimated as done previously[7] from the number of acidic end groups formed during the degradations. The end group data for the initial substrates and the degradation samples are presented in Table 23.

The strontium hydroxide treatment did cause substantial increases in the acidic end group contents of the two hydrocelluloses. However, the total end group contents of the fibrous and amorphous hydrocelluloses increased by 47% and 87%, respectively, during the degradations. Therefore, random chain cleavage must have occurred to significant extents in both substrates. In

addition, the larger increase in the total end group content of the amorphous hydrocellulose indicates that the molecules in the less ordered physical structure (see Cellulose Substrates) were more susceptible to chain cleavage. Consequently, the reducing end group contents of the initial substrates, determined as the numbers of acidic end groups formed during degradation, were 43% and 86% greater for the fibrous and amorphous hydrocelluloses, respectively, than the values obtained by reduction with sodium borotritiide (see Reducing End Groups).

Table 23. End group data[a] for the fibrous and amorphous hydrocelluloses before and after degradation in 1.0M strontium hydroxide at 100°C for 10 hours.

	Fibrous Hydrocellulose		Amorphous Hydrocellulose	
Sample	Untreated	Degraded	Untreated	Degraded
Reducing end groups	1.26×10^{-3} (1.80×10^{-3})[b]	0.57×10^{-3} -	3.45×10^{-3} (6.40×10^{-3})[b]	0.83×10^{-3} -
Acidic end groups	1.10×10^{-3}	2.90×10^{-3}	0.99×10^{-3}	7.39×10^{-3}
Total end groups	2.36×10^{-3}	3.47×10^{-3}	4.44×10^{-3}	8.22×10^{-3}

[a]Expressed as the mole fractions of the total monomer units in the untreated substrates.
[b]Reducing end group contents determined as the numbers of acidic end groups formed during degradation in strontium hydroxide.[7]

Thus, the use of strontium hydroxide to determine reducing end groups in cellulose, as described by Haas, et al.,[7] is not a reliable method. This is due to the fact that the proposed strontium hydroxide treatment causes significant chain cleavage, the extent of which depends upon the physical structure of the particular cellulose sample. As a result, additional reducing end groups are made available to the chemical stopping reaction, and the number of acidic end groups formed can exceed the total number of reducing end groups in the original sample.